

**EFFECTS OF THE BACTERIAL ALGICIDE IRI-160AA ON THE
MICROBIAL COMMUNITY COMPOSITION OF THE DELAWARE
INLAND BAYS**

by

Christopher R. Grasso

A thesis submitted to the Faculty of the University of Delaware in partial fulfillment of the requirements for the degree of Master of Science in Marine Studies

Fall 2018

© 2018 Christopher R. Grasso
All Rights Reserved

**EFFECTS OF THE BACTERIAL ALGICIDE IRI-160AA ON THE
MICROBIAL COMMUNITY COMPOSITION OF THE DELAWARE
INLAND BAYS**

by

Christopher R. Grasso

Approved: _____
Kathryn J. Coyne, Ph.D.
Professor in charge of thesis on behalf of the Advisory Committee

Approved: _____
Mark A. Moline, Ph.D.
Director of the School of Marine Science and Policy

Approved: _____
Estella Atekwana, Ph.D.
Dean of the College of Earth, Ocean, and Environment

Approved: _____
Douglas J. Doren, Ph.D.
Interim Vice Provost for Graduate and Professional Education

ACKNOWLEDGMENTS

I would like to first thank my advisor, Dr. Kathy Coyne, for her support, patience, and guidance as an advisor over the course of the last two years. I was very fortunate to have become a member of her lab and to have experienced so much of the world of molecular ecology. I have learned so much and am extremely grateful for the opportunities provided to me here at the University of Delaware.

I would like to thank my other two committee members, Drs. Mark Warner and Bill Ullman, for their support and interest in this research. It was always reassuring to know that I had a committee staffed with three excellent mentors. I would also like to thank my fellow lab members Yanfei Wang and Dr. Tye Pettay. Their expertise, knowledge, and friendship were also integral to the successful completion of this work.

I would like to thank the University of Delaware, Okie Fellowship, National Oceanic and Atmospheric Administration, and Delaware Sea Grant for funding various aspects of my research and employment as a graduate student.

Lastly, I would like to thank my family and friends, especially my girlfriend Emily Ruhl, without whom none of this would have been possible. Your support and encouragement over the years has been nothing short of amazing and has led me to where I am today. I love you all.

TABLE OF CONTENTS

LIST OF TABLES	vii
LIST OF FIGURES	ix
ABSTRACT	xiii
Chapter	
1 INTRODUCTION	1
1.1 Harmful Algal Blooms	1
1.2 IRI-160AA and Preexisting Work	3
1.3 Research Objectives	6
2 EFFECTS OF REPEATED DOSING ON MICROBIAL COMMUNITIES	7
2.1 Abstract	7
2.2 Introduction	8
2.3 Methods	11
2.3.1 Preparing Bacterial Algicide IRI-160AA	11
2.3.2 Measuring NH ₄ ⁺ Concentrations	11
2.3.3 Establishing IRI-160AA EC50 Concentrations	12
2.3.4 Repeated Dosing of Natural Phytoplankton Communities	12
2.3.5 DNA Extraction and Purification	13
2.3.6 Dissolved Nutrient and DOC Analysis	14
2.3.7 Community Sequencing	14
2.3.8 Dinoflagellate Response	15
2.3.9 Community Fingerprinting	16
2.3.10 Statistical Analyses	17
2.4 Results	18
2.4.1 Establishing IRI-160AA EC50 Concentrations	18
2.4.2 Repeated Dosing	18
2.4.2.1 June 28, 2017 Experiment	18
2.4.2.2 August 11, 2017	20
2.4.3 Community Composition Analysis	21
2.4.3.1 June 28, 2017	21
2.4.3.2 August 11, 2017	22

	2.4.3.2.1	Community Sequencing	23
	2.5	Discussion.....	25
3		EFFECTS OF IRI-160AA ON MICROZOOPLANKTON GRAZING	49
	3.1	Abstract.....	49
	3.2	Introduction	50
	3.3	Methods	52
	3.3.1	Preparing Bacterial Algicide IRI-160AA	52
	3.3.2	Experimental Setup	52
	3.3.3	Ammonium Effects on Community Composition.....	53
	3.3.4	DNA Extraction and Purification	54
	3.3.5	Community Fingerprinting via T-RFLP	54
	3.3.6	Statistical Analyses.....	54
	3.4	Results	55
	3.4.1	Grazing Results	55
	3.4.1.1	July 25, 2017	55
	3.4.1.2	September 25, 2017	55
	3.4.2	Ammonium Effects on Community Composition.....	56
	3.4.3	Molecular Analysis.....	56
	3.4.3.1	July 25, 2017	56
	3.4.3.2	September 25, 2017	57
	3.4.3.3	Ammonium Effects on Community Composition.....	57
	3.5	Discussion.....	58
4		CONTRIBUTION OF AMMONIUM TO THE ALGICIDAL EFFECTS OF IRI-160AA.....	71
	4.1	Abstract.....	71
	4.2	Introduction	72
	4.3	Methods	75
	4.3.1	Preparing Bacterial Algicide IRI-160AA	75
	4.3.2	Culture Conditions.....	76
	4.3.3	NH ₄ ⁺ Sensitivity	76
	4.3.4	Photochemical Response to NH ₄ ⁺ Alone vs. IRI-160AA.....	77
	4.3.5	NH ₄ ⁺ in Dose-Response Experiments	77

4.3.6	Dinoflagellate Photochemistry	78
4.3.7	Statistical Analyses.....	78
4.4	Results	79
4.4.1	NH ₄ ⁺ Sensitivity	79
4.4.2	Photochemical Response to NH ₄ ⁺ Alone vs. IRI-160AA.....	82
4.4.3	Dose Response.....	82
4.4.3.1	January 27, 2018 Experiment	82
4.4.3.2	April 11, 2018 Experiment	84
4.5	Discussion.....	85
5	CONCLUDING REMARKS	96
	REFERENCES	98
Appendix		
	PHOTOCHEMICAL RESPONSE TO NH ₄ ⁺ ALONE VS. IRI-160AA.....	113

LIST OF TABLES

Table 2.1 Environmental metadata and experimental specifications associated with the repeated dosing experiments conducted on June 28, 2017 and August 11, 2017.	33
Table 2.2 Sequences of primers and probes utilized in polymerase chain reactions as well as quantitative polymerase chain reactions. F denotes forward primer; R denotes reverse primer.	34
Table 2.3 Dissolved organic carbon (DOC) and nutrient concentrations corresponding to two repeated dosing experiments. All treatments not marked as “T ₀ ” are representative of T _{final} for its respective experiment. Values are presented as averages (SD). DOC values are averages of four measurements, each being the average of 3-5 detections of the same sample. Dissolved nutrient values are averages of four measurements. Asterisk (*) denotes significant difference (p < 0.05).....	35
Table 2.4 Percent community composition similarities to the T ₀ community based on Bray-Curtis similarity values derived from a resemblance matrix. Values in parentheses indicate standard deviation.	36
Table 2.5 Data collected from sequencing of the V4 region of the 18S rRNA gene performed on extracted DNA samples from the August 11, 2017 experiment. Pielou’s species evenness (J’) and Shannon-Wiener diversity index (H’) were calculated in PRIMER7 (Schmitz and Nagel, 1995).	37
Table 3.1 Environmental metadata and experimental specifications associated with the microzooplankton grazing experiments conducted on July 25, 2017, September 25, 2017, and September 28, 2017.	62
Table 3.2 Sequences of primers and probes utilized in polymerase chain reactions as well as quantitative polymerase chain reactions. F denotes forward primer; R denotes reverse primer.	63
Table 3.3 Percent community composition similarities compared to the T ₀ community based on Bray-Curtis similarity values derived from terminal restriction fragment data. Values in parentheses indicate standard deviation.....	64

- Table A1 Maximum yield of photosystem II (F_v/F_m) with standard deviation (SD) through after application of IRI-160AA at EC50 for *K. veneficum*. All values are representative of the mean of three biological replicates. 113
- Table A2 Maximum yield of photosystem II (F_v/F_m) with standard deviation (SD) through after application of IRI-160AA at EC50 for *P. minimum*. All values are representative of the mean of three biological replicates. 114
- Table A3 Maximum yield of photosystem II (F_v/F_m) with standard deviation (SD) through after application of IRI-160AA at EC50 for *G. instriatum*. All values are representative of the mean of three biological replicates. 115
- Table A4 Maximum yield of photosystem II (F_v/F_m) with standard deviation (SD) through after application of IRI-160AA at EC50 for *A. tamarense*. All values are representative of the mean of three biological replicates. 116

LIST OF FIGURES

- Figure 2.1 Sampling sites within the Delaware Inland Bays: Rehoboth Bay in Rehoboth Beach, DE at Love Creek (RB34) and Indian River Bay in Bethany Beach, DE at Holly Terrace Acres Canal (IR32). 38
- Figure 2.2 Procedural flowchart of sampling methodology for repeated dosing experiments. Asterisks (*) indicate days that were present in the June 28, 2017 experiment but not in the August 11, 2017 experiment. 39
- Figure 2.3 Mean daily growth rates (A and C) and relative abundance of dinoflagellates (B and D) for each of the two repeated dosing experiments (June 2017 and August 2017). All error bars represent standard deviation. *Top left*: Mean daily growth rate in the June 2017 experiment. *Top right*: Relative abundance of dinoflagellates on a logarithmic scale in the June 2017 experiment. *Bottom left*: Mean daily growth rates in the August 2017 experiment. *Bottom right*: Relative abundance of dinoflagellates in the August 2017 experiment. . 40
- Figure 2.4 Non-metric multi-dimensional scaling (nMDS) ordination based on a Bray-Curtis similarity matrix for the microzooplankton grazing experiment sampled on June 28, 2017. Timepoints: T₀ – black; T₃ – red; T₅ – green; T₇ – blue. 41
- Figure 2.5 Non-metric multi-dimensional scaling (nMDS) ordination based on a Bray-Curtis dissimilarity matrix for the microzooplankton grazing experiment sampled on August 11, 2017. Timepoints: T₀ – black; T₃ – red; T₅ – green. 42
- Figure 2.6 Relative abundance on a log-10 scale for prominent microbial eukaryotic classes detected through 18S rRNA sequencing in the August 11, 2017 experiment. Dino: Dinoflagellates (Dinophyceae); Cryp: Cryptophytes (Cryptophyta); Olig: Ciliates (Oligohymenophorea); Cosc: Diatoms (Coscinodiscophyceae); Raph: Raphidophytes (Raphidophyta). 43
- Figure 2.7 Dinoflagellate community in the August 11, 2017 repeated dosing experiment at T₀ as determined by sequencing of the V4 region of the 18S rRNA gene. Different tiers of the chart represent taxonomic groupings with the outermost ring representing species-level identification. Chart was constructed using the interactive metagenomic visualization program Krona (Ondov et al., 2011). 44

Figure 2.8 Dinoflagellate community in the August 11, 2017 repeated dosing experiment at T_{final} in the EC95 treatment as determined by sequencing of the V4 region of the 18S rRNA gene. Different tiers of the chart represent taxonomic groupings with the outermost ring representing species-level identification. Chart was constructed using the interactive metagenomic visualization program Krona (Ondov et al., 2011).....	45
Figure 2.9 Dinoflagellate community in the August 11, 2017 repeated dosing experiment at T_{final} in the EC50 treatment as determined by sequencing of the V4 region of the 18S rRNA gene. Different tiers of the chart represent taxonomic groupings with the outermost ring representing species-level identification. Chart was constructed using the interactive metagenomic visualization program Krona (Ondov et al., 2011).....	46
Figure 2.10 Dinoflagellate community in the August 11, 2017 repeated dosing experiment at T_{final} in the EC05 treatment as determined by sequencing of the V4 region of the 18S rRNA gene. Different tiers of the chart represent taxonomic groupings with the outermost ring representing species-level identification. Chart was constructed using the interactive metagenomic visualization program Krona (Ondov et al., 2011).....	47
Figure 2.11 Dinoflagellate community in the August 11, 2017 repeated dosing experiment at T_{final} in the control as determined by sequencing of the V4 region of the 18S rRNA gene. Different tiers of the chart represent taxonomic groupings with the outermost ring representing species-level identification. Chart was constructed using the interactive metagenomic visualization program Krona (Ondov et al., 2011).	48
Figure 3.1 Sampling sites within the Delaware Inland Bays: Rehoboth Bay in Rehoboth Beach, DE at Love Creek (RB34), Indian River Bay in Bethany Beach at Holly Terrace Acres Canal (IR32), and Little Assawoman Bay in South Bethany, DE at Russell Canal East (SB10E).	65
Figure 3.2 Dilution factor plotted against community growth rates derived from chlorophyll <i>a</i> concentrations for the (A) algicide treatment and (B) control in the July 25, 2017 microzooplankton grazing experiment. Grazing rates were calculated via linear regression analysis. Algicide treatment grazing rate: 0.396 d ⁻¹ ; control grazing rate: 0.400 d ⁻¹	66

Figure 3.3 Dilution factor plotted against community growth rates derived from chlorophyll <i>a</i> concentrations for the (A) algicide treatment and (B) control in the September 25, 2017 microzooplankton grazing experiment. Grazing rates were calculated via linear regression analysis. Algicide treatment grazing rate: 0.258 d ⁻¹ ; control grazing rate: 0.027 d ⁻¹	67
Figure 3.4 Non-metric multi-dimensional scaling (nMDS) ordination based on a Bray-Curtis similarity matrix for the microzooplankton grazing experiment sampled on July 25, 2017. Red coloration indicates the algicide treatment, blue indicates the control.	68
Figure 3.5 Non-metric multi-dimensional scaling (nMDS) ordination based on a Bray-Curtis similarity matrix for the microzooplankton grazing experiment sampled on September 25, 2017. Red coloration indicates the algicide treatment, blue indicates the control.	69
Figure 3.6 Non-metric multidimensional scaling (nMDS) ordination based on a Bray-Curtis similarity matrix for the microzooplankton grazing experiment sampled on September 28, 2017. All data represented were from the 100% undiluted samples at T _{final} . Red coloration indicates the algicide treatment, green indicates the ammonium treatment, blue indicates the control.....	70
Figure 4.1 Relative fluorescence of non-axenic cultured <i>Prorocentrum minimum</i> over the course of 8 days after initial exposure to varying concentrations of NH ₄ Cl dissolved in <i>f</i> /2 growth medium. Error bars represent standard deviation.....	90
Figure 4.2 Relative fluorescence of non-axenic cultured <i>Gyrodinium instriatum</i> over the course of 8 days after initial exposure to varying concentrations of NH ₄ Cl dissolved in <i>f</i> /2 growth medium. Error bars represent standard deviation.....	91
Figure 4.3 Relative fluorescence of non-axenic cultured <i>Karlodinium veneficum</i> over the course of 8 days after initial exposure to varying concentrations of NH ₄ Cl dissolved in <i>f</i> /2 growth medium. Error bars represent standard deviation.....	92

Figure 4.4 Growth rates for the three dinoflagellate species tested in the NH_4^+ sensitivity experiments. The dashed red line indicates the point at which growth becomes static. *K. veneficum* has a diminished range due to increased sensitivity. Highest NH_4^+ concentrations were omitted from calculations due to fluorescence measurements of 0 RFU. Error bars represent standard deviation. 93

Figure 4.5 Three parameters measured across three treatments during the 18-hour photochemical experiment conducted on January 27, 2018. F_v/F_m represents the maximum yield of PSII, ρ represents the photochemical connectivity between PSII reaction centers, and τ represents the amount of time it took to re-oxidize the primary quinone. Error bars are indicative of standard deviation..... 94

Figure 4.6 Three parameters measured across three treatments during the 18-hour photochemical experiment conducted on April 11, 2018. F_v/F_m represents the maximum yield of PSII, ρ represents the photochemical connectivity between PSII reaction centers, and τ represents the amount of time it took to re-oxidize the primary quinone. Error bars are indicative of standard deviation..... 95

ABSTRACT

Global increases in harmful algal blooms (HABs) have spurred interest in measures to control these blooms. Prevention, control, and mitigation of HABs are of human interest, and there are naturally-occurring compounds that may directly influence these processes. Use of these compounds appears promising, but effects to non-target organisms are also of concern. The Delaware Inland Bay (DIB; Delaware, United States) system is host to the algicidal marine bacterium *Shewanella* sp. IRI-160, which secretes one or more compounds having allelopathic effects to dinoflagellate algae. The research described here had three objectives: (1) to determine whether the algicide has a significant effect on microbial community composition during or after repeated dosing, (2) to determine whether the algicide has a significant effect on microzooplankton grazing rates in natural communities, and (3) to determine the extent to which ammonium contributes to the algicidal effect of IRI-160AA.

In Chapter 2, Quantitative PCR and DNA sequencing indicated a decline in natural dinoflagellate community abundance with repeated algicide daily dosing; however, community photosynthetic biomass was not negatively altered by the final timepoint. Additionally, community composition was shown to play a major role in dissolved nutrient and organic carbon assimilation.

In Chapter 3, microcosms were dosed with the algicide at EC50 concentrations and incubated for 24 hours at four dilution factors. Microzooplankton grazing rates did not significantly decrease in the presence of the algicide at EC50 concentrations yet dominant microeukaryotic groups within communities did shift after 24 hours of exposure.

In Chapter 4, photochemical parameters were used to investigate the extent to which ammonium contributes to the algicidal effect of IRI-160AA. Maximum yield of photosystem II (F_v/F_m), photochemical connectivity between photosystem II reaction centers (ρ), and the re-oxidation rate of the primary quinone (τ) all indicated that ammonium negatively affects the photosynthetic machinery of photosystem II but not to the same extent as IRI-160AA with equal NH_4^+ concentrations.

Chapter 1

INTRODUCTION

1.1 Harmful Algal Blooms

Harmful algal blooms (HABs) are events during which the population of a particular algal species reaches a critical density, potentially causing a multitude of negative environmental effects including, but not limited to: fish kills, loss of submerged vegetation, shellfish die-offs, etc. (Anderson et al., 2008). These events are caused by two categories of factors: natural and anthropogenic. Natural factors include processes such as circulation and temperature, while the dominant anthropogenic factor is eutrophication (Sellner et al., 2003). With ever-growing industrialization, varying forms of nitrogen have been increasingly added to the natural environment, spawning a greater frequency of HAB events (Hallegraeff, 1993). Efforts have been made globally and locally to stymie this major anthropogenic influence, yet eutrophication-induced blooms continue to occur (Boesch et al., 2001).

Historically, the impacts of HABs have been documented as far back as the late 18th century with explorers citing discolored waters associated with poisonous shellfish (Prakash et al., 1971). Earlier documentation of HABs may date back to the Biblical story of Moses turning the Nile River to blood. As discussed in National Geographic's series "The Ten Plagues of the Bible," empirically shown climate shifts coinciding with the end of Rameses II's reign may have caused a bloom of *Planktothrix rubescens*, causing the red coloration and fish kill described in the Bible. These blooms have become more common in recent decades (Smayda, 1989;

Anderson et al., 2002), and are of particular concern to modern fish and shellfish industries. Economically, HABs have the capacity to severely hamper these industries through varying mechanisms, sometimes costing regions millions of dollars in lost revenue or remediation efforts (Wolf et al., 2017). Furthermore, shellfish act as a common vector, transmitting HAB-produced toxins from the marine environment to humans, and subsequently yielding one of several potential HAB poisoning syndromes, such as paralytic shellfish poisoning, neurotoxic shellfish poisoning, diarrhetic shellfish poisoning, or amnesic shellfish poisoning (Anderson et al., 2008). Marine algal toxins vary greatly, but the group as a whole has steadily increased in both frequency of occurrence and recorded number of novel toxins alongside climate change (Van Dolah, 2000). Data suggest that the warming waters associated with climate change galvanize bloom events by altering the ecosystem enough to supplant a healthy mixture of marine microphotosynthesizers with one dominant bloom-forming species (O'Neil et al., 2012; Johnk et al., 2007). The bulk of toxic microalgae are members of the phylum Dinoflagellata, more commonly referred to as dinoflagellates (Smayda, 1997). Dinoflagellates are a diverse phylum of unicellular, marine eukaryotes that often exhibit strong relative motility due to their pair of flagella, with which they achieve forward (via longitudinal flagellum) and rotational (via transverse flagellum) motion (UNESCO, 2003).

Because of the increased frequencies of harmful algal bloom events, dinoflagellate-based and otherwise, there is considerable interest in methods of controlling HABs. HAB control can be broken down into two categories of response: prevention and reaction. Prevention refers to the proactive steps taken to reduce the likelihood of an HAB event, whereas reaction corresponds to treating or mitigating a

harmful algal bloom already underway. One of the most common preventative approaches in the field is the reduction of nutrient flux into a system which would in turn fuel phytoplankton growth. However, limiting nutrient input can be extremely challenging in non-fluvial systems such as the Delaware Inland Bays due to the sheer myriad of factors that go into estuarine or marine bloom formation (Smith and Schindler, 2009). Additionally, blooms that are not instigated by eutrophication require forms of prevention other than nutrient limitation (Tilney et al., 2014b; Bachmann et al., 2003). Anderson (2004) mentioned three categories of preventative HAB measures: nutrient limitation, limitation of activities potentially transporting HAB species to new environments, and the proper management and modification of physical conditions. In line with this last point, chemical and biological algicides have been studied as potential strategies for HAB prevention that do not rely on the concept of nutrient limitation and have shown promise in multiple studies. Jia et al. (2013) investigated the effects of copper sulfate, hydrogen peroxide, and even rice seed husks on algal species of the genus *Microcystis*, and saw the latter two exhibit successful HAB prevention. Other preventative measures studied have included natural clay for flocculation, strong oxidants, allelopathic seaweeds, and algicidal bacteria (Yang et al., 2014; Sengco, 2009). The results of these studies support the use of chemical and biological algicides as potential paths forward in the field of HAB prevention; however, understanding the ways in which these methods interact with both target and non-target organisms is pivotal to their continued viability.

1.2 IRI-160AA and Preexisting Work

The allelopathic compound being investigated here is an algicidal exudate produced by the naturally-occurring bacterium *Shewanella* sp. IRI-160 termed IRI-

160AA. Originally described by Hare et al. (2005), the bacterium itself was part of a study searching for algicidal activity across twenty-two bacterial isolates from the Delaware Inland Bays. The study showed that *Shewanella* sp. IRI-160 exhibited growth-inhibiting effects specific to dinoflagellates, while showing negligible or positive effects on other microalgal classes such as diatoms, prasinophytes, cryptophytes, and raphidophytes. Later, Pokrzywinski et al. (2012) found that this algicidal activity was attributed to a bioactive secretion containing a compound that was likely both small and hydrophilic. This qualitative characterization of the mode of algicidal activity supported earlier findings that the compound was dinoflagellate-specific, but also importantly found that the compound's efficacy was significantly greater during the logarithmic growth phase of the algal species. This latter finding supported the idea that this compound could be added to bloom-prone or bloom-forming systems to stop potential HAB events. Subsequently, Tilney et al. (2014a) investigated the effects of the algicide on dinoflagellates as well as the microbial community, but with naturally sampled communities rather than isolated dinoflagellate cultures. They found that the allelopathic algicidal activity was still observed, and that heterotrophic non-dinoflagellate protists in the bottled community exhibited dose-dependent growth alongside increasing IRI-160AA concentrations. The eukaryotic community was directly altered by the decline in dinoflagellates, yet the mixed community's total autotrophic biomass remained high. Because of this, and the fact that algicidal activity took slightly longer in mixed communities than in isolated cultures, it could be argued that non-dinoflagellate autotrophs may utilize components of the algicide for enhanced growth. Tilney et al. (2014b) went on to investigate the effects on dinoflagellate photobiology and found that responses to IRI-160AA were

species-specific, as thecate dinoflagellates were less sensitive than their athecate counterparts. This study was also the first regarding IRI-160AA to go beyond mortality when describing dinoflagellate responses to the algicide, citing PSII inactivation, lesser membrane integrity, and general inhibition of growth. More recently, Pokrzywinski et al. (2017) published a study showing that IRI-160AA may be dinoflagellate-specific due to the unique structure of dinoflagellate chromosomes. Various dinoflagellate species exhibited changes in cellular morphology and ultrastructure within two hours of algicide application, in some cases resulting in nuclear expulsion.

Most recently, focus has shifted from the cellular mode of algicidal activity to the composition of the compound itself. The undiluted algicide has been shown to have high concentrations of ammonium (NH_4^+), typically between 1 and 3mM. Although ammonium has been suggested to be one of the less toxic forms of inorganic nitrogen in aquatic systems (Camargo and Alonso, 2006), dinoflagellates are among the most susceptible microalgal classes to its potentially toxic effects (Collos and Harrison, 2014). Non-toxic concentrations, however, have been shown by many studies to stimulate growth in species across a broad range of algal classes, including diatoms, green algae, and others (Kuninao et al., 2009; Hii et al., 2011). Additional components of the algicide are under active investigation.

Even with the discovery of ammonium as a component of IRI-160AA, there are still a number of questions surrounding the algicide's composition and efficacy as an *in situ* control method for HAB events. This research was conducted to answer the following questions:

- To what extent does ammonium contribute to the algicidal activity of IRI-160AA?
- What is the effect on microbial community composition during proactive, repeated dosing with IRI-160AA?
- What is the effect of IRI-160AA on microzooplankton grazers?

The subsequent results will be used in the continued assessment of the bacterial algicide IRI-160AA as a naturally-isolated, acute or chronic response to harmful algal bloom events.

1.3 Research Objectives

This research project comprises three primary objectives relating to the characterization and potential implementation of the algicide: (1) to determine whether the algicide has a significant effect on microbial community composition during or after repeated dosing, (2) to determine whether the algicide has a significant effect on microzooplankton grazing rates in natural communities, and (3) to determine the extent to which ammonium contributes to the algicidal effect of IRI-160AA. The first two objectives contribute directly to a gap in knowing how this compound may affect non-target organisms in the ecosystem. This knowledge is integral to the larger project goal of *in situ* application of the algicide to bloom-susceptible systems. The third objective is directly related to the chemical characterization of the algicide by providing insight into IRI-160AA's active ingredient, information pertinent to understanding *in situ* effects on exposed biota.

Chapter 2

EFFECTS OF REPEATED DOSING ON MICROBIAL COMMUNITIES

2.1 Abstract

Global increases in harmful algal blooms (HABs) have spurred interest in measures to control these blooms. Prevention, control, and mitigation of HABs are of human interest, and there are naturally-occurring compounds that may directly influence these processes. Use of these compounds appears promising, but effects to non-target organisms are also of concern. The Delaware Inland Bay (DIB; Delaware, United States) system is host to the algicidal marine bacterium *Shewanella* sp. IRI-160, which secretes a compound(s) having allelopathic effects to dinoflagellate algae. Here, the effects of the algicide, designated IRI-160AA, on microbial communities in the DIB were evaluated. Natural community experiments were conducted to assess proactive application efficiency of the algicide to communities as a preventative measure. Repeated dosing was performed on natural, mixed dinoflagellate communities at various effective algicide concentrations, and changes in the microbial community were evaluated via *in vivo* fluorescence and molecular fingerprinting methodology. Statistically significant dose-dependent decreases in dinoflagellate abundance were observed, yet photosynthetic biomass increased overall. Dissolved organic carbon (DOC) analysis initially revealed a dose-dependent increase with higher concentrations of algicide exhibiting higher levels of measured DOC. A second experimental iteration on a separate community showed a small, treatment-independent decrease in DOC suggesting that community structure strongly influences these results. Next Generation Sequencing (NGS) was performed to track eukaryotic community changes. Overall increases in abundance between T_{final} and T_0 were

observed for diatoms (class Coscinodiscophyceae, Bacillariophyceae), cryptophytes (Cryptophyta), and ciliates (Oligohymenophorea). Decreases in abundance were observed for raphidophytes (Raphidophyceae), freshwater ciliates (Colpodea), chlorophytes (Chlorophyta), and dinoflagellates (Dinophyceae). Data from sequencing and molecular fingerprinting suggested that shifts in the eukaryotic community were dose-dependent. The results of this investigation demonstrate the efficacy of repeated, reactive dosing of IRI-160AA as a dinoflagellate-specific algicidal agent without negatively impacting the greater microalgal community in the Delaware Inland Bays.

2.2 Introduction

Global increases in frequency, geographic range, and duration of harmful algal blooms (HABs) have spurred interest in measures to control these blooms (Smayda et al., 1989; Hallegraeff et al., 1993; Van Dolah, 2000; Anderson et al., 2002). Anderson (2004) mentions three categories of preventative HAB measures: nutrient limitation, limitation of activities potentially transporting HAB species to new environments, and the proper management and modification of physical conditions. In line with this last point, chemical and biological algicides are potential strategies for HAB prevention. Allelopathy, or any process involving chemical compounds produced by organisms that influence the growth, development, and survival of other organisms (Roger et al., 2006), has been well documented in both terrestrial and aquatic environments (Bais et al., 2003; Levine et al., 2003; Gopal and Guel, 1993; Inderjit and Dashkini, 1994; Gross, 2003). Allelopathic compounds targeting HAB species have been studied with increasing frequency in recent decades, with algicidal allelochemicals shown to target dinoflagellates (Doucette et al., 1999; Jeong et al., 2003; Li et al., 2014),

raphidophytes (Kim et al., 2009), and green algae and cyanobacteria (Singh et al., 2001).

The allelopathic compound(s) investigated here is an algicidal exudate produced by the naturally-occurring bacterium *Shewanella* sp. IRI-160. Originally described by Hare et al. (2005), the bacterium itself was part of a study searching for algicidal activity across twenty-two bacterial isolates from the Delaware Inland Bays. The study showed that *Shewanella* sp. IRI-160 exhibited growth-inhibiting effects specific to dinoflagellates, while showing negligible or positive effects on other microalgal classes such as diatoms, prasinophytes, cryptophytes, and raphidophytes. Subsequently, Pokrzywinski et al. (2012) found that the algicidal activity could be attributed to a bioactive secretion containing a compound that was likely both small and hydrophilic. Qualitative characterization of algicidal activity was consistent with earlier findings in that the compound was dinoflagellate-specific, but also importantly the compound's efficacy was significantly greater when dinoflagellates were in logarithmic phase growth. This latter finding supported the idea that this compound could be added to bloom-prone or bloom-forming systems to prevent or mitigate potential HAB events in the early stages of a bloom. Tilney et al. (2014a) investigated the effects on dinoflagellate photobiology and found that responses to the algicidal exudate, termed "IRI-160AA", were species-specific, with less effect on thecate dinoflagellates compared to athecate species. This study was also the first regarding IRI-160AA to go beyond mortality when describing dinoflagellate responses to the algicide, citing PSII inactivation, impacts on membrane integrity, and general inhibition of growth. More recently, Pokrzywinski et al. (2017a) published a study suggesting that IRI-160AA may be dinoflagellate-specific due to the unique structure

of dinoflagellate chromosomes. Dinoflagellate species exhibited changes in cellular morphology and ultrastructure within two hours of algicide application, in some cases resulting in nuclear expulsion. A second study by Pokrzywinski et al. (2017b) evaluated biochemical changes in dinoflagellates, specifically those changes associated with cell death. In the presence of IRI-160AA, species exhibited significant increases in DNA degradation, intra- and extracellular reactive oxygen species (ROS), and DEVDase protease activity which have been associated with programmed cell death in other phytoplanktonic species (Vardi et al., 2007; Bidle and Bender, 2008; Vavilala et al., 2015).

Tilney et al. (2014b) investigated the effects of the algicide on dinoflagellates as well as the microbial community in mixed natural communities collected from Delaware's inland bays. They found that the allelopathic algicidal activity was still observed, and that heterotrophic non-dinoflagellate protists in the community exhibited dose-dependent growth with increasing IRI-160AA concentrations. The eukaryotic community was directly altered by the decline in dinoflagellates, yet the mixed community's total autotrophic biomass remained high, suggesting that components of the algicidal exudate may stimulate growth of non-dinoflagellate autotrophs.

Prior research by Tilney et al. (2014b) examined the dose-dependent effects of IRI-160AA after a single-dose. To effectively utilize allelopathic compounds for HAB management, however, the effects of repeated introduction to a single system must also be assessed. As such, the objective of this study was to investigate effects of IRI-160AA on the microbial community after repeated dosing. Expanding upon prior IRI-160AA work and seeking to better understand the capacity of IRI-160AA as a

preventative and/or reactive agent for HAB management, I investigated the effects on microbial communities repeatedly dosed with the algicide.

2.3 Methods

2.3.1 Preparing Bacterial Algicide IRI-160AA

Shewanella sp. IRI-160 was cultured on modified LM medium (Sambrook et al., 1989; Luria Bertani medium, 20 g/L NaCl, 10 g/L tryptone, 5 g/L yeast extract, 15 g/L agar) at room temperature for 48-72 hours. A colony was transferred into 100 mL of liquid LM medium (20 g/L NaCl, 10 g/L tryptone, 5 g/L yeast extract) and incubated with shaking at 25 °C overnight. This culture was inoculated into 1-L of f/2 medium (Guillard, 1975; Lananan et al., 2013) with 0.5% sterile casamino acids and incubated for three days with shaking before transferring into three 10L carboys of f/2 medium with 0.5% casamino acids. The cultures were incubated for 10 days with bubbling provided by air passed through a sterile 0.2 µm filter. The culture was subsequently filtered through a HemoFlow HF80S 60kDa dialysis cartridge (Fresenius Medical Care, Waltham, MA) to remove bacterial biomass and compounds >60 kDa. The bacteria-free filtrate (termed “IRI-160AA”) was used for experiments below.

2.3.2 Measuring NH₄⁺ Concentrations

The NH₄⁺ concentration of the IRI-160AA filtrate was determined via the salicylate-hypochlorite colorimetric method of Bower and Holm-Hansen (1980). Samples were diluted in duplicate to 2% (v/v) with deionized water prior to analysis. The NH₄⁺ concentrations of diluted samples were then determined by linear regression analysis.

2.3.3 Establishing IRI-160AA EC50 Concentrations

Karlodinium veneficum (family Kareniaceae) was cultured in sterile 20 PSU *f/2* medium at 25 °C, under a 12:12 light-dark cycle at 140 $\mu\text{mol photons m}^{-2} \text{s}^{-1}$ provided by fluorescent lighting. Algae were sampled during logarithmic growth phase, which has been shown to exhibit the greatest susceptibility to the effects of the algicide (Pokrzywinski et al., 2012). The effective concentrations of IRI-160AA to induce 5%, 50% and 95% mortality (EC05, EC50, and EC95) were determined as described in the EPA's Office of Chemical Safety and Pollution Prevention guidelines for testing the ecological effects of algal toxicity (United States Environmental Protection Agency, 2012).

2.3.4 Repeated Dosing of Natural Phytoplankton Communities

Natural communities were sampled during bloom events where dinoflagellate populations were still visible via light microscopy on two occasions: 28 June 2017 at site RB34, and 11 August 2017 at site IR32 (Figure 2.1). Temperature, salinity, dissolved oxygen, and pH were measured on-site using a YSI 556 MPS (Yellow Springs Instruments, Inc., Yellow Springs, OH). Water was prefiltered on site through a 100- μm mesh filter to remove zooplankton and detritus. Samples were collected for DNA as described below (Section 2.3.5). Field samples containing natural communities were diluted at 1:1 with 0.2 μm -filtered site water amended with NO_3^- and PO_4^{3-} at *f/2* medium levels (NO_3^- , 883 μM ; PO_4^{3-} , 36.3 μM). Treatments ($n = 4$) were 5% and 1% algicide in the June 2017 experiment, treatments were dosed to achieve final concentrations of EC95, EC50, and EC05 in the August 2017 experiment. Controls were dosed with an equal volume of *f/2* amended with 0.5% casamino acids (N-Z-Amine A, Millipore Sigma, Darmstadt, Germany), hereafter

known as “CAA”, which was the same media in which the algicide had been collected. Treatments and controls all had an equal volume of addition: as such, the algicide was diluted with $f/2 + 0.5\%$ CAA to achieve the correct effective concentration. Bulk samples were collected for dissolved nutrients and dissolved organic carbon (DOC) after addition of $f/2 + \text{CAA}$ as described below (Section 2.3.6). Growth was monitored via *in vivo* chlorophyll *a* measurements using the Aquafluor handheld fluorometer (Turner Designs, Sunnyvale, CA). Daily sampling is described in Figure 2.2. The repeated dosing experiment conducted in June 2017 was performed over the course of seven days with algicide dosing occurring on the initial day (T_0), then on days two through six (T_2 - T_6). The repeated dosing experiment conducted in August 2017 over the course of five days with algicide dosing every 24 hours for four days (T_4). The volume removed during sampling was replaced with nutrient-amended $0.2 \mu\text{m}$ -filtered site water and included the appropriate dosing volume of algicide or $f/2 + 0.5\%$ CAA required for each treatment or control.

2.3.5 DNA Extraction and Purification

Samples were filtered onto $3 \mu\text{m}$ Isopore™ polycarbonate filters (Millipore Sigma, Darmstadt, Germany) and submerged into $700 \mu\text{L}$ CTAB buffer amended with 20 ng mL^{-1} pGEM internal standard (100 mM Tris-HCl pH 8.0, 1.4 M NaCl, 1% (w/v) polyvinylpyrrolidone, 2% (w/v) cetyltrimethylammonium bromide, 20 mM EDTA pH 8.0, 0.4% (v/v) 2-mercaptoethanol, 20 ng/mL pGEM-3Z Vector, Promega, Cat. #P2151). DNA was extracted as in Coyne et al. (2001) and quantified via spectrophotometry (NanoDrop 2000, Thermo Fisher Scientific, Waltham, MA).

2.3.6 Dissolved Nutrient and DOC Analysis

Samples were filtered through a 0.2- μm Isopore™ polycarbonate filter (Millipore Sigma, Darmstadt, Germany) to remove biological material, and the resulting filtrate was stored at $-20\text{ }^{\circ}\text{C}$. Dissolved nutrient concentrations were analyzed at the initial and final timepoints, and included PO_4^{3-} , NO_x (NO_3^- and NO_2^-), and NH_4^+ . Samples were measured using a segmented-flow autoanalyzer (Seal Analytical, Mequon, WI). Prior to DOC analysis, samples were diluted 1:20 with ultrapure water to achieve DOC levels within the instrument's range of detection. Diluted samples were then acidified with reagent grade HCl and DOC was measured using a TOC-V total organic carbon analyzer (Shimadzu Corporation, Kyoto, Japan).

2.3.7 Community Sequencing

For the experiment conducted on August 11, 2017, DNA from the initial bulk sample and final timepoint of each treatment and control was shipped to Molecular Research LP (MR DNA; Shallowater, TX) on dry ice for 18S rRNA gene sequencing. DNA from replicates for the T_{final} EC95, EC50, and EC05 treatments and control samples were combined to make a composite DNA sample for each level of algicide treatment. Sequencing was performed on the MiSeq platform (Illumina Inc., San Diego, CA), using primers targeting the V4 region (EukV4F and EukV4R, Table 2.2). Sequence data were joined, depleted of barcodes, filtered to remove sequences <150 bp, and inspected for ambiguous base calls. OTUs were generated by clustering at 97% similarity and were taxonomically classified using BLASTn against the National Center for Biotechnology Information (NCBI) curated database (Altschul et al., 1990). Community sequencing data were visualized using the Krona program developed by Ondov et al. (2011).

2.3.8 Dinoflagellate Response

Quantitative polymerase chain reaction (qPCR) assays were conducted to assess relative changes in dinoflagellate abundance in each treatment and control at each time point. Reactions were performed in triplicate in 96-well plates using an ABI 7500 Real Time PCR System (Applied Biosystems, Foster City, CA). Two separate sets of reactions were conducted: one with dinoflagellate-specific primers, and one with primers targeting an internal pGEM plasmid (Table 2.2). Dinoflagellate-specific reaction volumes were 10 μL with 0.9 μM Dino06F (forward primer), 0.9 μM EukB (reverse primer), 5 μL *Power SYBR Green PCR Master Mix* (Thermo Fisher Scientific, Waltham, MA), and 1 μL of DNA template diluted to 25 $\text{ng}/\mu\text{L}$ in LoTE buffer. The thermal cycler profile was as follows: 50 $^{\circ}\text{C}$ for 2 min, 95 $^{\circ}\text{C}$ for 10 min, and then 40 cycles of 95 $^{\circ}\text{C}$ for 15 s, 56 $^{\circ}\text{C}$ for 30 s, and 72 $^{\circ}\text{C}$ for 1 min. This was followed by an additional dissociation analysis of 95 $^{\circ}\text{C}$ for 15 s, 60 $^{\circ}\text{C}$ for 1 min, 95 $^{\circ}\text{C}$ for 15 s, and 60 $^{\circ}\text{C}$ for 15 s. Reaction volumes for pGEM assays were 10 μL with 0.9 μM M13F (forward primer), 0.9 μM pGEM R (reverse primer), 0.2 μM pGEM probe, 5 μL *TaqMan Environmental Master Mix 2.0* (Thermo Fisher Scientific, Waltham, MA), and 1 μL of diluted DNA template. The thermal cycler profile was as follows: 50 $^{\circ}\text{C}$ for 2 min, 95 $^{\circ}\text{C}$ for 10 min, and then 40 cycles of 95 $^{\circ}\text{C}$ for 15 s, 60 $^{\circ}\text{C}$ for 30 s, and 72 $^{\circ}\text{C}$ for 1 min. Relative dinoflagellate abundance was determined by linear regression analysis using a standard curve generated from dinoflagellate-specific 18S rRNA plasmid and normalized to the relative abundance of pGEM in each sample.

2.3.9 Community Fingerprinting

Terminal restriction fragment length polymorphism (T-RFLP) was used to investigate changes in microbial eukaryote community composition. DNA template was used in each polymerase chain reaction (PCR) with primers targeting the 18S rRNA gene. Each PCR was 20 μ L, performed in triplicate and comprised 25 ng of DNA template, 1x PCR buffer, 0.2 mM dNTPs, 2.5 mM MgCl₂, 0.05 μ g/ μ L BSA, 2.5 μ M EUK1A (forward primer) and EUK517R (reverse primer, Table 2.2), 0.1 μ L JumpStart Taq polymerase, and sterile H₂O. Reaction conditions were as follows: an initial denaturation at 94 °C for 2 min, followed by 32 cycles of denaturation at 94 °C for 30 s, 52 °C for 30 s, and elongation at 72 °C for 1 min. The last of these cycles was followed by incubation at 72 °C for 7 min. Post-PCR amplicons were validated via gel electrophoresis on a 1% agarose gel (240 V, 500 mA, 10 min). Successful products were pooled and purified using the GeneJET PCR Purification Kit (Thermo Fisher Scientific).

Purified PCR products (200 ng) were digested in separate 20- μ L reactions comprising 10 U of either *Hae*III or *Mn*II and 1X CutSmart Buffer (New England Biolabs, Ipswich, MA) for approximately 15 hours at 37 °C. BSA (0.1 mg/mL) was added to the *Mn*II reaction. Reactions were stopped by heating at 80 °C and 65 °C for *Hae*III and *Mn*II, respectively (Kim et al., 2012). Samples were precipitated by addition of 20 μ g glycogen, 2 μ L 3M sodium acetate (pH 5.2), and 50 μ L 100% ice-cold ethanol, then resuspended in LoTE buffer (3mM Tris-HCl, 0.2mM EDTA, pH 7.5). Fragment size analysis was conducted at Delaware Biotechnology Institute (Newark, DE) on an Applied Biosystems 3130xl Genetic Analyzer (Foster City, CA). Fragment data were analyzed using the PeakScanner 2 software (Thermo Fisher Scientific), which constructed electropherograms for visual analysis and fragment

binning. Samples were binned by DNA fragment size, and data were collected for size, peak height, peak area, detected fluorophore, and peaks per sample. T-RFLP Analysis Expedited (T-REX; Culman et al., 2009) was used to analyze T-RFs present in samples and construct labeled data matrices for subsequent analyses. T-RF abundance bins were used as OTU proxies for taxonomic assignment and imported into PRIMER7 (PRIMER-E, Auckland, New Zealand) (Clarke and Gorley, 2015). Bins were manually inspected for stutter peaks and other anomalies prior to multivariate statistical analysis.

2.3.10 Statistical Analyses

Statistical comparisons were performed using ANOVA testing in R (<https://www.r-project.org/>) for relative *in vivo* fluorescence, growth rate, nutrient, DOC, and qPCR data. If data were found to be significantly different ($p \leq 0.05$) then the ANOVA was followed by a Tukey Honest Significant Difference test (Tukey HSD). All tests used a standard alpha value of 0.05, and all experiments were conducted with comparable sample sizes ($n = 3$ or 4). Correlation testing was performed using Spearman rank correlations to nullify the need for bivariate normality in the data.

T-RFLP data were imported into PRIMER7, standardized, and square-root transformed to down-weight exceptionally disparate variables. Resemblance matrices based on Bray-Curtis similarity were constructed for biological data and used to construct multidimensional scaling (MDS) ordinations for data visualization. One-way and two-way analysis of similarity (ANOSIM) testing was used in place of analysis of variance (ANOVA) testing for variance in biological data due to the data being both non-normally distributed and exhibiting heteroscedasticity. The null hypotheses tested

via ANOSIM were that (1) time had no significant effect on the resemblance matrix, (2) treatment had no significant effect on the resemblance matrix, and (3) there was no significant cross-effect of time and treatment on the resemblance matrix. Significance in all tests was dictated by a P value < 0.05 . Pielou's species evenness and the Shannon-Wiener diversity index were used to assess ecological stability (Schmitz and Nagel, 1995 and references within).

2.4 Results

2.4.1 Establishing IRI-160AA EC50 Concentrations

Two separate batches of IRI-160AA were used in the repeated dosing experiments, one for each experiment, due to volumetric constraints. A batch designated "03-01" was used for the June 2017 repeated dosing experiment. Volume constraints necessitated that the June 2017 experiment be conducted with addition of the algicide at 5% and 1% addition. An alternative batch designated "4-5-6 Combined" was used in the August 2017 experiment. Batch 4-5-6 Combined achieved EC50 at 1% addition, which had a measured NH_4^+ concentration of 65.66 μM .

2.4.2 Repeated Dosing

2.4.2.1 June 28, 2017 Experiment

DOC analysis revealed a dose-dependent response in which the DOC levels increased significantly in the 5% algicide treatment (Table 2.3). DOC values measured at T_{final} in the 5% algicide treatment were 1.86-fold greater than those of the 1% algicide treatment and 2.41-fold greater than those of the control. Within the T_{final} timepoint, NO_x concentrations were significantly higher in the 1% algicide treatment

when compared to both the 5% algicide treatment (1.25-fold, $p < 0.005$) and the control (1.32-fold, $p < 0.001$, Table 2.3). The NO_x concentrations of the 5% algicide treatment and control did not significantly differ from one another. Ammonium concentrations were significantly higher in the 5% algicide treatment when compared to both the 1% algicide treatment (1.9-fold, $p < 0.001$) and the control (3.0-fold, $p < 0.001$). The ammonium concentrations in the 1% algicide treatment were also significantly higher than the control (1.6-fold, $p < 0.05$). Phosphate concentrations were significantly lower in the 5% algicide treatment when compared to both the 1% algicide treatment (3.0-fold, $p < 0.01$) and the control (3.4-fold, $p < 0.005$). The phosphate concentrations of the 1% algicide treatment and control did not significantly differ from one another.

The community growth rates, based on relative *in vivo* chlorophyll *a* fluorescence, were positive for all time points. Daily growth rates increased from T_1 to T_3 across all treatments, then decreased through T_{final} (Figure 2.3). Growth rates were significantly lower in the 5% algicide treatment at both T_3 ($p < 0.001$) and T_5 ($p < 0.01$) when compared to both the 1% algicide treatment and control, which did not significantly differ from one another. By T_{final} , there were no significant differences in daily growth rate among any of the treatments.

There was a significant decline in the relative abundance of dinoflagellates for both treatments and control over the course of the June 2017 experiment ($p < 0.05$). The relative dinoflagellate abundance at T_3 of both the control and 1% algicide treatment were not significantly different, yet both were approximately 200-fold greater than the relative abundance of dinoflagellates in the 5% algicide treatment ($p < 0.001$, Figure 2.3). Significant differences among all three treatments were first

observed at T_5 , at which point the relative abundance in the 1% algicide treatment was 3.5-fold greater than that of the 5% algicide treatment, but 7.2-fold less than that of the control. By T_{final} , the relative abundance of dinoflagellates in the 1% algicide treatment was 4.3-fold greater than that of the 5% algicide treatment and 3.0-fold less than that of the control. August 11, 2017 Experiment

2.4.2.2 August 11, 2017

There was a significant decrease in DOC independent of treatment between T_0 and all four T_{final} treatments ($p < 0.05$), but there were no significant differences among the four T_{final} treatments alone. On average, the DOC of the initial bulk sample with $f/2 + 0.5\%$ CAA was 2.6-fold greater than that of any T_{final} treatment (Table 2.3). NO_x concentrations were significantly less across all treatments at T_{final} when compared to the initial sample ($p < 0.05$), although none of the T_{final} treatments differed significantly from one another. Ammonium levels were significantly higher in the EC95 (15.7-fold, $p < 0.001$) and EC50 (13.2-fold, $p < 0.01$) treatments at T_{final} when compared to the initial sample, but insignificant when the initial samples was compared to EC05 and the control. The ammonium concentrations of the EC95 and EC50 treatments at T_{final} did not significantly differ from one another, nor was there any significant difference between the EC05 treatment and control ($p < 0.01$) (Table 2.3). The ammonium concentration of EC95 and EC50 treatments were significantly higher than the EC05 treatment and control ($p < 0.01$).

Daily growth rates across treatments were positive for all time points. Growth rates increased uniformly across treatments from T_1 to T_2 , remained steady for 24 hours, then decreased uniformly across treatments through T_{final} (Figure 2.3). Growth rates measured across all treatments were not significantly different at any timepoint

except between the EC95 and EC05 treatments at T_2 , at which point EC95 had a growth rate 11.9% greater than that of EC05 ($p < 0.05$) but did not significantly differ from either the EC50 treatment or control.

There were significant differences in relative dinoflagellate abundance with increasing algicide concentration of the treatments (Figure 2.3). In contrast to the June 2017 experiment, the relative abundance of dinoflagellates increased in control and the EC05 treatment over the course of the experiment. After 24 hours (T_1), the relative abundances of dinoflagellates in both the EC05 treatment and control were significantly higher than either the EC95 or EC50 treatments by 1.7-fold ($p < 0.05$). By T_{final} , the relative abundances of dinoflagellates within the EC95 and EC50 treatments did not significantly differ from one another but were significantly lower than both the EC05 treatment (11.2-fold, $p < 0.001$) and the control (29.2-fold, $p < 0.001$). The relative dinoflagellate abundances of the EC95 and EC50 treatments were significantly lower than the relative abundance at T_0 (4.0-fold, $p < 0.001$). Notably, the relative abundance of dinoflagellates of the control treatment was 2.6-fold greater ($p < 0.001$) than that of the EC05 treatment at T_{final} .

2.4.3 Community Composition Analysis

2.4.3.1 June 28, 2017

Relative changes in community composition were evaluated using the multivariate statistical package PRIMER-E. Fragment data were used to construct a Bray-Curtis similarity matrix and assigned Bray-Curtis distances were compared against T_0 for each timepoint as each treatment within each timepoint was significantly different from the bulk sample (Table 2.4). Sample interrelatedness was

visualized using a non-metric multidimensional scaling (nMDS) ordination constructed based on the Bray-Curtis similarity matrix derived from the DNA fragment data (Figure 2.4). One-way ANOSIM testing of the DNA fragment data from the June 2017 experiment revealed that time and treatment both had significant effects on the eukaryotic microbial community composition ($p < 0.001$ and $p < 0.05$, respectively). Time and treatment also exhibited a significant cross-effect on the resemblance matrix ($p < 0.001$). These data reject all three tested null hypotheses, exhibiting strong relationships between time and treatment as they affect the microbial community.

2.4.3.2 August 11, 2017

Fragment data were used to construct a Bray-Curtis similarity matrix as described above (Section 2.4.3.2) and each Bray-Curtis distance for each treatment at each timepoint was significantly different from the initial community at T_0 (Table 2.4). The interrelatedness of the biological community within the T_0 and T_{final} samples based on T-RFLP fragment data from the August 2017 experiment, was visualized using an nMDS ordination (Figure 2.5). One-way ANOSIM testing of the DNA fragment data revealed that both time and treatment had significant effects on the eukaryotic microbial community composition when comparing the bulk sample, or T_0 , to the samples taken at T_{final} ($p < 0.05$). Pertaining to treatment, each of the three treatment levels and the control differed significantly from the bulk sample ($p < 0.05$). Within the treatments at T_{final} , ANOSIM revealed that the only significant differences were between the EC95 treatment and control, as well as between the EC50 treatment and control ($p < 0.05$). A two-way crossed ANOSIM test performed on all collected time points confirmed that there were significant differences caused by cross-effects

among all treatments ($p < 0.05$), with the exception of the EC95-EC50 relationship. All three tested null hypotheses are thereby rejected by these data, suggesting that both time and treatment had independent and dependent effects on the composition of the microbial community.

2.4.3.2.1 Community Sequencing

Sequencing of the V4 region of the 18S rRNA gene revealed 3,450 independent operational taxonomic units, or OTUs, present within the five samples (one initial timepoint and one from composite samples from the final timepoint of the EC95, EC50, and EC05 treatments, and control) submitted from the August 11, 2017 experiment (Table 2.5). These OTUs, binned at 97% similarity, comprised 299 genera in 80 distinct classes. Substantially-contributing groups in the initial bulk sample (those contributing $\geq 1\%$ of detections) included dinoflagellates (class Dinophyceae, 64.1%), cryptophytes (Cryptophyta, 15.5%), ciliates (seven classes, 10.7%), raphidophytes (Raphidophyceae, 3.7%), and diatoms (three classes, 2.4%). Dinoflagellates (class Dinophyceae) exhibited a negative, dose-dependent response when compared to the relative abundance in the initial sample. At the final timepoint, Dinophyceae OTU relative abundance within the community fell by 89.4% in EC95, 85.0% in EC50, 13.4% in EC05, and rose by 7.1% in the control treatment (Figure 2.6). Cryptophytes increased in relative OTU abundance in the EC95, EC50, and EC05 treatments (69.6%, 103.9%, 36.3%, respectively), but remained relatively unchanged in the control treatment (1.8% increase) compared to the initial sample. Ciliates had class-dependent responses such as a decrease in the relative OTU abundance of classes Colpodea and Litostomatea (99.1-99.8% and 77.3-89.5%, respectively), as well as a large increase in relative OTU abundance of class

Oligohymenophorea (755.1-981.1%). Raphidophyte relative abundance of OTUs decreased across all treatments to varying degrees (45.9-93.3%). All three classes of diatoms detected increased across all treatments, seemingly independent of algicide concentration. These included classes Bacillariophyceae (317.2-400.9%), Coscinodiscophyceae (390.0-1020.0%), and Mediophyceae (358.8-1058.5%).

Dinoflagellate relative OTU abundances at T_0 were dominated by an OTU most similar to *Azadinium obesum*, a non-toxic thecate dinoflagellate accounting for 42% of the OTUs detected (Figure 2.7). OTUs for 31 other dinoflagellate genera were detected at T_0 . Dinoflagellate populations differed greatly at T_{final} among the four treatments. Within EC95, EC50, EC05, and in the control, dinoflagellate relative OTU abundances comprised 8%, 11%, 42%, and 51% of the library, respectively. In the EC95 treatment, the two dinoflagellate OTUs with the highest relative abundance were most similar to sequences from *A. obesum* and *Duboscquodinium collinii*, accounting for a combined 40% of the dinoflagellate OTUs present (Figure 2.8). In the EC50 treatment, sequences related to *A. obesum* and *D. collinii* were again dominant (30% of dinoflagellate OTUs), but sequences related to an unidentified species of the genus *Gyrodinium* as well as *G. helveticum* also contributed a combined 34% of species OTUs (Figure 2.9). In both the EC05 treatment and control, dinoflagellate relative OTU abundances were dominated by sequences related to an unidentified species of *Gyrodinium* accounting for 62% and 57%, respectively (Figure 2.10, Figure 2.11).

Pielou's species evenness and the Shannon-Wiener diversity index were calculated for T_0 and for each of the treatments at T_{final} based on the 18S rRNA gene sequencing results (Schmitz and Nagel, 1995 and references within). In spite of the

changes in species composition, both parameters remained relatively constant between T_0 and T_{final} , as well as among T_{final} treatments. Species evenness varied from 0.839 to 0.856, while the diversity indices ranged from 6.175 to 6.535 (Table 2.5).

2.5 Discussion

In this study I examined the effects of repeated dosing with a dinoflagellate-specific algicide, IRI-160AA, on eukaryotic microbial community composition using a combination of terminal restriction fragment length polymorphism (T-RFLP) analysis and community sequencing of the V4 region of the 18S rRNA gene. This suite of methods was chosen to better understand the effects on natural communities after introduction of the algicide as a proactive or reactive HAB measure. T-RFLP analysis was developed as a rapid method of analyzing microbial community diversity in both eukaryotes and prokaryotes and has been used in many studies (Liu et al., 1997; Osborn et al., 2000; Lord et al., 2002; Casamayor et al., 2002; Duran et al., 2015; Lindstrom et al., 2018). Additionally, ribosomal RNA sequences are commonly used for accurate differentiation of species due to their unique mixture of conserved and variable regions (Diaz et al., 2010). Further, community shifts were evaluated using growth rates based on relative chlorophyll *a* fluorescence, as well as dinoflagellate-specific quantitative polymerase chain reactions (qPCR). This combination of techniques provided insight into both the changes within the overall photosynthetic community as well as within the target microalgal class of dinoflagellates.

Dissolved NO_3^- and PO_4^{3-} were added to all treatments and controls at the same *f/2* concentrations to eliminate nutrient limitations within microcosms. However ammonium concentrations were expected to differ based on the amount of IRI-160AA added. Of the three nutrient analytes, the concentrations of ammonium increased with

increasing algicide concentrations due to algicide input independent of experiment while still predominantly remaining at sub-toxic levels based on a literature review conducted by Collos and Harrison (2014). NO_x and PO_4^{3-} concentration trends differed strongly between the June 2017 and August 2017 experiments even though they were amended with the same initial concentrations. Algal groups have been shown to exhibit preferential uptake of nitrogen source on a class-by-class basis (Cochlan et al., 2008; Yamada et al., 2009), which could potentially explain the difference in results between the two experiments. Regarding PO_4^{3-} , because the growth rates of phototrophs were not significantly different at T_{final} , we can infer that microalgal groups growing in the stead of the decreasing dinoflagellate population may have utilized more PO_4^{3-} on a cell-by-cell basis compared to their dinoflagellate counterparts in the June experiment as has been shown in past studies (Azad and Borchardt, 1970). PO_4^{3-} limitation across treatments and controls in the August experiment may have obscured a similar trend. Overall, dissolved nutrient concentrations of NH_4^+ were in step with the amount of algicide added while NO_x and PO_4^{3-} concentrations appeared to be much more dependent on the experiments' respective communities.

Dissolved organic carbon (DOC) levels were analyzed in both the June 2017 and August 2017 experiments. DOC in the June experiment at T_{final} increased with algicide concentrations (Table 2.4) which differs from the August 2017 experiment where DOC concentrations were not significantly different between treatments and control at T_{final} . While initial assumptions may be that increased algicide levels leads to increased cell lysis which leads to higher DOC concentrations, these results indicate that community structure strongly influences the DOC available in the system. It is

possible that the community dynamics between dinoflagellates and heterotrophic predators account for the variations in microcosm DOC (Saba et al., 2009). Autochthonous DOC is derived primarily from phytoplankton, but microzooplankton grazing increases the accessibility of DOC through violent feeding mechanisms, excretion, egestion, and fecal pellet leaching (Moller, 2007). A study by Strom et al. (1997) highlighted the importance of algae-consuming grazers in DOC production by demonstrating that grazers release 16-37% of an algal cell's total carbon content as DOC, while typical exudation from algal cells releases 3-7%. Because microzooplankton grazers were not excluded from these microcosms, this variability in DOC production and utilization likely contributes to the results shown here. DOC in aquatic ecosystems is especially important in microalgal communities given many autotrophic species' ability to assimilate DOC as an auxiliary energy source (Richardson and Fogg, 1982 and references within). Studies have also demonstrated the importance of DOC in heterotrophs such as invertebrate larvae when supplementary energy sources are integral before the development of raptorial feeding mechanisms (Manahan and Crisp, 1982 and references within). With the exception of the 5% addition treatment in the June experiment, application of the algicide does not appear to significantly affect DOC concentrations compared to the controls.

The bulk community response in both experiments, as measured by *in vivo* chlorophyll fluorescence, illustrates that there was no difference in photosynthetic biomass at T_{final} even after repeatedly dosing with IRI-160AA. For microzooplankton and other grazers, this finding points toward a retention of overall prey abundance with potential implications for renewed diversity, which is integral to the structural integrity of the community (Yang et al., 2018). qPCR analysis revealed dose-

dependent decreases in relative dinoflagellate abundance, which is in contrast with the lack of significant differences in the bulk community response. The microcosms employed here indicate that microalgal communities are capable of maintaining certain levels of photosynthetic biomass across treatment concentrations of a dinoflagellate-specific algicide. These data are not only consistent with the earlier findings of Hare et al. (2005) and Tilney et al. (2014b) in which they observed stimulated growth in non-dinoflagellate microalgal species comprising a diatom, cryptophyte, raphidophyte, and prasinophyte, but also demonstrate that such effects are not limited to single-dose application of IRI-160AA. This study shows that repeated dosing of communities with IRI-160AA will cause decreases in bloom-prone dinoflagellate species without negatively impacting the greater microalgal community.

The results of the community sequencing support the findings of the photosynthetic community response in that several non-dinoflagellate groups exhibited increases in proportion of the 18S library, such as diatoms and cryptophytes. Additionally, an increase in relative abundance was observed for one class of ciliates (Oligohymenophorea), however it is unlikely that these ciliates contributed to relative *in vivo* fluorescence data and the growth rates derived thereafter. It should also be noted that of the two classes of ciliates that exhibited decreases in relative abundance, one includes anaerobic endosymbionts of larger species (Litostomatea), while the other (Colpodea) is more commonly found terrestrially than in the marine environment (Vd'acny et al., 2010; Bourland et al., 2014). As predicted, dinoflagellate relative OTU abundance decreased in an algicide dose-dependent manner. The simplest explanation for the increase in non-dinoflagellate relative abundance is the increase of available nitrogen from the *f/2* control and algicide treatment that is no longer being

drawn down by dinoflagellates combined with decreases in dinoflagellate relative abundance. Perhaps most interesting in the lens of algicide-based growth stimulation is the fact that cryptophytes exhibited a large increase in proportion of the 18S library in all algicidal treatments yet not in the control, as observed in the August 11, 2017 experiment. Horner-Rosser and Thompson (2001) observed active cryptophyte migration based on nitrogen availability, underlining its importance, and showed that NH_4^+ was preferentially utilized over NO_3^- by the cryptophytes. Therefore, the increases in cryptophyte relative OTU abundance in all treatments may be due to a class affinity for the NH_4^+ present within the algicide.

The T-RFLP analysis of eukaryotic community structure illustrated the relative shifts in microbial community composition over the course of repeated algicide application. By T_{final} in both experiments, there were significant differences in treatments and controls respective to each experiment based on ANOSIM. The greatest concentration of algicide in each experiment (5% addition and EC95, respectively) resulted in community composition that was significantly different from the communities of all other treatments and controls. Additionally, the EC50 treatment in the August 2017 experiment exhibited a composition that significantly differed from all other treatments and the control. In the context of the qPCR data, the decrease in relative abundance of dinoflagellates is strongly linked to the microbial community structure (Zhou et al., 2018).

Dinoflagellate sequencing results, beyond the overarching trend of decreased OTU abundance, provided insight into species-specific responses. It is important to note that all mentions of species in the context of these sequencing results are actually representative of OTUs yielding 97% similarity with documented genomes of those

species. OTU abundance is different than cellular abundance in that the 18S rRNA gene copies may vary by multiple orders of magnitude among species. As such, comparisons can only be made on relative abundances to assess how proportions change over time and treatment, and not in absolute abundance of cells.

A consistent shift was observed regarding the dominant dinoflagellate in the sequence library within each sample as algicide concentrations decreased. At T₀, the OTU that shared 97% similarity with *A. obesum* accounted for 42% of the dinoflagellate OTUs detected. *A. obesum* is a small (13-18 μm), thecate dinoflagellate that was originally isolated from the North Sea along the coast of Scotland by Tillmann et al. (2010), however there has been no documentation of *A. obesum* outside of this geographic range. *A. obesum* was initially characterized by Tillmann et al. (2010) using a suite of methods, including sequencing of the 18S rRNA gene, 28S rRNA gene, ITS region, and the cytochrome c oxidase subunit 1 (COI) gene. The results of the 18S sequencing showed that *A. obesum* and a sister species, *A. spinosum*, differed only by four bases. Sequence alignment also revealed that this OTU is 98% similar to both *A. obesum* as well as *A. spinosum*. Because *A. spinosum* has been documented as having a geographic distribution extending to the western Atlantic Ocean (Akselman et al., 2012; Akselman et al., 2014), it is more likely that the OTU attributed here to *A. obesum* is actually that of *A. spinosum*. Even so, this is the first report of this particular species in the northwest Atlantic Ocean. *A. spinosum* is a thecate dinoflagellate similar in size to *A. obesum*, and *A. spinosum* is also the largest known producer of lipophilic marine biotoxins called azaspiracids (Tillmann et al., 2009; Salas et al., 2011; Toebe et al., 2013). Azaspiracids are a relatively novel group of marine biotoxins but they have been shown to cause illness in humans similar to

those of diarrhetic shellfish poisoning (Twiner et al., 2008). As such, demonstrating the efficacy of IRI-160AA against a potent, novel toxin-producer further supports the potential importance of this algicide in maintaining both community and human health.

Because the 18S sequencing results do attribute this OTU to *A. obesum*, that notation will continue throughout this paper in spite of the evidence discussed above. The relative abundance of *A. obesum* decreased in all treatments and control at T_{final} while *Gyrodinium* spp. increased in relative abundance in T_{final} compared to T_0 . *Gyrodinium*, unlike *Azadinium*, is a genus comprised of larger, mixotrophic, athecate dinoflagellates (Li et al., 1999; Li et al., 2000). With the increase in heterotrophic grazers and small diatoms and cryptophytes in algicide-treated samples, it is possible that *Gyrodinium* spp. were able to employ both their mixotrophic feeding strategies and size in order to prey on smaller organisms and avoid grazing predation themselves, respectively. In spite of the overall decrease in relative abundance of OTUs related to *Azadinium* in T_{final} samples, the proportion of this OTU within the dinoflagellate community alone increased with increasing algicide concentration. Tilney et al. (2014a) provides one potential explanation for this trend in that thecate dinoflagellates were found to be less susceptible to the algicide compared to athecate dinoflagellates. This would explain an increased proportion of *A. obesum* OTUs within the dinoflagellate community as IRI-160AA concentrations increased, while the relative abundance of athecate dinoflagellates such as *Gyrodinium* spp. decreased with increasing algicide concentration at T_{final} . Other thecate dinoflagellates, such as *Scrippsiella trochoidea* and *Duboscquodinium collinii*, also had increased proportions further supporting this explanation (Janofske, 2000; Coats et al., 2010).

This study provides information about changes to the microbial eukaryotic community after repeated dosing with the algicide IRI-160AA. Consistent with results of single-application microcosm experiments (Tilney et al., 2014b), results here show that some microalgal groups like diatoms and cryptophytes, as well as ciliate grazers, dominate the microbial eukaryotic community upon the removal of dominant dinoflagellates even in cases of prolonged, repeated dosing of various concentrations. Results also indicate that repeated application of IRI-160AA at EC50 levels would be an effective course of action to mitigate blooms of dinoflagellates with minimal impact on the rest of the community. Based on parameters analyzed here, repeated dosing of EC50 concentrations of the algicide significantly reduced the dinoflagellate community while having no significant detrimental effect on relative *in vivo* fluorescence, dissolved nutrients, or certain microalgal classes compared to controls. Future work may investigate the effects on microbial communities at a wider range of sub-EC50 concentrations to maximize efficacy while minimizing application volume. Additionally, work on this project should aim to analyze the effects of repeated algicide exposure on other relevant metazoan species. Investigating the effects of repeated dosing creates a more robust body of research that will more clearly indicate whether IRI-160AA could be a viable form of HAB dinoflagellate control and mitigation in the Delaware Inland Bays.

Table 2.1 Environmental metadata and experimental specifications associated with the repeated dosing experiments conducted on June 28, 2017 and August 11, 2017.

Experiment Date	June 28, 2017			August 11, 2017			
Study Length (Days Dosed)	7 days (0, 2, 3, 4, 5, 6)			5 days (0, 1, 2, 3, 4)			
Sampling Location	RB34 Rehoboth Beach, DE			IR32 Bethany Beach, DE			
Latitude	38° 42' 10'' N			38° 41' 56'' N			
Longitude	75° 09' 39'' W			75° 06' 44'' W			
Temperature (°C)	24.88			26.11			
Salinity (PSU)	9.72			23.05			
Dominant Dinoflagellate	<i>Karlodinium veneficum</i>			<i>Azadinium obesum</i>			
Algicide Batch	Batch 03-01			Batch 4-5-6 Combined			
Algicide Concentrations	5%	1%	Control	EC95	EC50	EC05	Control
[NH ₄ ⁺] in μM	176.5	35.3	0	124.7	65.66	6.57	0

Table 2.2 Sequences of primers and probes utilized in polymerase chain reactions as well as quantitative polymerase chain reactions. F denotes forward primer; R denotes reverse primer.

Primer or Probe	Sequence (5'-3')	Target	Reference
Euk1A	HEX/CTGGTTGATCCTGCCAG	Eukarya 18S rRNA	Sogin and Gunderson, 1987
Euk517R	FAM/CACCAGACTTGCCCTC	Eukarya 18S rRNA	Coyne et al., 2005
Dino06F	CCGATTGAGTGWTCCGGTGAATAA	Dinoflagellate 18S	Handy et al., 2008
EukB	GATCCWTCTGCAGGTTACCTAC	Dinoflagellate 18S	Handy et al., 2008
M13F	CCCAGTCACGACGTTGT	pGEM plasmid DNA	Coyne et al., 2005
pGEMR	TGTGTGGAATTGTGAG	pGEM plasmid DNA	Coyne et al., 2005
pGEM probe	FAM/CACTATAGA/ZEN/ATACTCAAG/3IABkFQ	pGEM plasmid DNA	Coyne et al., 2005
EukV4F	CCAGCASCYGCGGTAATTCC	Eukarya 18S V4 region	Orsi et al., 2013
EukV4R	ACTTTCGTTCTTGATYRA	Eukarya 18S V4 region	Orsi et al., 2013

Table 2.3 Dissolved organic carbon (DOC) and nutrient concentrations corresponding to two repeated dosing experiments. All treatments not marked as “T₀” are representative of T_{final} for its respective experiment. Values are presented as averages (SD). DOC values are averages of four measurements, each being the average of 3-5 detections of the same sample. Dissolved nutrient values are averages of four measurements. Asterisk (*) denotes significant difference (p < 0.05).

	Treatment	DOC (ppm)	NO _x (μM)	NH ₄ ⁺ (μM)	PO ₄ ³⁻ (μM)
June 28, 2017	5%	5469.0* (864.5)	98.19 (8.06)	141.70** (3.61)	3.83* (0.52)
	1%	2937.3 (65.9)	121.90* (6.51)	74.83* (8.78)	11.38 (3.08)
	Control	2272.9 (384.7)	92.43 (5.67)	46.67 (16.62)	13.03 (3.75)
	Treatment	DOC (ppm)	NO _x (μM)	NH ₄ ⁺ (μM)	PO ₄ ³⁻ (μM)
August 11, 2017	T ₀	6237.0* (321.0)	253.5* (6.33)	2.71** (0.14)	26.45* (0.27)
	EC95	2348.6 (310.9)	221.8 (5.62)	42.61* (16.14)	1.49 (2.54)
	EC50	2529.1 (299.9)	224.2 (7.44)	35.83* (15.28)	Below detection
	EC05	2440.1 (134.1)	212.6 (12.48)	14.51 (9.00)	Below detection
	Control	2258.1 (352.9)	225.0 (5.27)	14.40 (7.65)	Below detection

Table 2.4 Percent community composition similarities to the T₀ community based on Bray-Curtis similarity values derived from a resemblance matrix. Values in parentheses indicate standard deviation.

	Treatment	T ₃	T ₅	T ₇
June 28, 2017	5%	37.62 (2.70)	27.75 (5.74)	15.39 (2.14)
	1%	49.63 (1.60)	14.93 (3.26)	16.66 (3.35)
	Control	55.11 (2.62)	21.72 (5.51)	15.30 (5.22)
	Treatment	T ₃	T ₅	
August 11, 2017	EC95	24.52 (2.09)	37.37 (5.24)	
	EC50	19.78 (1.34)	33.48 (7.29)	
	EC05	29.53 (1.38)	41.11 (9.62)	
	Control	33.12 (2.47)	44.64 (7.70)	

Table 2.5 Data collected from sequencing of the V4 region of the 18S rRNA gene performed on extracted DNA samples from the August 11, 2017 experiment. Pielou's species evenness (J') and Shannon-Wiener diversity index (H') were calculated in PRIMER7 (Schmitz and Nagel, 1995).

Treatment	No. OTUs	No. Sequences	J'	H'
T ₀	1798	109,518	0.86	6.45
T _{final} EC95	1482	99,850	0.84	6.18
T _{final} EC50	1565	95,540	0.84	6.25
T _{final} EC05	2185	148,136	0.85	6.58
T _{final} Control	2185	149,075	0.85	6.54

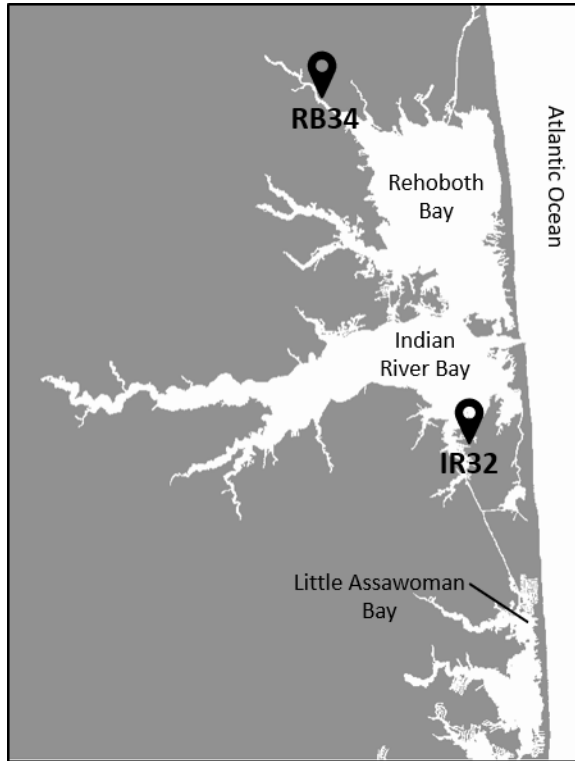


Figure 2.1 Sampling sites within the Delaware Inland Bays: Rehoboth Bay in Rehoboth Beach, DE at Love Creek (RB34) and Indian River Bay in Bethany Beach, DE at Holly Terrace Acres Canal (IR32).

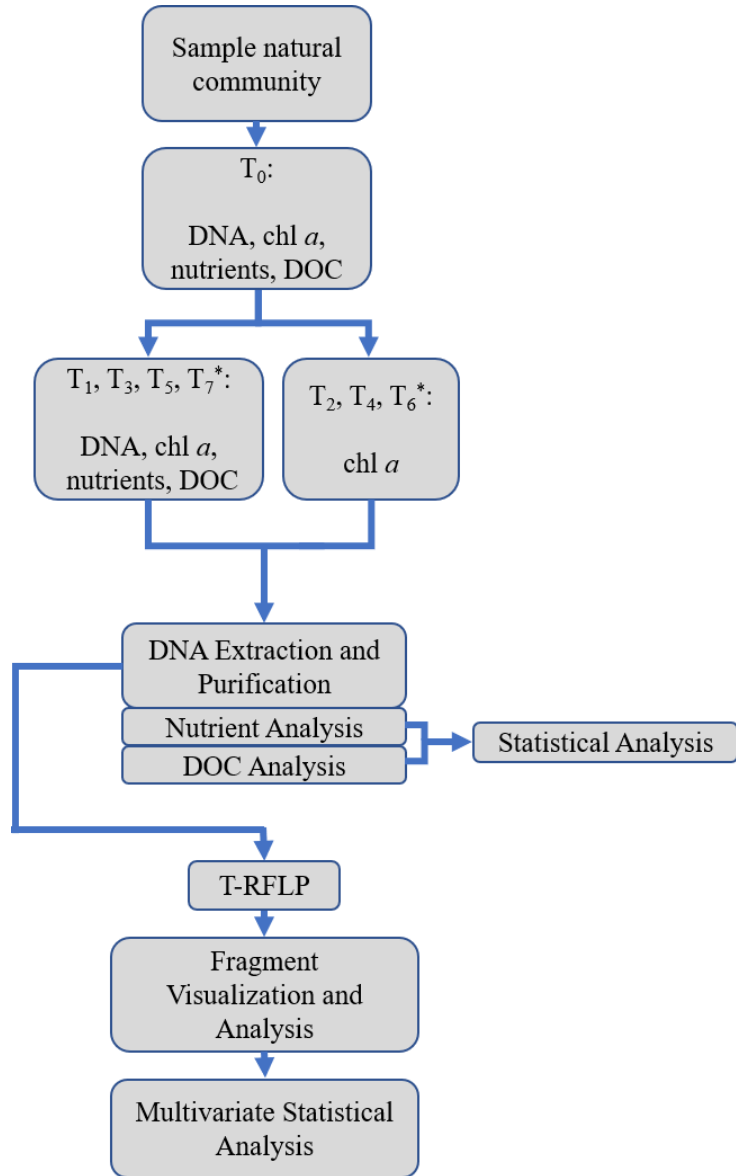


Figure 2.2 Procedural flowchart of sampling methodology for repeated dosing experiments. Asterisks (*) indicate days that were present in the June 28, 2017 experiment but not in the August 11, 2017 experiment.

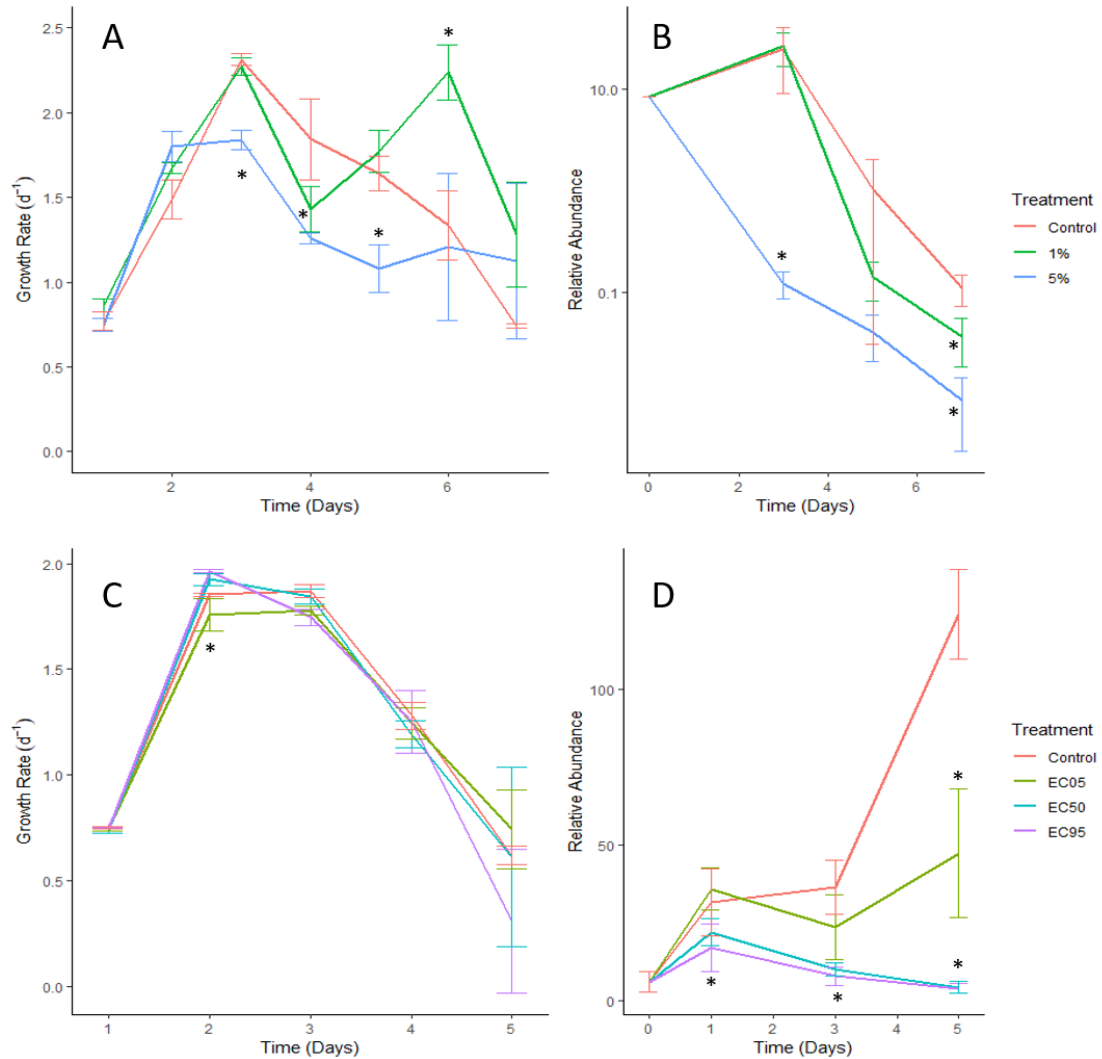


Figure 2.3 Mean daily growth rates (A and C) and relative abundance of dinoflagellates (B and D) for each of the two repeated dosing experiments (June 2017 and August 2017). All error bars represent standard deviation. *Top left*: Mean daily growth rate in the June 2017 experiment. *Top right*: Relative abundance of dinoflagellates on a logarithmic scale in the June 2017 experiment. *Bottom left*: Mean daily growth rates in the August 2017 experiment. *Bottom right*: Relative abundance of dinoflagellates in the August 2017 experiment.

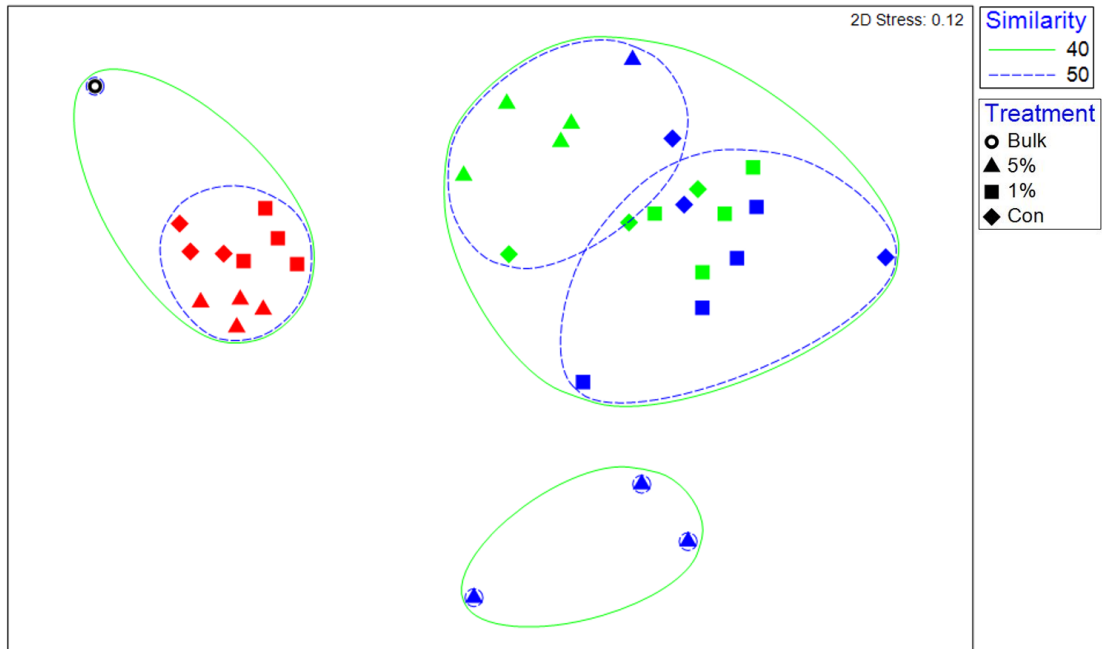


Figure 2.4 Non-metric multi-dimensional scaling (nMDS) ordination based on a Bray-Curtis similarity matrix for the microzooplankton grazing experiment sampled on June 28, 2017. Timepoints: T₀ – black; T₃ – red; T₅ – green; T₇ – blue.

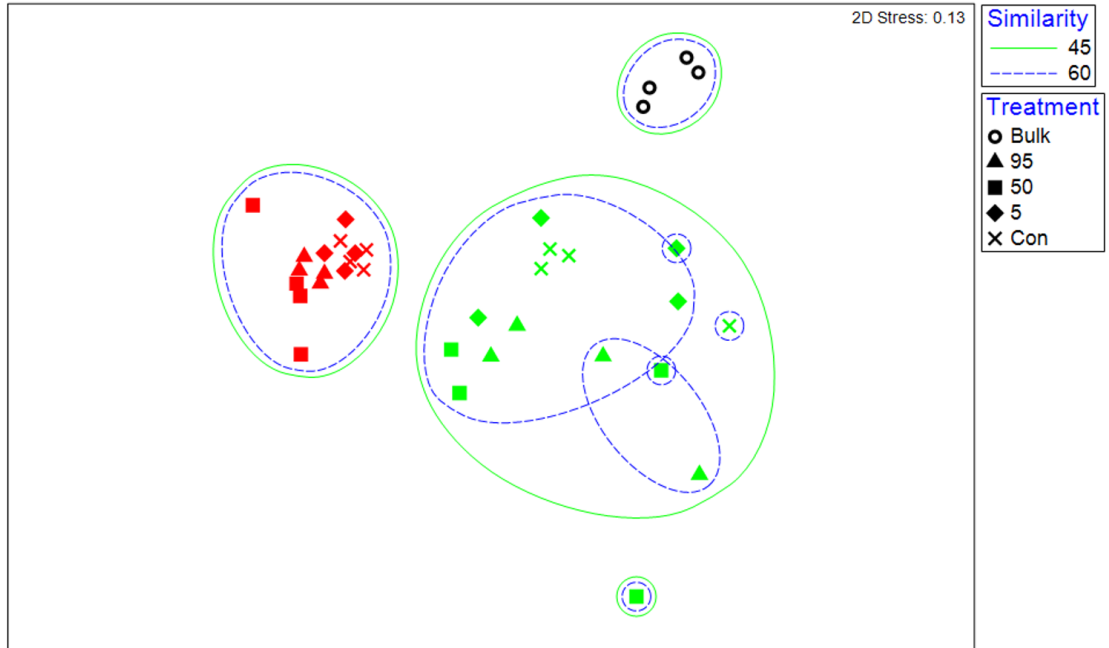


Figure 2.5 Non-metric multi-dimensional scaling (nMDS) ordination based on a Bray-Curtis dissimilarity matrix for the microzooplankton grazing experiment sampled on August 11, 2017. Timepoints: T₀ – black; T₃ – red; T₅ – green.

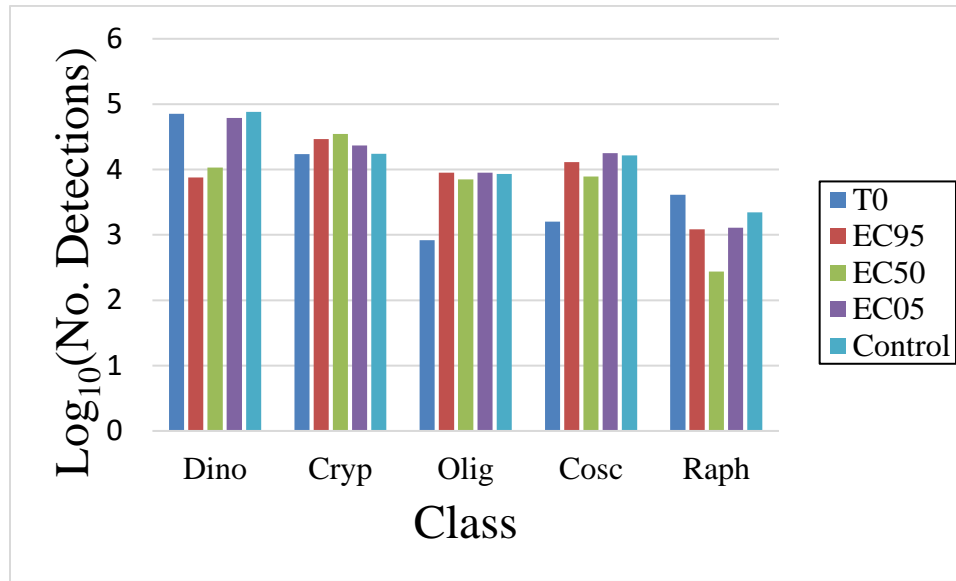


Figure 2.6 Relative abundance on a log-10 scale for prominent microbial eukaryotic classes detected through 18S rRNA sequencing in the August 11, 2017 experiment. Dino: Dinoflagellates (Dinophyceae); Cryp: Cryptophytes (Cryptophyta); Olig: Ciliates (Oligohymenophorea); Cosc: Diatoms (Coscinodiscophyceae); Raph: Raphidophytes (Raphidophyta).

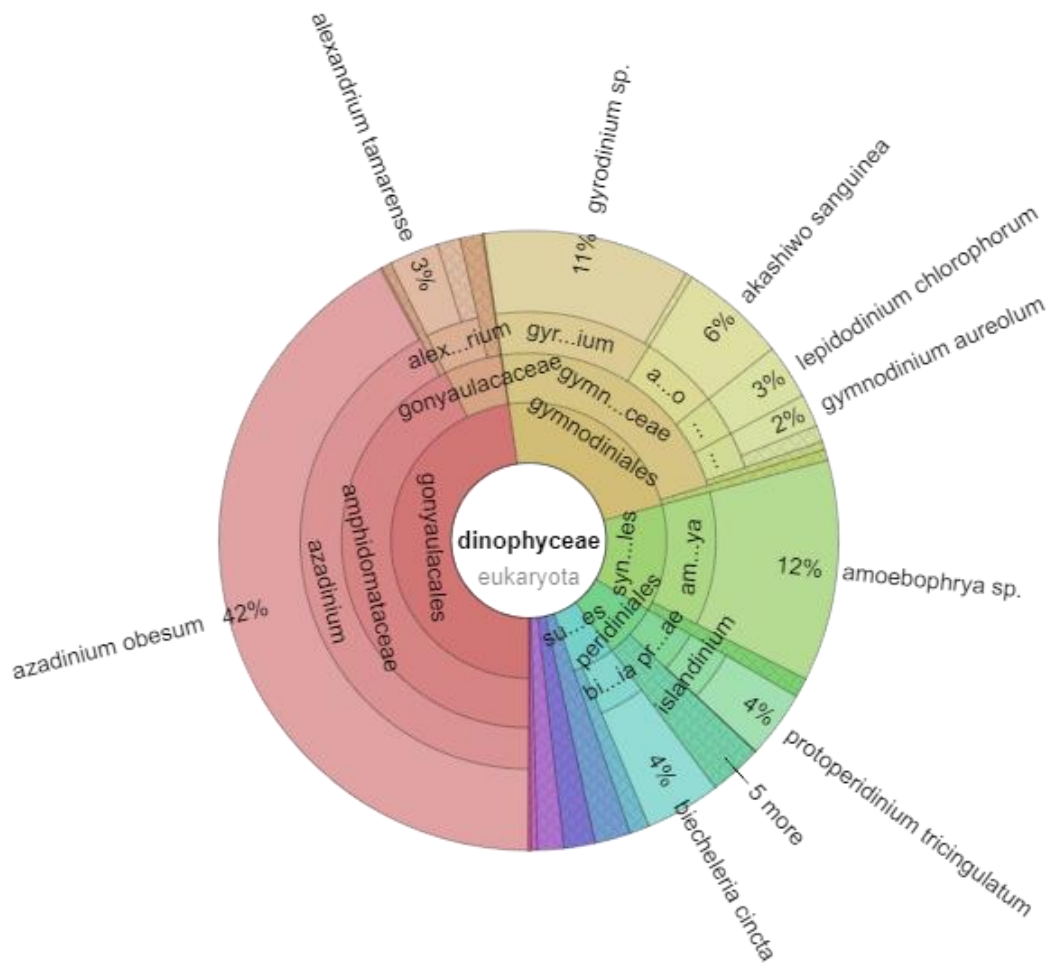


Figure 2.7 Dinoflagellate community in the August 11, 2017 repeated dosing experiment at T₀ as determined by sequencing of the V4 region of the 18S rRNA gene. Different tiers of the chart represent taxonomic groupings with the outermost ring representing species-level identification. Chart was constructed using the interactive metagenomic visualization program Krona (Ondov et al., 2011).

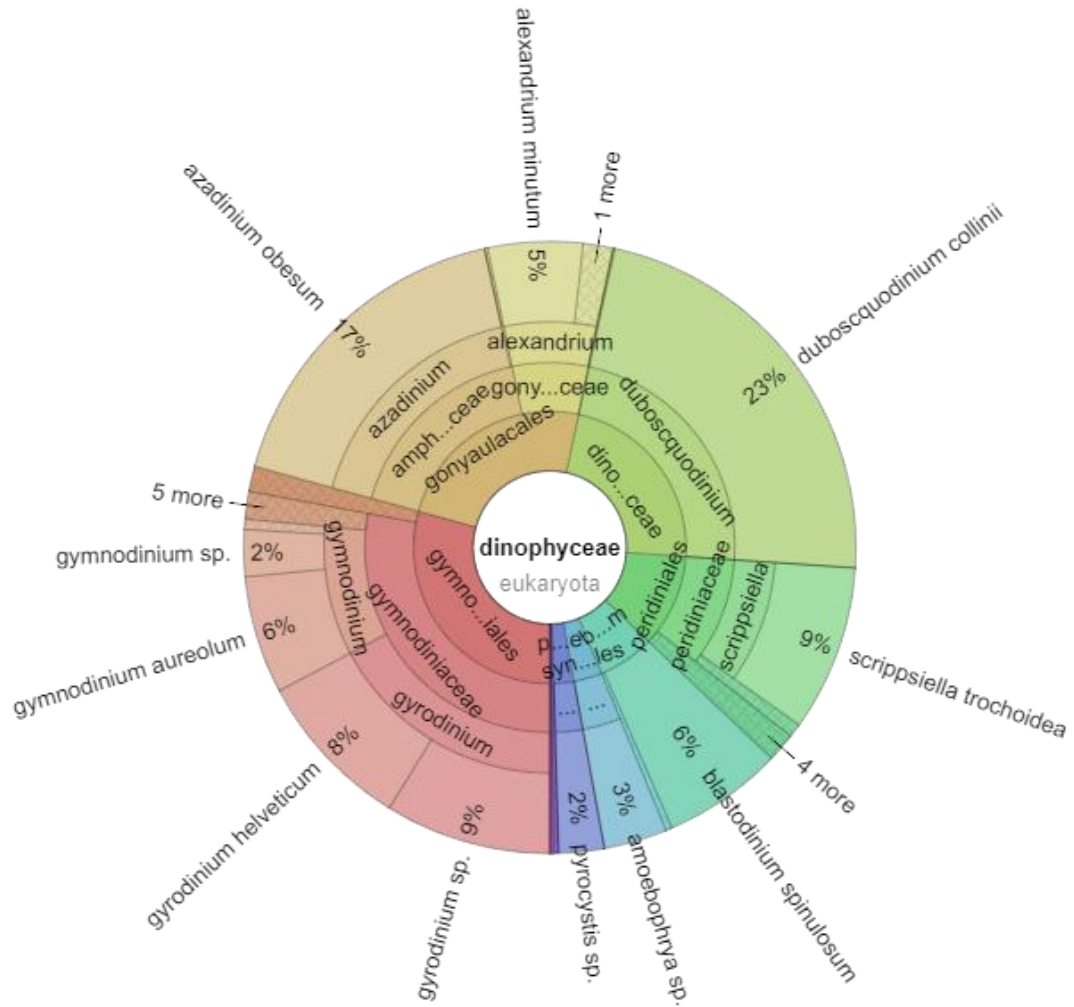


Figure 2.8 Dinoflagellate community in the August 11, 2017 repeated dosing experiment at T_{final} in the EC95 treatment as determined by sequencing of the V4 region of the 18S rRNA gene. Different tiers of the chart represent taxonomic groupings with the outermost ring representing species-level identification. Chart was constructed using the interactive metagenomic visualization program Krona (Ondov et al., 2011).

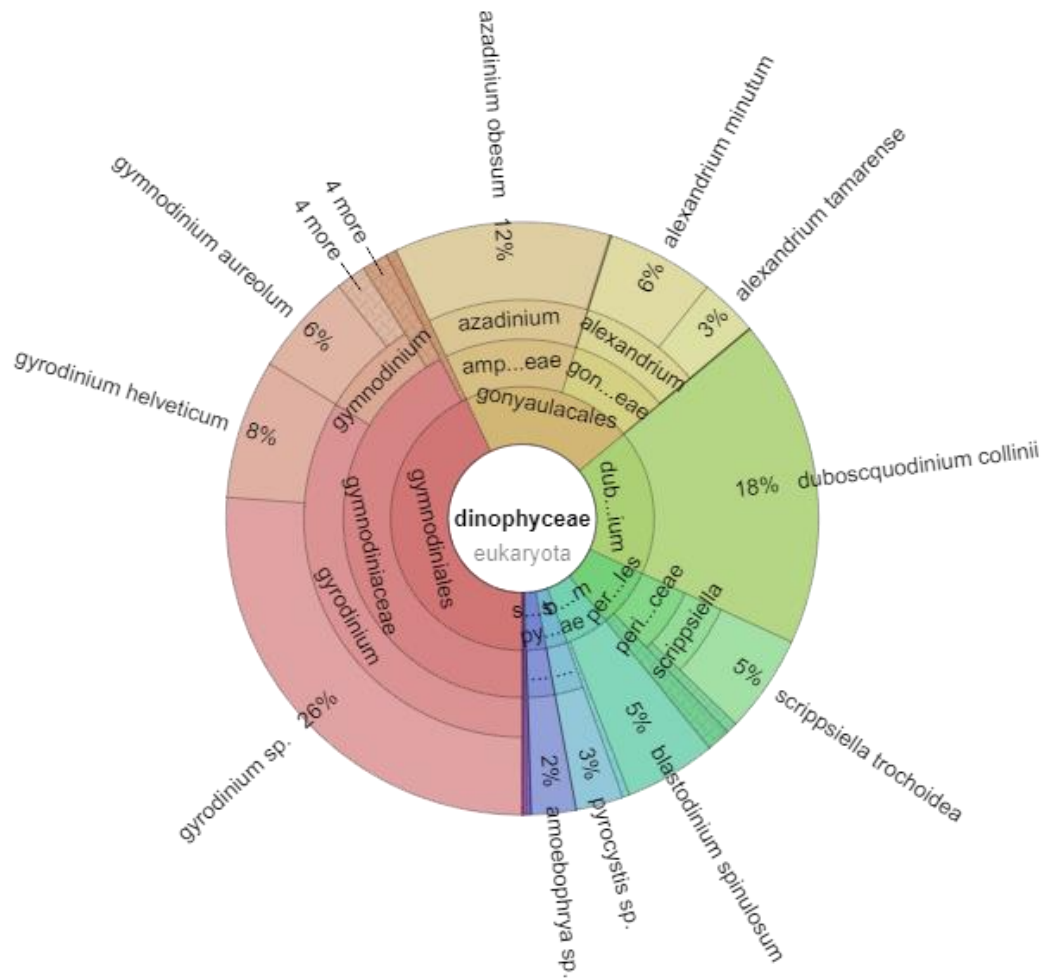


Figure 2.9 Dinoflagellate community in the August 11, 2017 repeated dosing experiment at T_{final} in the EC50 treatment as determined by sequencing of the V4 region of the 18S rRNA gene. Different tiers of the chart represent taxonomic groupings with the outermost ring representing species-level identification. Chart was constructed using the interactive metagenomic visualization program Krona (Ondov et al., 2011).

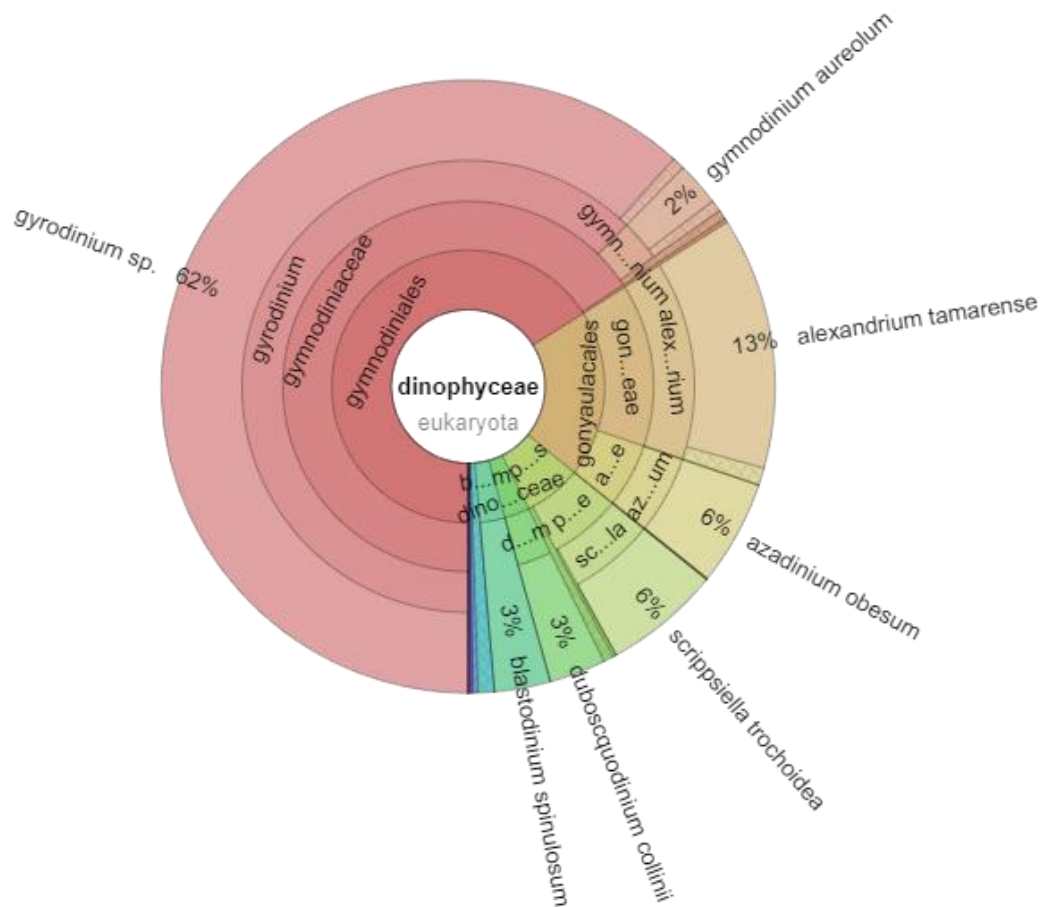


Figure 2.10 Dinoflagellate community in the August 11, 2017 repeated dosing experiment at T_{final} in the EC05 treatment as determined by sequencing of the V4 region of the 18S rRNA gene. Different tiers of the chart represent taxonomic groupings with the outermost ring representing species-level identification. Chart was constructed using the interactive metagenomic visualization program Krona (Ondov et al., 2011).

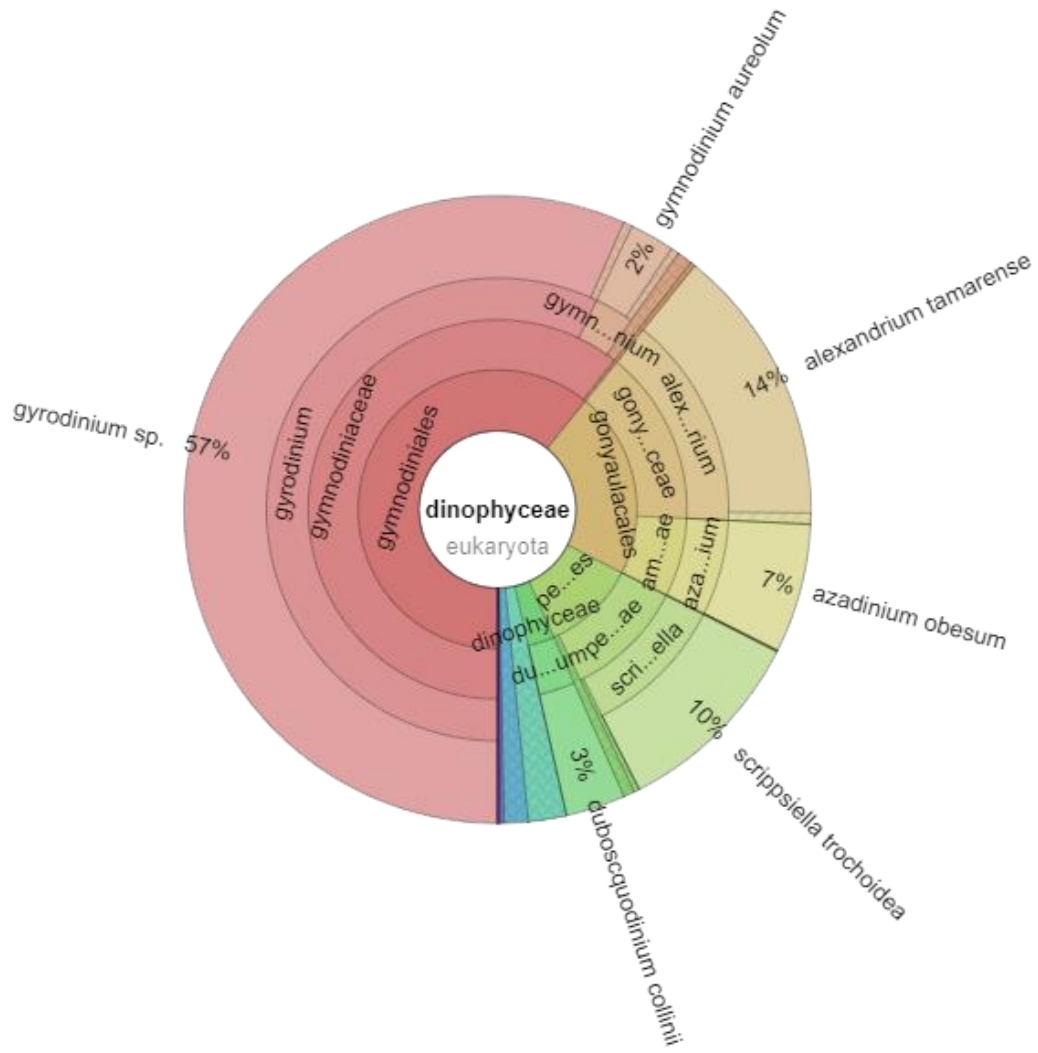


Figure 2.11 Dinoflagellate community in the August 11, 2017 repeated dosing experiment at T_{final} in the control as determined by sequencing of the V4 region of the 18S rRNA gene. Different tiers of the chart represent taxonomic groupings with the outermost ring representing species-level identification. Chart was constructed using the interactive metagenomic visualization program Krona (Ondov et al., 2011).

Chapter 3

EFFECTS OF IRI-160AA ON MICROZOOPLANKTON GRAZING

3.1 Abstract

Global increases in harmful algal blooms (HABs) have spurred interest in measures to control these blooms. Prevention, control, and mitigation of HABs are of human interest, and there are naturally-occurring compounds that may directly influence these processes. Use of these compounds appears promising, but effects to non-target organisms are also of concern. The Delaware Inland Bay (DIB; Delaware, United States) system is host to the algicidal marine bacterium *Shewanella* sp. IRI-160, which secretes a compound(s) having allelopathic effects to dinoflagellate algae. In investigating the viability of this compound(s) as a preventative or reactive HAB control measure, this study examined the effects of IRI-160AA on microzooplankton grazing. Natural microcosms were exposed to either IRI-160AA at EC50 levels or a control at four dilution factors (100%, 75%, 50%, and 25% undiluted) and incubated for 24 hours. Grazing rates were calculated via linear regression analysis of growth rate vs dilution factor. One trial demonstrated that IRI-160AA had no significant effect on grazing rate while a second trial demonstrated a significant increase in grazing rate when comparing the algicide treatment to the control. DNA fragment analysis revealed greater similarity between the initial sampled community and the algicide-treated community at T_{final} than that of the initial community and the control community. One smaller experiment was conducted comparing the effects of the algicide and an equal concentration of NH_4^+ to that of the control. This experiment yielded no significant difference in fragment-derived communities between the NH_4^+ treatment and control, but both were significantly more similar to the T_0 community

than that of the algicide treatment at T_{final} . Overall, this study suggests that shifts in microbial communities are caused by the application of IRI-160AA, however those shifts do not negatively impact the rates of microzooplankton grazers.

3.2 Introduction

Harmful algal blooms (HABs) have been expanding in frequency, duration, geographic extent, and overall impact in recent decades (Smayda et al., 1989; Hallegraeff et al., 1993; Anderson et al., 2002; Glibert et al., 2005). With environmental and economic burdens growing (Heisler et al., 2008), there has been an increased interest in the prevention, mitigation, and control of HABs. Anderson (2004) mentions three categories of preventative HAB measures: nutrient limitation, limitation of activities potentially transporting HAB species to new environments, and the proper management and modification of physical conditions. In line with this last point, chemical and biological algicides are commonly studied as potential strategies for HAB prevention, with many of these allelopathic compounds showing promise when tested on dinoflagellates (Doucette et al., 1999; Jeong et al., 2003; Li et al., 2014), raphidophytes (Kim et al., 2009), and other microalgal classes (Gleason and Baxa, 1986; Singh et al., 2001). A bacterial algicide described by Hare et al. (2005) exhibited algicidal effects on three tested dinoflagellates, but had little to no effect on non-dinoflagellate species including diatoms, prasinophytes, cryptophytes, and raphidophytes. A naturally-occurring exudate isolated from *Shewanella* sp. IRI-160, the algicide was termed “IRI-160AA” and was shown to be most effective during logarithmic-phase dinoflagellate growth (Pokrzywinski et al., 2012). These findings propelled further research into whether this compound to be added to bloom-prone or bloom-forming events in order to stymy growing HABs. To that end, understanding

the potential effects of IRI-160AA on non-target species is critical. One group of particularly important non-target organisms is microzooplankton grazers. Grazing in itself is an effective natural control mechanism for bloom-prone microalgal populations. Given the general ubiquity of these microalgae, one could assume that grazing effects would not greatly affect algal population densities; however, studies of microzooplankton grazing impacts have shown that 65-70% of standing algal biomass can be grazed in a single day (Burkill et al., 1987), although these results vary seasonally (Linacre et al., 2017). Other studies suggest these rates could be even higher, depending on multiple compounding factors (Gobler et al., 2004). These grazing rates, though, are representative of systems not experiencing bloom events. Studies have shown that grazing rates decrease during HAB events (Gobler et al., 2004), and grazers in blooms experience the harmful effects of toxic algae in these conditions due to the limitation of non-toxic prey (Graham and Strom, 2010). The effects on non-target organisms should always be of concern in toxicity studies where *in situ* compound introduction is a possibility, especially regarding keystone organisms in the target environment. Here, the potential effects of a novel algicidal compound on microzooplankton grazers is assessed via relative fluorescence measurements to estimate autotrophic growth alongside a dilution approach adapted from Landry and Hassett (1982), an approach commonly used today (Gutierrez-Rodriguez et al., 2016; Calbet and Saiz, 2017; Selph et al., 2018).

3.3 Methods

3.3.1 Preparing Bacterial Algicide IRI-160AA

Bacterial species *Shewanella sp.* IRI-160 was cultured on a plate of modified LM medium (Sambrook et al., 1989; Luria Bertani medium, 20 g/L NaCl, 10 g/L tryptone, 5 g/L yeast extract, 15 g/L agar). Plates were then incubated at room temperature for 48-72 hours. A colony was transferred into 100 mL of liquid LM medium (20 g/L NaCl, 10 g/L tryptone, 5 g/L yeast extract) and incubated with shaking at 25 °C overnight. This culture was inoculated into 1-L of f/2 medium (Guillard, 1975; Lananan et al., 2013) with 0.5% sterile casamino acids and incubated for three days before transferring into three 10L carboys of f/2 medium with 0.5% casamino acids. The cultures were incubated for 10 days with bubbling provided by air passed through a sterile 0.2 µm filter. The culture was subsequently filtered through a HemoFlow HF80S 60kDa dialysis cartridge (Fresenius Medical Care, Waltham, MA) to remove bacterial biomass. The bacteria-free filtrate (termed “IRI-160AA”) was used for experiments below.

3.3.2 Experimental Setup

Natural communities were sampled during non-bloom events where dinoflagellate populations were still prominent and visible via light microscopy on two occasions: at site SB10E on 25 July 2017 and at site RB34 on 25 September 2017. Temperature, salinity, dissolved oxygen, and pH were measured on-site using a YSI 556 MPS (Yellow Springs Instruments, Inc., Yellow Springs, OH). Water was prefiltered on site through a 100-µm mesh filter to remove macroscopic zooplankton and detritus. Eukaryotic DNA was sampled via filtration through a 3.0-µm filter, with that filter being stored and processed as described below. A subset of the prefiltered

site water was then sequentially filtered to obtain 0.2 μm -filtered seawater (“filtered”). To assess grazing rates based on microzooplankton grazers present in each sample, a dilution series was constructed. The prefiltered and 0.2 μm -filtered water was mixed in a total volume of 360mL ($n = 4$) in ratios of 1:0, 3:1, 1:1, and 1:3. NO_3^- and PO_4^{3-} concentrations consistent with *f/2* medium were added to each sample. 5 mL aliquots in duplicate from each sample were filtered over a 25-mm GFF filter for T_0 chlorophyll analysis. IRI-160AA was added to each treatment bottle ($n = 4$, four dilution factors) in order to achieve the EC50 specific to the batch of algicide used. Controls were equal volume of the nutrient medium to each control bottle ($n = 4$, four dilution factors). Experimental NH_4^+ concentrations were determined using the spectrophotometric approach described in Chapter 2, Section 2.2.2. Samples were incubated for 24 hours (25 °C, 12:12 dark:light, 140 $\mu\text{mol photons m}^{-2} \text{s}^{-1}$) with intermittent mixing to prevent settling of biotic communities. A second set of chlorophyll, DNA, size structure, and bacterial samples will be taken for T_{24} . Chlorophyll analysis was done using a 24-hour 90% acetone extraction followed by readings on a Turner fluorometer. Chlorophyll concentrations were used as a proxy for phytoplankton growth. Linear regression analyses of growth versus dilution factor were used to estimate grazing rates in each treatment (Landry and Hassett, 1982).

3.3.3 Ammonium Effects on Community Composition

A natural community was sampled during a non-bloom event where dinoflagellate populations were still prominent and visible via light microscopy at site IR32 on September 25, 2017. The sample was processed as described in Section 3.3.2 but remained as 100% sample and was not subjected to a dilution series. The algicide treatment and control were constructed as described in Section 3.3.2. A second

treatment of NH₄Cl in *f*/2 medium (n = 4, four dilution factors) was added to achieve the same concentration of NH₄Cl present in the IRI-160AA at EC50 levels. Incubation and parameter analysis were performed as described in Section 3.3.2.

3.3.4 DNA Extraction and Purification

Samples were filtered onto 3 µm Isopore™ polycarbonate filters (Millipore Sigma, Darmstadt, Germany) and DNA extracted as described in Section 2.3.5.

3.3.5 Community Fingerprinting via T-RFLP

Terminal restriction fragment length polymorphism (T-RFLP) was used to investigate changes in microbial eukaryote community composition and was performed as described in Section 2.3.9.

3.3.6 Statistical Analyses

Statistical analyses outside of PRIMER 7 were performed in R (<https://www.r-project.org/>) with a standard alpha of 0.05. Comparisons between grazing rates were conducted using Student's t-test on the slopes of linear regression lines. Student's t-test was also used to compare Bray-Curtis distances as proxies for community composition similarity. ANOVA testing was used to compare mean relative abundances within a treatment but across dilution factors. Correlation testing was performed using Spearman rank correlations to nullify the need for bivariate normality in the data. All other analyses were performed in PRIMER 7 as described in Section 2.3.10.

3.4 Results

3.4.1 Grazing Results

3.4.1.1 July 25, 2017

A prominent dinoflagellate population below bloom levels was confirmed via light microscopy. The dominant dinoflagellate was *Heterocapsa rotundata*, and the dominant grazer was the heterotrophic dinoflagellate *Oxyrrhis marina*. The experiment was conducted using a batch of algicide designated “Batch 4-5-6 Combined” which had an EC50 value of 1% addition with a corresponding NH_4^+ concentration of 65.66 μM . A control was tested directly against the algicide at EC50. After 24 hours, there was no significant difference between the two grazing rates. The grazing rate for the algicide treatment was 0.396 d^{-1} while the grazing rate calculated for the control microcosm was 0.400 d^{-1} (Figure 3.2). Apparent growth rates for the 100% undiluted samples were 1.003 d^{-1} for the algicide treatment and 0.909 d^{-1} for the control, which were not significantly different.

3.4.1.2 September 25, 2017

A prominent dinoflagellate community was confirmed via light microscopy, and the dominant dinoflagellate was identified as *Gyrodinium instriatum* and the dominant grazer was a comparably smaller ciliate. The experiment was conducted using an algicide designated as “Batch 7” which achieved EC50 at 2.5% addition with an NH_4^+ concentration of 177.75 μM . After 24 hours, the grazing rate measured for the algicide treatment (0.258 d^{-1}) was significantly greater than the rate for the control (0.027 d^{-1} , $p < 0.005$, Figure 3.3). Apparent growth rates for the 100% undiluted

samples were 0.343 d^{-1} for the algicide treatment and 0.396 d^{-1} for the control, which were not significantly different.

3.4.2 Ammonium Effects on Community Composition

Due to time elapsed between sampling and experiment initiation, the sample had low photosynthetic biomass as assessed via fluorometry. The dominant dinoflagellate was *Prorocentrum minimum* while the dominant grazer was an unidentified ciliate. A one-way ANOVA test was performed with Tukey HSD post-hoc analysis and found that the average growth rate of the control (0.532 d^{-1}) was significantly greater than either that of the algicide (0.186 d^{-1} , $p < 0.001$) or ammonium (0.258 d^{-1} , $p < 0.005$) treatments by factors of 2.9-fold and 2.1-fold, respectively, but the two treatments did not significantly differ from one another.

3.4.3 Molecular Analysis

3.4.3.1 July 25, 2017

Relative changes in community composition were evaluated using the multivariate statistical package PRIMER-E. Fragment data were used to construct a Bray-Curtis similarity matrix and assigned Bray-Curtis distances were compared against T_0 for each dilution factor (Table 3.3). Sample interrelatedness was visualized using a non-metric multidimensional scaling (nMDS) ordination constructed based on the Bray-Curtis similarity matrix derived from the DNA fragment data (Figure 3.4).

A one-way ANOSIM based on treatment found a significant difference between the algicide and control communities at T_{final} ($p = 0.038$), and both treatments' resemblance matrices significantly differed from T_0 ($p < 0.005$). A two-

way ANOSIM factoring in both treatment and dilution found a significant difference between the algicide and control treatment communities ($p < 0.001$).

3.4.3.2 September 25, 2017

Fragment data were used to construct a Bray-Curtis similarity matrix and data were analyzed as described above (Section 3.4.3.1, Table 3.3). Sample interrelatedness was visualized using a non-metric multidimensional scaling (nMDS) ordination constructed based on the Bray-Curtis similarity matrix derived from the DNA fragment data (Figure 3.5).

A one-way ANOSIM based on treatment revealed that the community composition of the control significantly differed from the composition of both the algicide treatment ($p < 0.001$) and the initial bulk community ($p < 0.001$). No significant differences were observed between the community composition in the algicide treatment and in the initial bulk sample. A two-way ANOSIM found that the resemblance matrices for the algicide treatment and control significantly differed ($p < 0.001$).

3.4.3.3 Ammonium Effects on Community Composition

Fragment data were used to construct a Bray-Curtis similarity matrix and data were analyzed as described above (Section 3.4.3.1, Table 3.3). Sample interrelatedness was visualized using an agglomerative hierarchical clustering dendrogram based on the Bray-Curtis similarity matrix derived from the DNA fragment data (Figure 3.6).

A one-way ANOSIM test was conducted on the samples at T_{final} and found that the fragment-derived resemblance matrix of the ammonium treatment significantly differed from both the algicide treatment and control ($p < 0.05$), however the algicide

treatment and control resemblance matrices did not significantly differ from one another.

3.5 Discussion

The primary goal of this work was to assess whether application of the algicide IRI-160AA had a negative effect on the grazing rate of microzooplankton in microcosm experiments. The data supported the null hypothesis that the algicide would have no significant negative effect on microzooplankton grazing in both the July 25, 2017 and September 25, 2017 experiments. Due to low photosynthetic biomass in the September 28, 2017 experiment, grazing rates were unable to be calculated. While the grazing rates within the July experiment were very nearly equal, the grazing rate calculated in the algicide treatment of the September 25, 2017 experiment was significantly greater than that of the control by a factor of 9.5 ($p < 0.005$, Figure 3.3). The dominant dinoflagellate in the July experiment was *Heterocapsa rotundata*, a small (9-14 μm), non-toxic, mixotrophic dinoflagellate that is found many places throughout the world including South Korea, India, Germany, Australia, and Chesapeake Bay (Hansen 1995; Millette et al., 2016 and references within). Additionally, the dominant grazer was a larger (20-30 μm), phagotrophic and non-photosynthetic dinoflagellate, *Oxyrrhis marina*, that has been shown to actively feed on cells equal to its own size (Droop, 1953; Hansen et al., 1996). Given that both the most prominent predator and prey in the July experiment were both dinoflagellates, it is likely that the addition of the algicide at EC50 levels caused decreases in both populations over the course of the 24-hour experiment. Grazing rates, which were derived from chlorophyll *a* measurements at their base, would have only remained equal if the growth rates within the experiments had remained

relatively equal between the two treatments. For that to hold true, it can be inferred that non-dinoflagellate phototrophs may have grown in place of *H. rotundata* and other dinoflagellates within the sample to effectively compensate for the loss of dinoflagellate chlorophyll. This is supported by prior studies that have shown diatoms, cryptophytes, raphidophytes, and prasinophytes all exhibiting increases in growth in the presence of IRI-160AA (Hare et al., 2005; Tilney et al., 2014b). The September 25, 2017 grazing experiment resulted in a significant increase in grazing rate in the algicide treatment when compared to the control, which can likely be attributed to an increase in consumable prey for the dominant ciliate grazers. *Gyrodinium instriatum* is a large-celled, mixotrophic, athecate dinoflagellate (Li et al., 1999; Li et al., 2000) that may be too large for some grazers to consume. In the presence of IRI-160AA, this trend of smaller, non-dinoflagellate species growing in their stead (such as the diatoms and cryptophytes in Section 2.4.3.2.1) may have allowed the ciliates present in the microcosm to increase their grazing rates.

The community composition, based on resemblance matrices derived from the DNA fragment data, was predominantly similar across dilution factors in the July grazing experiment. There were no significant differences in community between the algicide treatment and control in the 75%, 50%, or 25% dilution factors. The exception, the 100% dilution factor, was the only point at which the respective communities of the algicide treatment and control significantly differed, at which point the community composition at T_0 was more similar to that of the algicide treatment than to the control community after 24 hours. One-way similarity percentage (SIMPER) analysis based on treatment identified a 375-bp T-RF as the primary contributor (>10%) to intra-treatment similarity with the exception of this 100%

dilution factor. A 336-bp T-RF, found in both the initial bulk sample and the algicide treatment after 24 hours, accounted for greater than 27% of the similarity between the two. The September 25, 2017 experiment yielded similar results in that the community composition at T_0 was once again more similar to that of the algicide treatment than the control after 24 hours in the 100%, 75%, and 50% dilution factors. Here, a 153-bp T-RF was the dominant contributor to similarity between the bulk and algicide treatment across dilution factors (10-12%). Alternatively, a SIMPER analysis performed on the bulk and control found that this 153-bp fragment was not detectable. This trend of increased similarity to initial bulk samples in the algicide treatment is not what one would expect given the algicide known efficacy against dinoflagellates. Additionally, the control experienced minimal grazing as well as a lower growth rate which would suggest fewer changes between the initial community and that of the control.

The September 28, 2017 ammonium effects experiment revealed that the community of the algicide treatment significantly differed from both the respective ammonium treatment and control communities. However, in comparing the communities of the two treatments and control to the community at T_0 , the community of the algicide was the least similar to that of T_0 .

Microzooplankton grazing is a critical component of natural harmful algal bloom prevention, control, and mitigation (Burkill et al., 1987; Gobler et al., 2004; Linacre et al., 2017). Beyond algal consumption, microzooplankton grazers positively impact their respective communities through their roles in nutrient regeneration and as a food source for larger grazers (Graham and Strom, 2010 and references within). This

study indicates that IRI-160AA application will not have a negative effect on this process in natural phytoplankton communities.

Table 3.1 Environmental metadata and experimental specifications associated with the microzooplankton grazing experiments conducted on July 25, 2017, September 25, 2017, and September 28, 2017.

Experiment Date	July 25, 2017	September 25, 2017	September 28, 2017
Sampling Location	SB10E South Bethany, DE	RB34 Rehoboth Beach, DE	IR32 Bethany Beach, DE
Latitude	38° 31' 15'' N	38° 42' 10'' N	38° 41' 56'' N
Longitude	75° 03' 39'' W	75° 09' 39'' W	75° 06' 44'' W
Temperature (°C)	30.85	24.10	23.69
Salinity (PSU)	23.04	15.99	24.28
Dominant Dinoflagellate	<i>Heterocapsa rotundata</i>	<i>Gyrodinium instriatum</i>	<i>Prorocentrum minimum</i>
Dominant Grazer	<i>Oxyrrhis marina</i>	<i>Ciliates</i>	<i>Ciliates</i>
Algicide Batch	Batch 4-5-6 Combined	Batch 7	Batch 7
[NH ₄ ⁺] in μM	65.66	177.75	177.75

Table 3.2 Sequences of primers and probes utilized in polymerase chain reactions as well as quantitative polymerase chain reactions. F denotes forward primer; R denotes reverse primer.

Primer or Probe	Sequence (5'-3')	Target
Euk1A	HEX/CTGGTTGATCCTGCCAG	Eukarya 18S rRNA
Euk517R	FAM/CACCAGACTTGCCCTC	Eukarya 18S rRNA
Dino06F	CCGATTGAGTGWTCGGTGAATAA	Dinoflagellate 18S
EukB	GATCCWTCTGCAGGTTACCTAC	Dinoflagellate 18S
M13F	CCCAGTCACGACGTTGT	pGEM plasmid DNA
pGEMR	TGTGTGGAATTGTGAG	pGEM plasmid DNA
pGEM probe	FAM/CACTATAGA/ZEN/ATACTCAAG	pGEM plasmid DNA

Table 3.3 Percent community composition similarities compared to the T₀ community based on Bray-Curtis similarity values derived from terminal restriction fragment data. Values in parentheses indicate standard deviation.

	Treatment	100%	75%	50%	25%
July 25, 2017	Algicide	81.18 (2.57)	75.41 (4.91)	62.64 (1.54)	59.59 (1.17)
	Control	65.05 (1.97)	72.06 (2.96)	61.97 (6.71)	53.17 (4.06)
	Treatment	100%	75%	50%	25%
September 25, 2017	Algicide	76.04 (2.66)	72.17 (4.34)	75.04 (3.62)	39.89 (16.27)
	Control	50.83 (1.91)	43.11 (2.74)	50.32 (2.65)	38.89 (7.02)
	Treatment	100%			
September 28, 2017	Algicide	52.37 (2.30)			
	NH ₄ ⁺	71.86 (1.90)			
	Control	71.00 (3.57)			

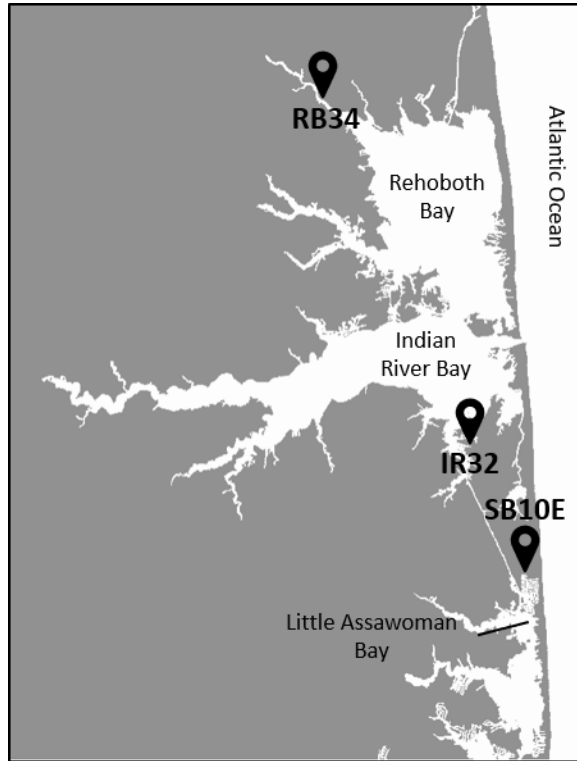


Figure 3.1 Sampling sites within the Delaware Inland Bays: Rehoboth Bay in Rehoboth Beach, DE at Love Creek (RB34), Indian River Bay in Bethany Beach at Holly Terrace Acres Canal (IR32), and Little Assawoman Bay in South Bethany, DE at Russell Canal East (SB10E).

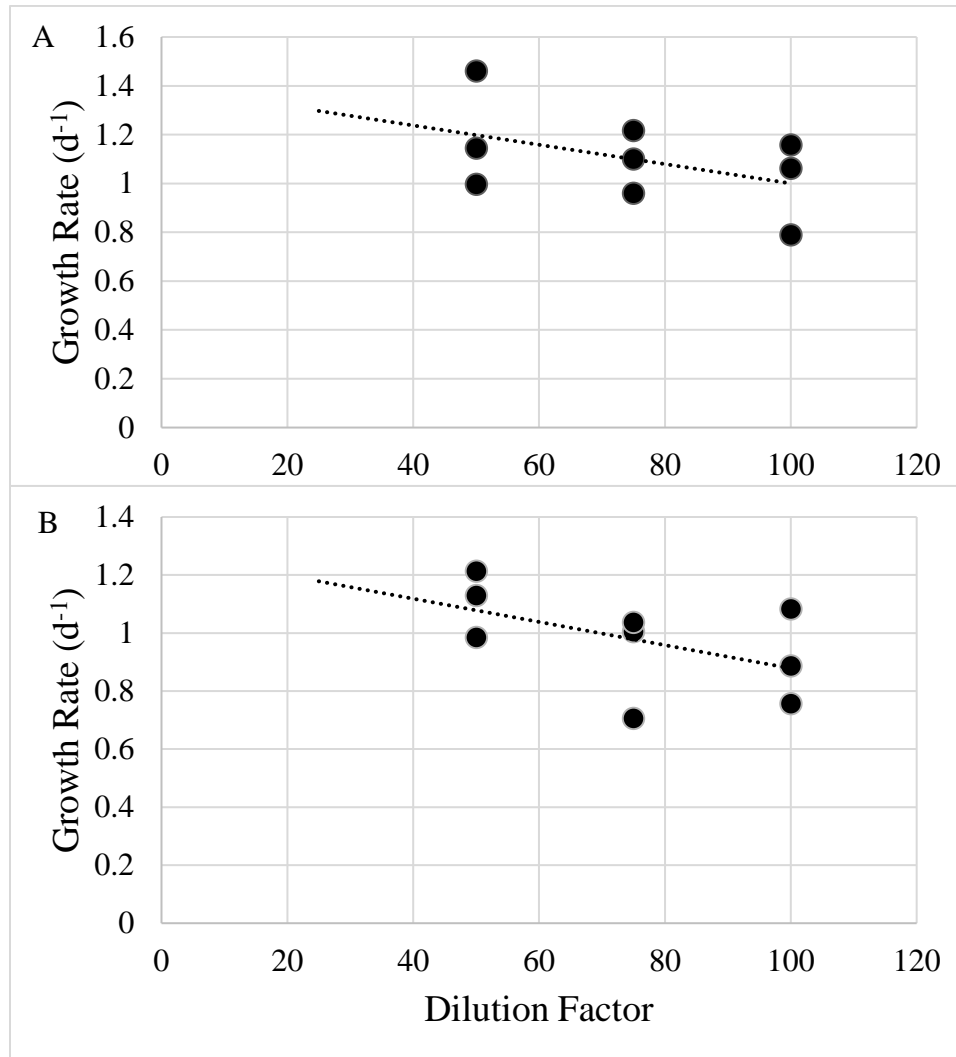


Figure 3.2 Dilution factor plotted against community growth rates derived from chlorophyll *a* concentrations for the (A) algicide treatment and (B) control in the July 25, 2017 microzooplankton grazing experiment. Grazing rates were calculated via linear regression analysis. Algicide treatment grazing rate: 0.396 d⁻¹; control grazing rate: 0.400 d⁻¹.

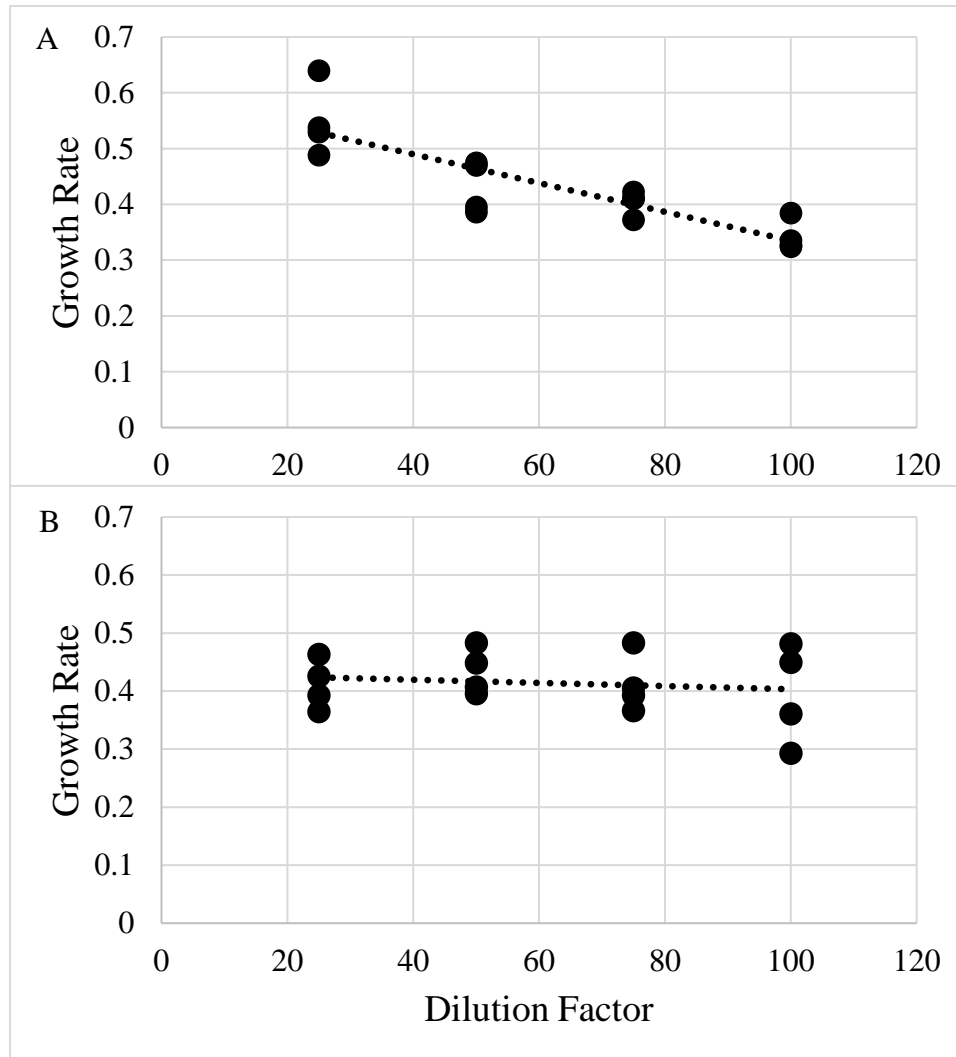


Figure 3.3 Dilution factor plotted against community growth rates derived from chlorophyll *a* concentrations for the (A) algicide treatment and (B) control in the September 25, 2017 microzooplankton grazing experiment. Grazing rates were calculated via linear regression analysis. Algicide treatment grazing rate: 0.258 d⁻¹; control grazing rate: 0.027 d⁻¹.

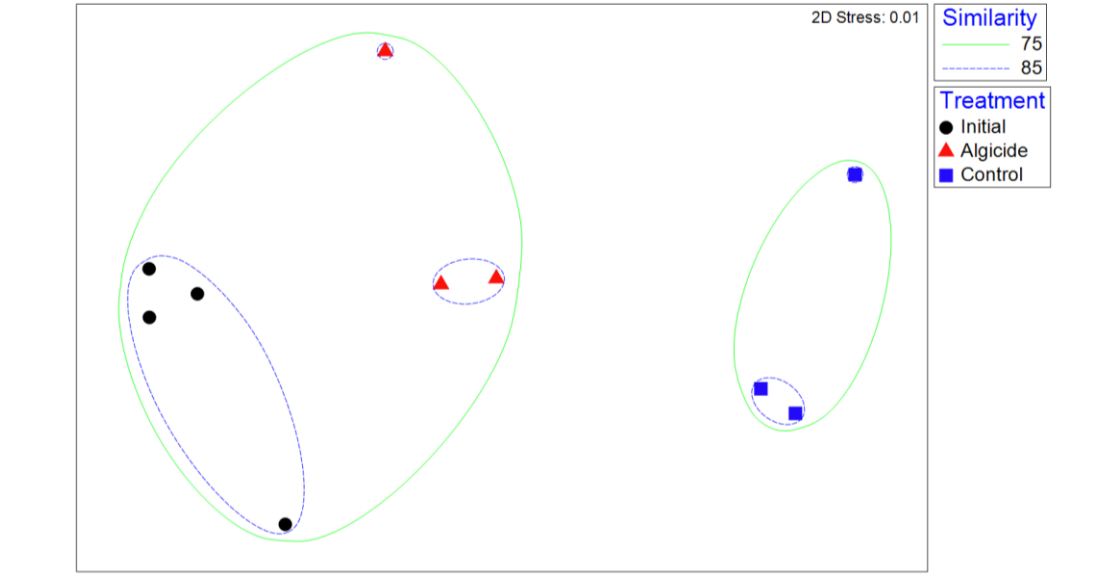


Figure 3.4 Non-metric multi-dimensional scaling (nMDS) ordination based on a Bray-Curtis similarity matrix for the microzooplankton grazing experiment sampled on July 25, 2017. Only the initial bulk sample and the 100% undiluted algicide treatment and control are shown.

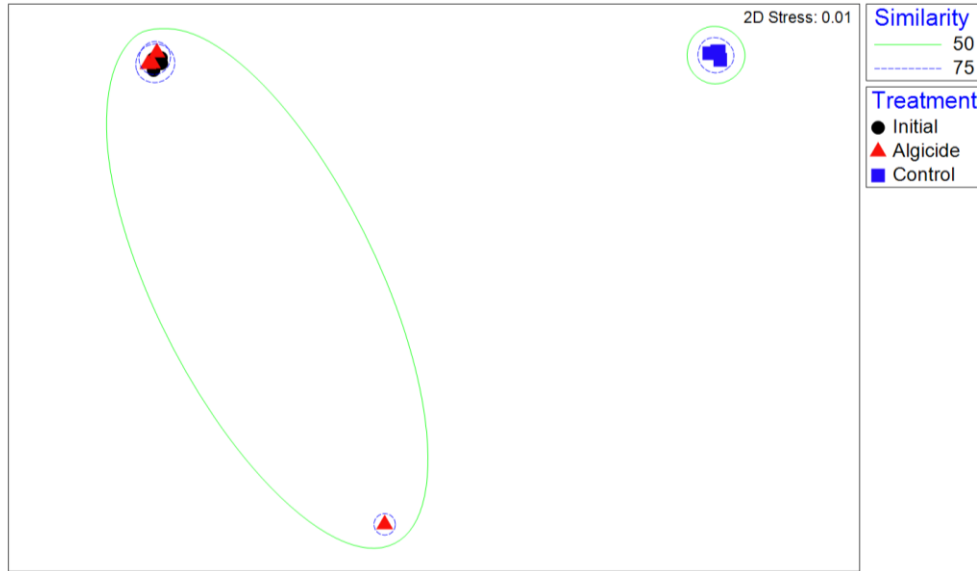


Figure 3.5 Non-metric multi-dimensional scaling (nMDS) ordination based on a Bray-Curtis similarity matrix for the microzooplankton grazing experiment sampled on September 25, 2017. Only the initial bulk sample and the 100% undiluted algicide treatment and control are shown.

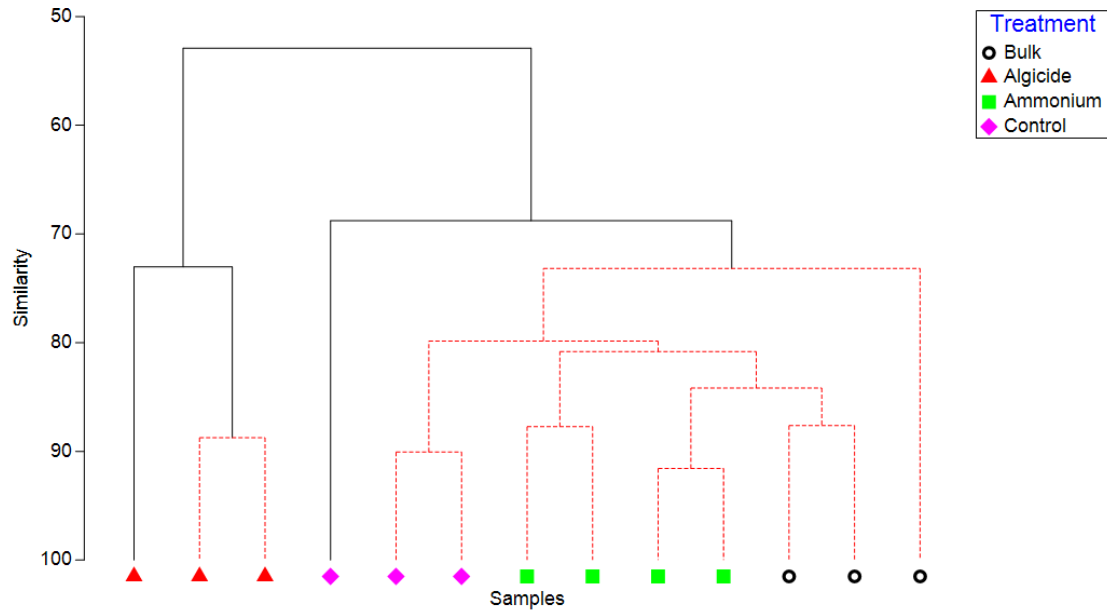


Figure 3.6 Agglomerative hierarchical cluster showing the percent similarities among the initial bulk sample, algicide treatment, ammonium treatment, and control based on terminal restriction fragment data. Icons represent individual replicates. Black lines indicate significant differences, red lines indicate a lack thereof.

Chapter 4

CONTRIBUTION OF AMMONIUM TO THE ALGICIDAL EFFECTS OF IRI-160AA

4.1 Abstract

Increasing prevalence of harmful algal blooms has led to increases in research studying potential forms of prevention, control, and mitigation. In the Delaware Inland Bays, one species of bacteria, *Shewanella* sp. IRI-160, has been shown to naturally produce a bacterial algicide specific to dinoflagellates. Free ammonium (NH_4^+) concentrations within the algicide, termed IRI-160AA, vary between 1-3 mM which brings to question the extent to which ammonium contributes to the compound's algicidal activity. NH_4^+ sensitivity was tested via 24-hour bioassay in three dinoflagellates (*Prorocentrum minimum*, *Gyrodinium instriatum*, *Karlodinium veneficum*) and one cryptophyte as a biological control (*Rhodomonas* sp. 757). To assess the comparative effects of NH_4^+ alone vs. IRI-160AA, laboratory monocultures of *K. veneficum* incubated for 18-h with NH_4^+ or with IRI-160AA at the same NH_4^+ concentration, after which photochemical parameters were measured: maximum quantum yield of PSII (F_v/F_m), photochemical connectivity between PSII reaction centers (ρ), and primary quinone re-oxidation rate (τ). At IRI-160AA concentrations exhibiting 50% lethality (EC50) in *K. veneficum*, F_v/F_m values did not significantly differ between the NH_4^+ treatment and control, yet F_v/F_m decreased by 14% in the IRI-160AA treatment. ρ decreased by as much as 24% near EC50 with IRI-160AA, which was significantly greater than the effects of the NH_4^+ treatment. Both the NH_4^+ and IRI-160AA treatments exhibited τ values greater than that of the control, however those of the NH_4^+ were never significantly greater than those of the IRI-160AA treatment. These results indicate that NH_4^+ , while toxic to microalgal populations at

levels that are species-specific, is not the sole cause of the algicidal effect observed in IRI-160AA.

4.2 Introduction

With harmful algal blooms (HABs) steadily increasing in both frequency and geographic range (Smayda et al., 1989; Hallegraeff, 1993; Anderson et al., 2002), resources are consistently being invested in establishing effective practices for HAB management. These events are capable of causing significant damage to coasts and coastal communities by means of fish kills, loss of submerged vegetation, shellfish die-offs, etc. (Anderson et al., 2008). All of these factors can lead to annual costs greater than US\$82 million in the United States alone (Hoagland and Scatasta, 2006), further promoting interest in HAB prevention, control, and management. One of the most common preventative approaches in the field is the restriction of nutrient flux into a system to limit anthropogenic eutrophication. However, limiting nutrient input can be extremely challenging in non-fluvial systems due to the sheer myriad of factors that go into estuarine or marine bloom formation (Smith and Schindler, 2009). Additionally, blooms that are not instigated by eutrophication require forms of prevention other than nutrient limitation (Tilney et al., 2014a; Bachmann et al., 2003). Chemical and biological algicides have been studied as potential strategies for HAB prevention that do not rely on the concept of nutrient limitation and have shown promise in multiple studies. Jia et al. (2013) investigated the effects of copper sulfate, hydrogen peroxide, and rice seed husks on algal species of the genus *Microcystis*, and saw the latter two exhibit varying degrees of successful HAB prevention. Other preventative measures studied have included natural clay for flocculation, strong

oxidants, allelopathic seaweeds, and algicidal bacteria (Yang et al., 2014; Sengco, 2009).

Hare et al. (2005) originally described an algicidal exudate isolated from the gammaproteobacterium *Shewanella* sp. IRI-160 which exhibited algicidal effects on three dinoflagellate species but had negligible effects on non-dinoflagellate microalgae such as diatoms, prasinophytes, cryptophytes, and raphidophytes. Subsequent studies sought to characterize the algicidal agent, termed “IRI-160AA”, and Pokrzywinski et al. (2012) found that the algicidal activity could be attributed to a bioactive secretion that was small, polar, and hydrophilic. Undiluted, IRI-160AA exhibits concentrations of ammonium (NH_4^+) between 1 and 3 mM. Current research also suggests that the algicide comprises several small polyamines in addition to the free ammonium. To understand the way these nitrogen-based compounds may be interacting with dinoflagellates, it is important to review the relationship between nitrogen and phytoplankton in general.

Nitrogen is a required element in the synthesis of biological molecules like nucleotides and amino acids, and as such is an integral nutrient for phytoplankton growth and development (Terrado et al., 2015). Nitrogen is a limiting nutrient for primary productivity and growth for coastal phytoplankton populations (Heckey and Kilham 1988). Algal species have been known to utilize forms of dissolved organic nitrogen (DON), as well as dissolved inorganic nitrogen (DIN) (Burford and Pearson, 1998; Twomey et al., 2005), in order to satisfy their biological requirements. Of these nitrogen forms, ammonium and nitrate (NH_4^+ and NO_3^- , respectively) are the forms most commonly available and assimilated by photosynthetic algae (Gruber, 2008). Between the two, ammonium is taken up more readily due to its oxidation state

matching that of most amino acids (Berges, 1997), while nitrate must be enzymatically reduced to ammonium prior to any assimilation (Guerrero et al., 1981; Malerba et al., 2015): however, ammonium can also have detrimental effects on algae in larger concentrations. Unlike nitrate, ammonium freely permeates cell membranes in its unprotonated state (NH_3), which is why it is so readily taken up. Once it has passed through the thylakoid membrane, the NH_3 is protonated and the ammonium acts as an uncoupling reagent (Mills, 1986, p. 151-153). Ammonium does this by taking the place of a proton, thereby decreasing the ΔpH across the thylakoid membrane and inhibiting ATP synthesis. A review by Collos and Harrison (2014) explored the acclimation and toxicity of high ammonium concentrations on microalgal classes, including class Dinophyceae which carries particular significance for this study. Dinoflagellates exhibited the lowest tolerance of all tested microalgal classes with a mean optimal ammonium concentration of 100 μM .

In an effort to understand the effects of the algicide beyond senescence, Tilney et al. (2014a) utilized a photobiological approach and found that dinoflagellate responses to the algicide included significant PSII inactivation. Studies investigating the effects of natural allelochemicals on photosynthetic algae have been documented as having an array of negative effects on the photosynthetic apparatus. Compounds derived from the cyanobacterium *Fischerella muscicola* have been shown to act at several sites along the photosynthetic electron transport chain, especially the primary quinone (Smith and Doan, 1999). An algicidal polyphenol, tellimagrandin II, is produced by the macrophyte *Myriophyllum spicatum* and inhibits both microalgal exoenzymes and PSII (Leu et al., 2002). A biosurfactant produced by the bacterium *Pseudomonas aeruginosa* has been shown to decrease photosynthetic efficiency and

cell viability in various microalgal classes (Gustafsson et al., 2009). The cyanobacterium *Scytonema hofmanni* produces a diaryl substituted γ -lactone called cyanobacterin that acts on the oxidizing side of the quinone-B electron acceptor (Gleason and Paulson, 1984). In short, oxygenic photosynthesis requires a complex set of biological machinery that is vulnerable to disruption at a myriad of key junctures by naturally produced compounds and allelochemicals. This study investigates the extent to which ammonium contributes to the algicidal activity of IRI-160AA by examining multiple photochemical parameters described below (Section 4.3.6).

4.3 Methods

4.3.1 Preparing Bacterial Algicide IRI-160AA

Shewanella sp. IRI-160 was cultured on modified LM medium (Sambrook et al., 1989; Luria Bertani medium, 20 g/L NaCl, 10 g/L tryptone, 5 g/L yeast extract, 15 g/L agar) at room temperature for 48-72 hours. A colony was transferred into 100 mL of liquid LM medium (20 g/L NaCl, 10 g/L tryptone, 5 g/L yeast extract) and incubated with shaking at 25 °C overnight. 900 mL of liquid LM medium was then inoculated with the suspended bacteria and incubated with shaking at 25 °C for an additional 6 hours. Samples were subsequently spun down, the supernatant discarded, and the cells were washed twice in 20 PSU *f/2* medium (Guillard, 1975). The cells were then resuspended in *f/2* medium and incubated for one week. Cells were then removed via filtration through a 0.2- μ m IsoporeTM polycarbonate filters (Millipore Sigma, Darmstadt, Germany) and the resulting filtrate, termed “IRI-160AA”, was stored at 4 °C.

4.3.2 Culture Conditions

Prorocentrum minimum (DIB), *Karlodinium veneficum* (DIB), *Gyrodinium instriatum* (DIB), and *Rhodomonas sp.* (CCMP 757) were batch cultured in sterile 20 PSU *f/2* medium at 25 °C and experienced a 12:12 light-dark cycle at 140 $\mu\text{mol photons m}^{-2} \text{ s}^{-1}$ provided by fluorescent lighting. *Alexandrium tamarense* (DIB) was batch cultured in sterile 32 PSU *f/2* medium at 18 °C and experienced a light-dark cycle equal to that of the aforementioned cultures. For all photochemical experiments, algae were sampled during logarithmic growth as this growth phase has been shown to exhibit the greatest susceptibility to the effects of the algicide (Pokrzywinski et al., 2012).

4.3.3 NH_4^+ Sensitivity

NH_4^+ sensitivity experiments were conducted on three dinoflagellate species (*P. minimum*, *G. instriatum*, and *K. veneficum*), as well as the cryptophyte *Rhodomonas sp.* as a non-dinoflagellate control. All algal species were cultured as described above. A dilution series was generated from a 2 mM stock solution of NH_4Cl in sterile 20 PSU *f/2* medium (including NO_3^-) to achieve final NH_4^+ concentrations of 1 mM, 500 μM , 250 μM , 125 μM , and 0 μM (*f/2* only, $n = 3$). *K. veneficum* exhibited a greater increased sensitivity to NH_4^+ , so the final NH_4^+ concentrations were adjusted to 250 μM , 100 μM , 50 μM , and 25 μM . Relative *in vivo* fluorescence measurements were taken using the Aquafluor handheld fluorometer (Turner Designs) at 0, 2, 4, 6, and 8 days. Samples were kept at growth conditions described above for the duration of the experiment. Growth rates and algistic points were calculated using linear regression analysis based on the relative *in vivo* fluorescence of chlorophyll in the samples tested.

4.3.4 Photochemical Response to NH₄⁺ Alone vs. IRI-160AA

The suite of concentrations used to compare the effects of IRI-160AA and NH₄⁺ on dinoflagellate species was specific to the batch of IRI-160AA used. These concentrations were determined by a *Karlodinium veneficum* bioassay. The EC50 was found to be at 2.85% addition with an NH₄⁺ concentration of 3.9 mM at full strength (111.15 μM at EC50 level). Four dinoflagellate species (*K. veneficum*, *Prorocentrum minimum*, *Gyrodinium instriatum*, and *Alexandrium tamarense*) were tested in 30 mL autoclaved glass test tubes using 20 mL volumes with treatments for both IRI-160AA and NH₄⁺, as well as *f/2* control ($n = 4$). IRI-160AA treatments had a 2.85% addition of algicide (final concentration = EC50), while NH₄⁺ treatments also had a 2.85% addition to achieve the same final concentration of NH₄⁺ to each treatment. Cultures were sampled for both photochemistry after 18 hours of exposure as described below (Section 4.3.6).

4.3.5 NH₄⁺ in Dose-Response Experiments

The response of *K. veneficum* was assessed in two separate experiments (January 27, 2018 and April 11, 2018) using 10 mL reactions ($n = 3$ or 4) with 0.5%, 1%, 2%, 3%, 5%, 8%, and 10% addition of either IRI-160AA or NH₄Cl. These percentages as concentrations of NH₄⁺ are 19.5, 39, 78, 117, 195, 312, and 390 μM, respectively. The NH₄Cl was made up in 20 PSU *f/2* medium with a final concentration of 3.9 mM to mirror the concentration found in the full-strength IRI-160AA, ensuring equal NH₄⁺ concentrations at the same percent additions between treatments. An *f/2* control was included at 10%. Cultures were sampled for photochemical parameters after an 18-h incubation period as described below (Section

4.3.6). Samples fixed with 3% Lugol's Iodine solution were collected and stored at 4 °C.

4.3.6 Dinoflagellate Photochemistry

The extent to which NH_4^+ contributed to the algicidal effect of IRI-160AA was investigated using PSII function as a proxy for algal health. Fast repetition rate fluorometry was used to assess this function using 100 subsaturating LED flashlets, applied at 1 μs intervals, to create a single turnover fluorescence transient (FAST*tracka* II and FAST*act* system, Chelsea Instruments, UK). Fluorescence transients were used to evaluate several photochemical parameters: the maximum quantum yield of PSII (F_v/F_m), the photochemical connectivity between PSII reaction centers (ρ), and the rate of primary quinone re-oxidation (τ) (Kolber et al., 1998; Cosgrove and Borowitzka, 2010). Samples were dark-acclimated for 20-30 minutes prior to measurement to re-open PSII reaction centers. The FRR sample chamber was maintained at 25 °C. The fluorescence measurement protocol comprised 40 repetitions of the following: 100 flashlets at 1- μs intervals, then 50 flashlets at 49- μs intervals. Curve-fitting and analysis software was provided with the fluorometer (FAST*pro* v3.0, Chelsea Instruments, UK). Data were manually inspected in real time.

4.3.7 Statistical Analyses

Statistical comparisons were performed using ANOVA testing in R (<https://www.r-project.org/>). If data were found to be significantly different ($p \leq 0.05$), then the ANOVA was followed by a Tukey Honest Significant Difference test (Tukey HSD). All tests used a standard alpha value of 0.05, and all experiments were conducted with comparable sample sizes ($n = 3$ or 4).

4.4 Results

4.4.1 NH₄⁺ Sensitivity

Cultures of *P. minimum* exhibited continual growth throughout the experiment in the control and 125 μM NH₄⁺ treatment (Figure 4.1). The 250 μM, 500 μM, and 1 mM NH₄⁺ treatments all exhibited dose-dependent decreases in relative *in vivo* fluorescence by T₂, however *P. minimum* in the 250 μM treatment had increases in fluorescence at subsequent timepoints indicating sustained growth. *In vivo* fluorescence of the cells in the 500 μM treatment remained relatively stagnant throughout the experiment at a measurement significantly lower than that of the treatments with lower NH₄⁺ concentrations, suggesting 500 μM caused a mostly algistatic effect on the culture. The 1 mM NH₄⁺ treatment resulted in total senescence of cells based on fluorescence measurements.

Fluorescence values of *P. minimum* responded in a dose-dependent manner with higher NH₄⁺ concentrations resulting in lower fluorescence measurements. By the final timepoint, T₈, significant differences ($p < 0.05$) existed between all treatments and the control except for between the 125 μM NH₄⁺ treatment and the control, as well as between the 1 mM and 500 μM NH₄⁺ treatments. The relative fluorescence values of the control were 1.3-fold greater than that of the 250 μM treatment, 4.6-fold greater than that of the 500 μM treatment, and 74.2-fold greater than that of the 1 mM treatment. While not statistically significant, the 125 μM treatment did have a higher mean relative fluorescence value at T₈ when compared to the control by a factor of 1.1. Calculated growth rates revealed that approximately 430 μM was the NH₄⁺ concentration at which *P. minimum* exhibited algistatic effects, or where the growth rate was equal to zero.

Cultures of *G. instriatum* exhibited increasingly positive relative *in vivo* fluorescence values throughout the experiment in both the control and 125 μM NH_4^+ treatment (Figure 4.2). The 250 μM , 500 μM , and 1 mM NH_4^+ treatments all exhibited dose-dependent decreases in relative *in vivo* fluorescence by T_2 , a trend which continued through to T_{final} . Cells exposed to 1 mM concentrations of NH_4^+ were the only samples of these three highest concentrations to have total senescence as early as T_2 based on fluorescence measurements.

Relative fluorescence measurements of the *G. instriatum* monocultures over time yielded a strictly dose-dependent response in which the highest NH_4^+ concentrations used resulted in the lowest fluorescence values. By T_{final} , there were significant differences among all treatments with only two exceptions: the 1 mM and 500 μM NH_4^+ treatments did not significantly differ, nor did the 500 μM and 250 μM treatments. At this point, the mean relative fluorescence value of the control was 58.7-fold greater than that of the 1 mM treatment. The algistatic point for *G. instriatum* was calculated to be approximately 185 μM NH_4^+ .

Cultures of *K. veneficum* exhibited increases in fluorescence throughout the entirety of the experiment in the 25 μM , 50 μM , and 100 μM NH_4^+ treatments as well as in the control (Figure 4.3). The 250 μM NH_4^+ treatment was the only treatment in which fluorescence values below that of T_0 were measured, which occurred by T_2 . Cells exposed to this concentration of NH_4^+ exhibited total senescence based on fluorescence measurements.

K. veneficum was exposed to a gradient of NH_4^+ treatments with a lower maximum value than the other two dinoflagellates due to a preliminary study showing increased sensitivity to NH_4^+ compared to the other two species. No significant

differences in fluorescence were observed at T₀. At T₂, the 25 μM and 50 μM NH₄⁺ treatments registered significantly greater (p < 0.05) fluorescence values when compared to the 100 μM treatment and control. The 25 μM and 50 μM NH₄⁺ treatment relative fluorescence values at T₂ did not significantly differ from one another, but were significantly greater than the 100 μM treatment and control by factors of 1.5- and 1.3-fold, respectively. There were no significant differences between the 25 μM and 50 μM treatments or between the 100 μM treatment and controls, but *in vivo* fluorescence of all four treatments were significantly greater than the 250 μM treatment. At T₄, the 50 μM treatment once again had the greatest measured fluorescence levels but only significantly differed (p < 0.01) from the 100 μM and 250 μM treatments. The control only differed significantly (p < 0.001) from the 250 μM treatment. 50 μM exhibited the greatest relative fluorescence values at both T₆ and T₈, being significantly greater than all other treatments by T₈ (p < 0.05). The 100 μM treatment, the 25 μM treatment, and the control had no statistical difference between them by T₈, but the grouping was both significantly less than 50 μM (p < 0.05) as well as significantly greater than the 250 μM treatment (p < 0.001). The mean relative fluorescence of the control was 72.9-fold greater than that of the 250 μM treatment at T₈, but the 50 μM treatment was calculated as 100.9-fold greater than the 250 μM treatment (1.4-fold greater than the control). The algistic point for *K. veneficum* was unable to be calculated due to a lack of data points exhibiting negative growth rates.

Up to the maximum tested concentration of 1 mM NH₄⁺, *Rhodmonas* sp. 757 exhibited a strictly positive growth rate. In both the 125 μM treatment and control, fluorescence values were over the limit of detection at both T₆ and T₈. Data for

Rhodomonas sp. 757 are not pictured below due to these missing data as well as a lack of necessity in the context of the experiment. These data suggest that its role as a biological control was fulfilled, and its results have no bearing on the efficacy of IRI-160AA on target dinoflagellates.

4.4.2 Photochemical Response to NH₄⁺ Alone vs. IRI-160AA

The same batch of IRI-160AA was used in both the dose response experiments as well as the experiment testing the effects of NH₄⁺ versus IRI-160AA on dinoflagellate photochemistry among species. The EC50 value of 2.85% addition (111.15 μM NH₄⁺) was used across the four dinoflagellates tested in this experiment. This EC50 was established on the basis of relative fluorescence and growth as opposed to any photochemical parameter and photochemical effects in all dinoflagellates over the course of the experiment were negligible due to the concentration being too low to elicit a response. Full data are included in the appendix.

4.4.3 Dose Response

A preliminary bioassay was conducted on a laboratory monoculture of *K. veneficum* in logarithmic growth phase using the same batch of algicide to be used for photochemical experiments. The EC50 value for this batch was calculated to be 2.85% addition with an approximate ammonium concentration of 111.15 μM at this level.

4.4.3.1 January 27, 2018 Experiment

The F_v/F_m values of the control treatment were significantly greater ($p < 0.05$) than the algicide and ammonium treatments at 10%, 8%, and 5% addition (Figure 4.5). The mean F_v/F_m value of the control, which was amended with 20 PSU $f/2$ medium, at 10% addition was 1.8- and 2-fold greater than the ammonium and

algicide treatment, respectively. At 3% and 2% addition, the mean F_v/F_m value of the control was significantly greater than the algicide treatment (1.16- and 1.06-fold, respectively), but there were no significant differences between the controls and the ammonium treatment at these levels. None of the three treatments differed significantly from one another at 1% addition, and the ammonium treatment exhibited a significantly greater F_v/F_m value at 0.5% addition when compared to both the algicide and control treatments.

The photochemical connectivity between PSII reaction centers, ρ , exhibited a clearer separation of effects between the algicide and ammonium alone (Figure 4.5). At 10% addition, the ρ values differed significantly between each treatment and between treatments and controls ($p < 0.05$) with the control treatment having a mean value 6.9- and 1.6-fold greater than the algicide and ammonium treatment, respectively. At 8% addition, the ρ values of the control treatment were significantly higher than either the algicide or ammonium treatment, which did not significantly differ from one another. The control and ammonium treatments did not differ from one another at 5%, 3%, or 2% addition, however both of those treatments had significantly higher ρ values than those measured in the algicide treatment. The 1% addition treatment yielded no significant differences among any treatments. Lastly, the 0.5% addition yielded significantly higher ρ values in the ammonium treatment compared to the control.

At 10%, 8%, 3%, 2%, and 1% addition, the value of τ in the ammonium treatment was significantly higher than that of the control treatment ($p < 0.05$) by factors as large as 1.5-fold at 10% addition down to 1.04-fold at 1% addition (Figure 4.5). The 5% and 0.5% treatments yielded no significant differences among any

treatments. The algicide treatment yielded no significant differences between either treatment or between the treatments and control at any percent addition.

4.4.3.2 April 11, 2018 Experiment

The F_v/F_m values of treatments and controls were significantly different from each other ($p < 0.05$) at 10% and 8% addition, with the control treatment exhibiting the highest mean F_v/F_m value 1.7-fold greater than that of the ammonium treatment and 3.3-fold greater than that of the algicide treatment (Figure 4.6). At 5% addition, both of the average F_v/F_m values of the ammonium and control treatments were significantly greater than the average F_v/F_m value in the algicide treatment by factors of 1.18 and 1.23, respectively, but the two did not significantly differ from one another. From 3% down to 0.5% addition, none of the treatments significantly differed from one another.

There were significant differences in connectivity (ρ) between both of the treatments and between the treatments and the control at both 10% and 8% addition ($p < 0.05$) with the ρ values being higher in the control treatment compared to either the ammonium or algicide treatments by factors of 1.7 and 5.7, respectively at 10% addition (Figure 4.6). At 5% addition, ρ was significantly higher in the control compared to the algicide treatment, but neither of those significantly differed from the ammonium treatment. There was a marked decrease in the average ρ value in the ammonium treatment at 3% addition, leading to significantly lower values in the ammonium treatment compared to both the algicide and control. 2%, 1%, and 0.5% addition each yielded no significant differences in ρ between the treatments or the control.

Across both treatments and the control, those dosed with algicide had the greatest average τ values while the control exhibited the lowest (Figure 4.6). Large standard deviations contributed to no significant differences between treatments and control at both 10% and 8% addition. Data were analyzed for outlier presence using Dixon's Q test, but none qualified. The average τ value in the control was significantly lower than that of the algicide treatment at 5%, 3%, 2%, and 0.5% addition ($p < 0.05$). The average τ value in the control was also significantly lower than that of the ammonium treatment at both 5% and 2% addition, but not at 3% and 0.5%. However, the re-oxidation rate of the ammonium treatment was significantly lower than that of the algicide at both 3% and 0.5% addition. There were no significant differences among treatments at 1% addition.

4.5 Discussion

The NH_4^+ sensitivity measured above indicates that *P. minimum* was the most tolerant of ammonium (algistatic point of 430 μM) while *K. veneficum* was the least tolerant. Due to increased sensitivity to ammonium compared to other species tested, the highest ammonium concentration tested for *K. veneficum* was 250 μM . *P. minimum* was the only thecate dinoflagellate of the three species tested, an anatomical distinction that has been shown to decrease the effects of IRI-160AA when compared to athecate dinoflagellates (Tilney et al., 2014a). It is possible that the thecal plates of certain dinoflagellates, which serve to limit cell membrane-environment interfacing, restrict the cell's exposure to and uptake of certain nutrients. Unlike *P. minimum*, *G. instriatum* and *K. veneficum* are athecate dinoflagellates with no protective plates. Given the number of similarities shared by these two species, it is difficult to infer what the driving factor or factors may be regarding the discrepancy in their NH_4^+

sensitivity. One potential explanation could be the size of the respective cells: *G. instriatum* is a much larger cell measuring approximately 50 μm in length while *K. veneficum* is approximately 15 μm in length (Freudenthal and Lee, 1963; Uchida et al., 1997; Dai et al., 2014). Toxicity of various compounds decreases in larger organisms when compared to smaller ones, which is intuitive given that equal levels of exposure would result in a greater body mass percentage of toxin present in a smaller cell. As previously mentioned, a literature review conducted by Collos and Harrison (2014) and references within estimated that a mean optimal NH_4^+ concentration for dinoflagellates was approximately 100 μM , an estimate that is supported by the data here. While not significant, relative fluorescence measurements of *P. minimum* were greater on average at 125 μM NH_4^+ when compared to the control. Additionally, 50 μM NH_4^+ yielded significantly greater fluorescence measurements by T_{final} in *K. veneficum* when compared to all other treatments and the control. The 25 μM treatment, while not significant, also had greater fluorescence values on average than the control in *K. veneficum*. The *f/2* medium used in the control had the same concentration of nutrients as the *f/2* used to make the NH_4^+ treatment, including sufficient levels of NO_3^- for algal growth (883 μM ; Guillard, 1975). Therefore, these effects can be attributed solely to the presence and potential toxicity of NH_4^+ as opposed to some form of nitrogen limitation within the cells. Overall, the data shown here agree with the current literature regarding NH_4^+ sensitivity in dinoflagellates as a microalgal class (Collos and Harrison, 2014 and references within).

A key distinction to be made is how NH_4^+ , which is a primary nitrogen source for many algae, can be toxic at higher concentrations. As previously stated, NH_4^+ and NO_3^- are the two most dominant forms of nitrogen available for most algal species,

with NH_4^+ being taken up more readily due to its oxidation state matching that of most amino acids (Gruber, 2008; Berges, 1997). However, it is the ease with which NH_4^+ is taken up and utilized that actually causes its toxic effects on algae. In its unprotonated state (NH_3), it is able to freely pass through cell membranes and eventually through the thylakoid membrane where it bonds with a free proton to become NH_4^+ . This bonding decreases the pH gradient necessary to drive ATP synthesis thereby inhibiting the cell from creating the appropriate amount of energy required for survival. That being said, IRI-160AA has been shown to affect photosynthetic and non-photosynthetic dinoflagellates alike at the nuclear level with morphological changes and even nuclear expulsion occurring post-application (Pokrzywinski et al., 2012; Pokrzywinski et al., 2017). Dose-response experiments were conducted and measured via photochemical parameters to assess the extent to which NH_4^+ contributed to the algicidal effects observed by the introduction of IRI-160AA. These comparative effects were investigated through two separate experiments performed on January 27, 2018 and April 11, 2018, respectively. In both experiments, trends observed in both the IRI-160AA and NH_4^+ treatments were similar to one another. The F_v/F_m parameter, or the maximum quantum yield of PSII, is commonly used as a metric for the overall photosynthetic health of photoautotrophs (Aquino-Cruz and Okolodkov, 2016; Xu et al., 2016; Higo et al., 2017). Broadly, both the January and April experiments showed that F_v/F_m values in both the ammonium and algicide treatments were significantly lower than that of the control at greater percent addition and approached the values measured in the control as the percent addition approached the EC50 value of 2.85% addition. In fact, this trend held true in both the photochemical connectivity between PSII reaction centers (ρ) and the rate of primary quinone re-

oxidation (τ) as well. The EC50 value of 2.85% addition was calculated based on growth rates derived from relative fluorescence measurements, not through photochemical means. These data suggest that, although there were some significant differences described above, 2.85% addition of the algicide is not a large enough application to induce a significant deficiency in photochemical parameters. This would indicate that the photosynthetic apparatus is not the primary target of algicidal activity but is instead a secondary target of IRI-160AA. Additionally, 2.85% addition of the algicide equates to a final concentration of 111.15 μM NH_4^+ in the *K. veneficum* cultures. The overall lack of significant differences in photochemical parameters among treatments at lower concentrations can be explained by the earlier NH_4^+ sensitivity findings in which a 100 μM NH_4^+ treatment did not significantly differ in relative fluorescence from the control by T_{final} . While 2.85% addition of the algicide reduced cell density by 50% in the controls, these sensitivity findings suggest that this was unlikely due to the ammonium present within the algicide, as well as unlikely due to impacts on the chloroplast function.

These results indicate that, while high NH_4^+ concentrations can be toxic, it is not solely responsible for the algicidal activity of IRI-160AA. The photochemical parameters investigated here consistently exhibited significantly different results between the NH_4^+ and IRI-160AA treatments. Exposure to the algicide resulted in greater detrimental effects to photosystem II function compared to NH_4^+ alone. Future research should focus on the chemical characterization of other active compounds within IRI-160AA. A number of small polyamines including, but not limited to, putrescine, n-butylamine, diethylamine, spermine, and spermidine have been identified in IRI-160AA (Ternon et al. in prep). Some of these compounds have been

shown to affect algal growth, metabolism, and photosynthetic apparatus function (Kotzabasis et al., 1999; Czerpak et al., 2003; Theiss et al., 2004). The potential for independent or synergistic algicidal effects of these compounds is of great interest and will elucidate key facets of IRI-160AA function.

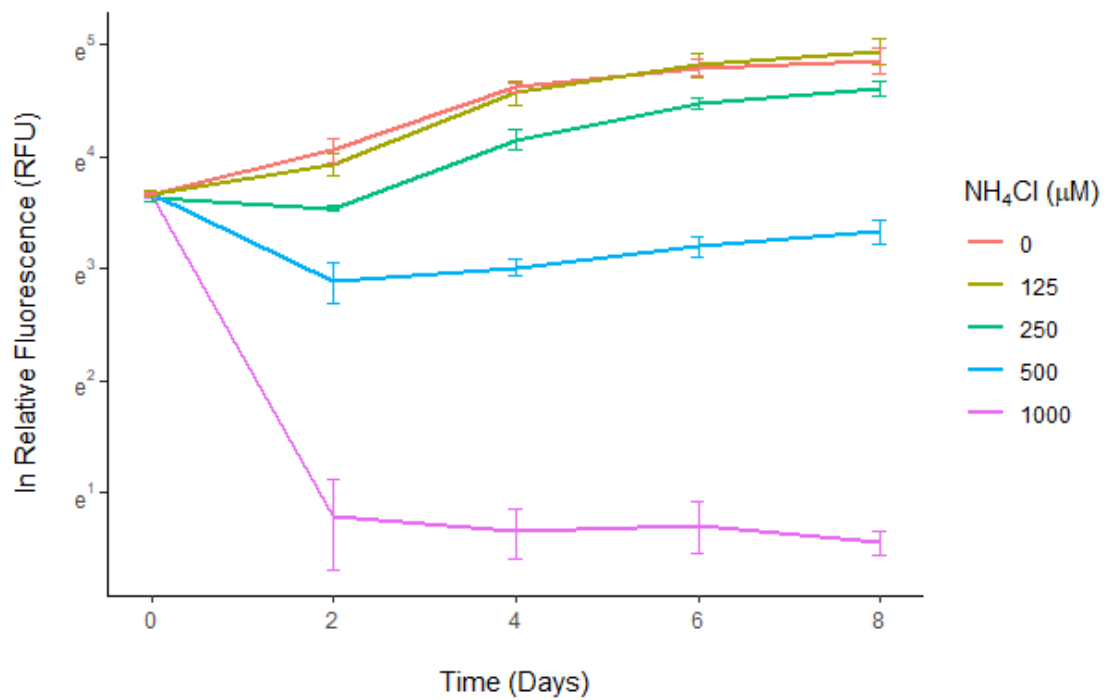


Figure 4.1 Relative fluorescence of non-axenic cultured *Prorocentrum minimum* over the course of 8 days after initial exposure to varying concentrations of NH_4Cl dissolved in *f/2* growth medium. Error bars represent standard deviation.

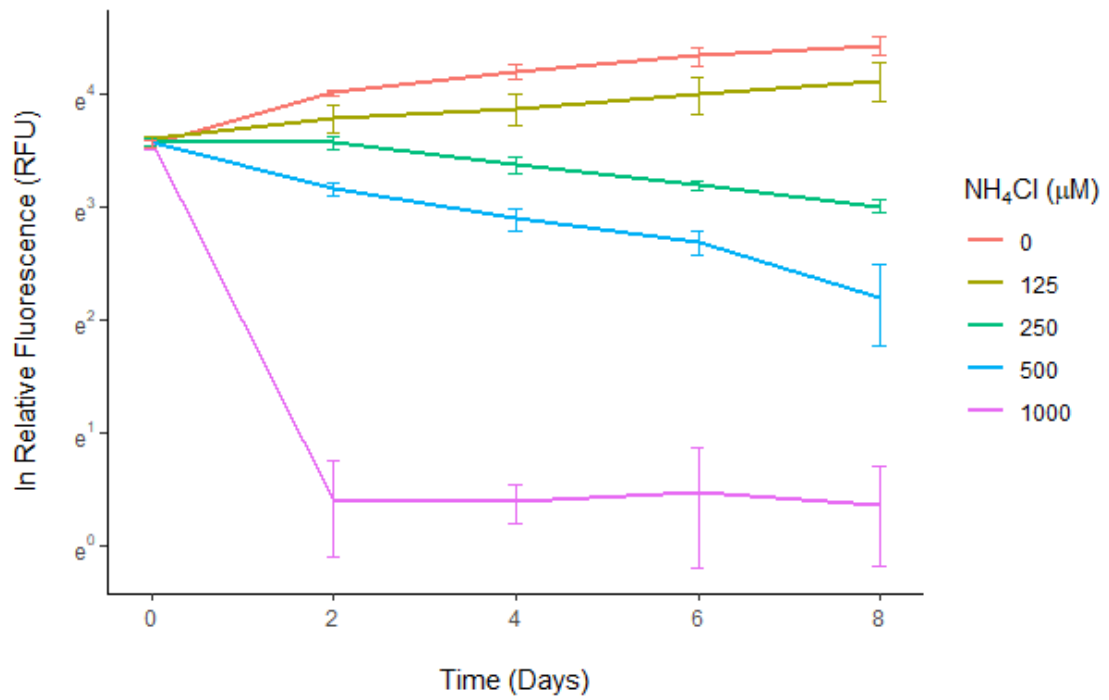


Figure 4.2 Relative fluorescence of non-axenic cultured *Gyrodinium instriatum* over the course of 8 days after initial exposure to varying concentrations of NH_4Cl dissolved in *f/2* growth medium. Error bars represent standard deviation.

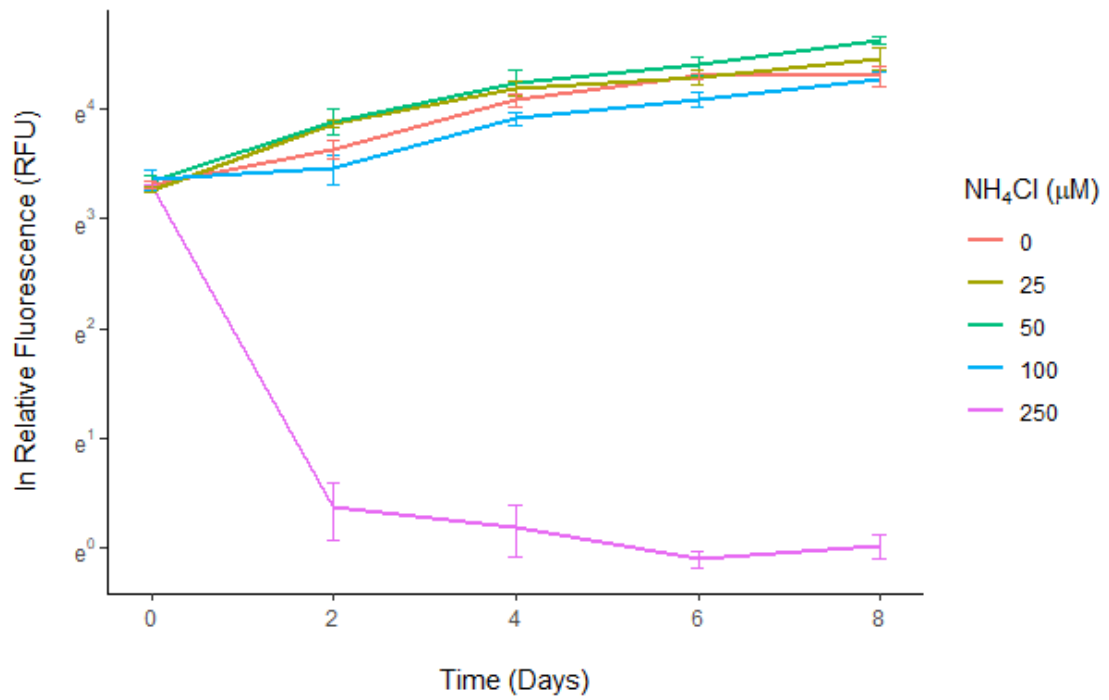


Figure 4.3 Relative fluorescence of non-axenic cultured *Karlodinium veneficum* over the course of 8 days after initial exposure to varying concentrations of NH_4Cl dissolved in *f/2* growth medium. Error bars represent standard deviation.

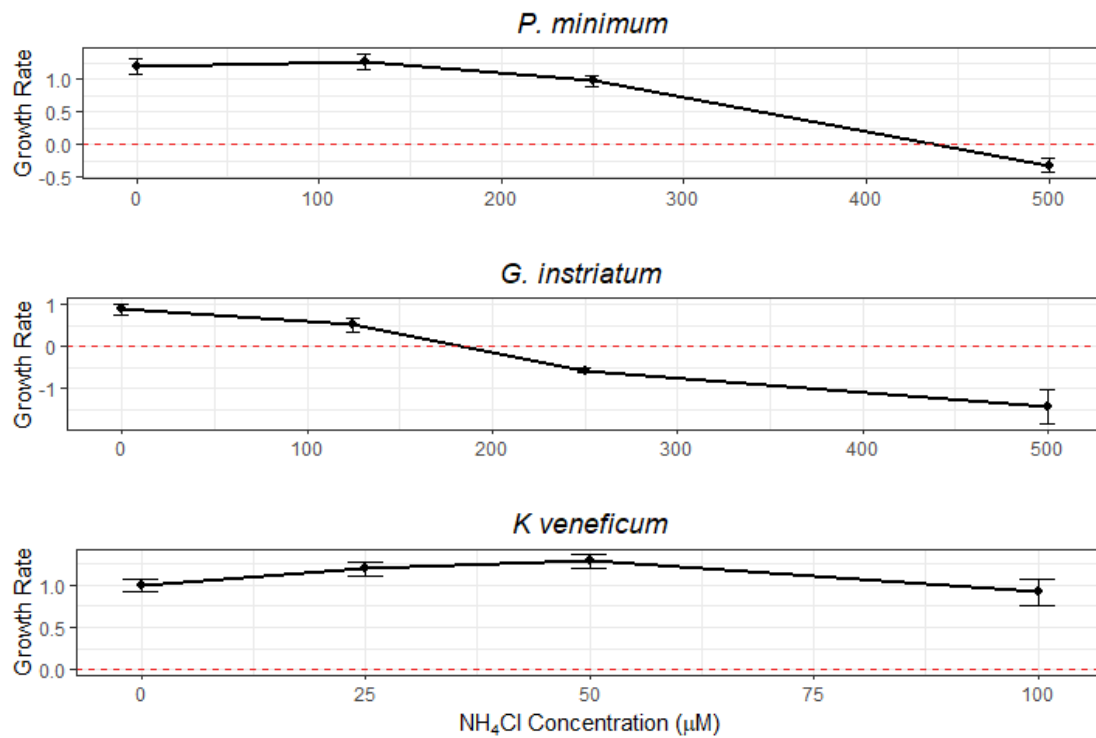


Figure 4.4 Growth rates for the three dinoflagellate species tested in the NH₄⁺ sensitivity experiments. The dashed red line indicates the point at which growth becomes static. *K. veneficum* has a diminished range due to increased sensitivity. Highest NH₄⁺ concentrations were omitted from calculations due to fluorescence measurements of 0 RFU. Error bars represent standard deviation.

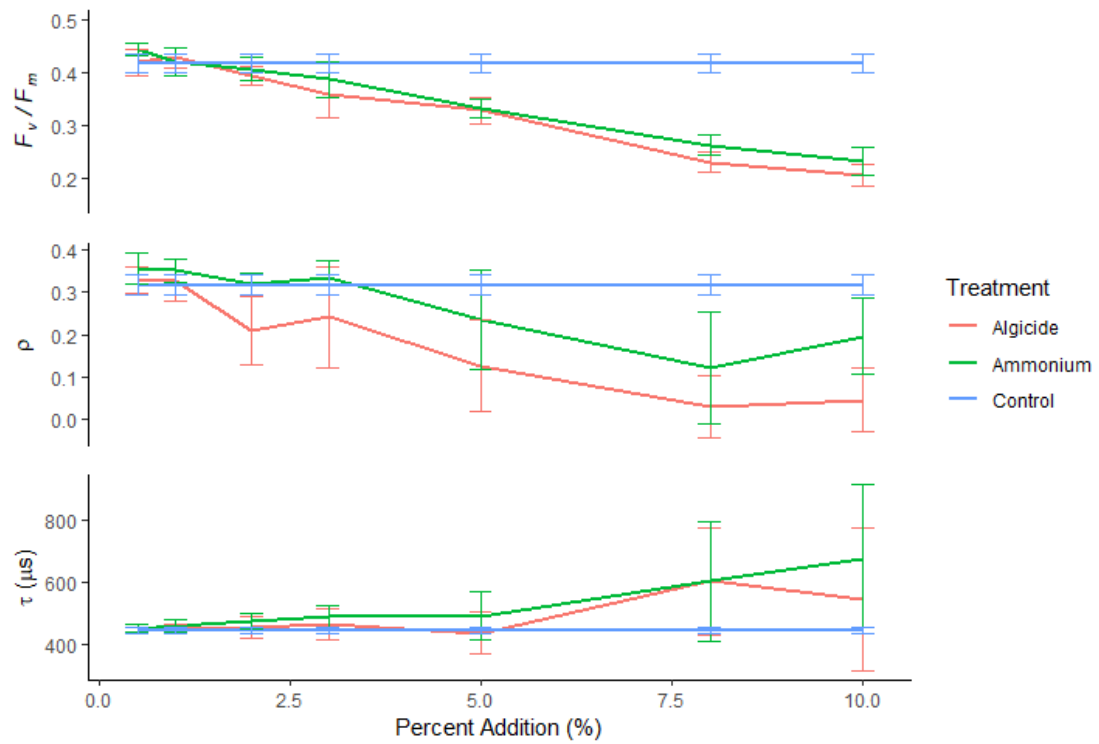


Figure 4.5 Three parameters measured across three treatments during the 18-hour photochemical experiment conducted on January 27, 2018. F_v/F_m represents the maximum yield of PSII, ρ represents the photochemical connectivity between PSII reaction centers, and τ represents the amount of time it took to re-oxidize the primary quinone. Error bars are indicative of standard deviation.

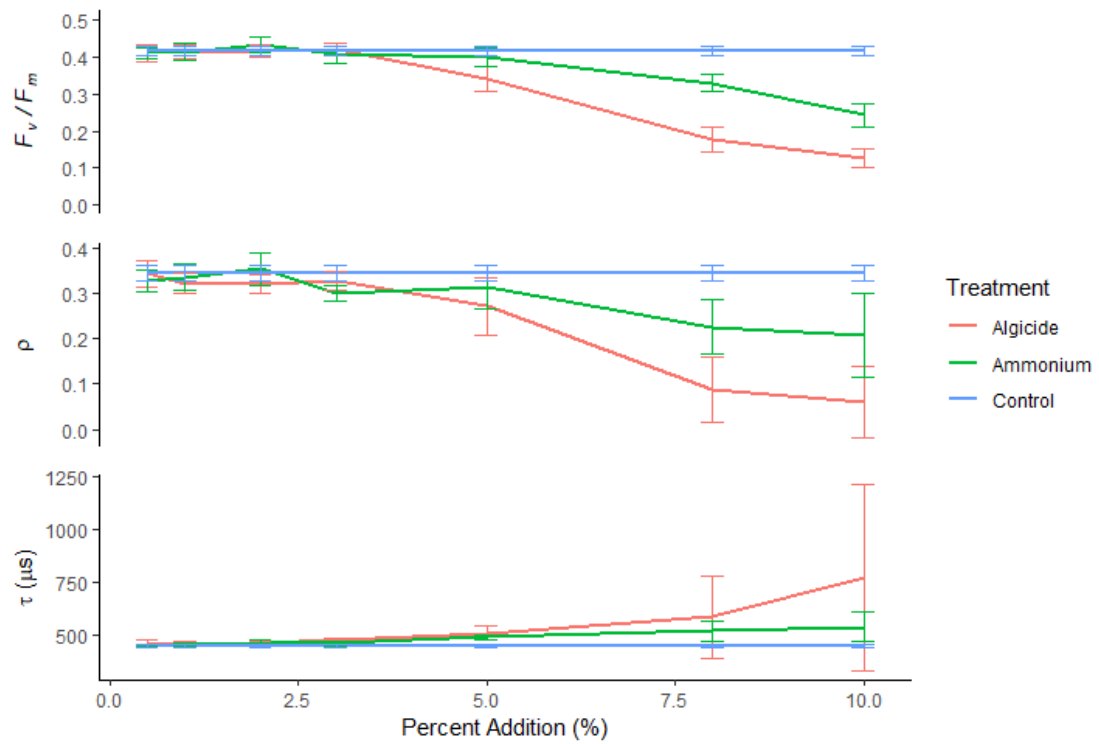


Figure 4.6 Three parameters measured across three treatments during the 18-hour photochemical experiment conducted on April 11, 2018. F_v/F_m represents the maximum yield of PSII, ρ represents the photochemical connectivity between PSII reaction centers, and τ represents the amount of time it took to re-oxidize the primary quinone. Error bars are indicative of standard deviation.

Chapter 5

CONCLUDING REMARKS

This research project assessed three primary objectives relating to the characterization and potential implementation of the algicide IRI-160AA: (1) to determine whether the algicide has a significant effect on microbial community composition during or after repeated dosing, (2) to determine whether the algicide has a significant effect on microzooplankton grazing rates in natural communities, and (3) to determine the extent to which ammonium contributes to the algicidal effect of IRI-160AA.

The community response results discussed in Chapter 2 demonstrate that microalgal communities are capable of maintaining certain levels of photosynthetic biomass across treatment concentrations in the presence of repeatedly-dosed, dinoflagellate-specific algicide. Dinoflagellates were removed from the communities at higher IRI-160AA concentrations as evidenced by both qPCR and sequencing data yet mean daily growth rates were not significantly different by T_{final} . The T-RFLP data showed that community composition was shifting as a result of both exposure to the algicide as well as experiment duration, and those shifts in composition likely strongly affect the cycling of dissolved nutrients and DOC. Overall, the research discussed in Chapter 2 demonstrates that repeated application of the algicide to natural communities will effectively decrease dinoflagellate abundance. This will cause shifts in the microbial eukaryotic community but will not perturb the function of the ecosystem based on the parameters considered here.

The results of Chapter 3 indicate that application of the algicide at EC50 levels will not negatively impact microzooplankton grazing rates in natural communities.

Grazing rates associated with algicide treatment were shown to either be significantly greater than those in the control or not significantly different from those in the control based on community composition. Communities did shift based on T-RFLP data but, just as in the repeated dosing experiments, shifts in community structure did not result in negative impacts to non-target, microbial, eukaryotic organisms.

The ammonium sensitivity results in Chapter 4, in combination with the photochemical results, suggest that ammonium is not solely responsible for the full extent of the algicidal effects of IRI-160AA. Data collected for maximum yield of photosystem II (F_v/F_m), photochemical connectivity between photosystem II reaction centers (ρ), and the re-oxidation rate of the primary quinone (τ) all indicate that ammonium negatively affects the photosynthetic machinery of photosystem II but not to the same extent as the algicide. This holds true across multiple concentrations of application, not just at EC50 levels. Additionally, a growth-derived EC50 concentration for the algicide was not potent enough to be a photochemically-derived EC50 suggesting that photosystem II is perhaps a secondary target of IRI-160AA.

This study demonstrates that application of the algicide to communities densely populated with dinoflagellates is an effective, highly-specific approach to preventing, controlling, and mitigating harmful algal blooms. Prior to a proper field demonstration, future work should aim to understand potential impacts on other relevant metazoan species including invertebrates and fish, as well as bacterial assemblages. Additionally, ongoing characterization efforts are integral to assessing impacts to target and non-target species alike. Elucidating the extent of the algicide's specificity will help determine the viability of this compound as HAB control measure in the Delaware Inland Bays and perhaps elsewhere.

REFERENCES

- Akselman, R., Negri, R.M., 2012. Blooms of *Azadinium* cf. *spinosum* Elbrächter et Tillmann (Dinophyceae) in northern shelf waters of Argentina, Southwestern Atlantic. *Harmful Algae* 19, 30–38. <https://doi.org/10.1016/j.hal.2012.05.004>
- Akselman, R., Negri, R.M., Cozzolino, E., 2014. *Azadinium* (Amphidomataceae, Dinophyceae) in the Southwest Atlantic: In situ and satellite observations. *Rev. Biol. Mar. Oceanogr.* 49, 511–526. <https://doi.org/10.4067/S0718-19572014000300008>
- Altschul, S.F., Gish, W., Miller, W., Myers, E.W., Lipman, D.J., 1990. Basic local alignment search tool. *J. Mol. Biol.* 215, 403–410. [https://doi.org/10.1016/S0022-2836\(05\)80360-2](https://doi.org/10.1016/S0022-2836(05)80360-2)
- Anderson, D.M., 2004. Prevention, control, and mitigation of harmful algal blooms: multiple approaches to HAB management, in: Hall, S., Etheridge, S., Anderson, D., Kleindinst, J., Zhu, M., Zou, Y. (Eds.), *Harmful Algae Management and Mitigation*. Asia-Pacific Economic Cooperation, Singapore, pp. 123–130.
- Anderson, D.M., Burkholder, J.M., Cochlan, W.P., Glibert, P.M., Gobler, C.J., Heil, C.A., Kudela, R.M., Parsons, M.L., Jack Rensel, J.E., Townsend, D.W., Trainer, V.L., Vargo, G.A., 2008. Harmful algal blooms and eutrophication: Examining linkages from selected coastal regions of the United States. *Harmful Algae* 39–53. <https://doi.org/10.1016/j.hal.2008.08.017>
- Anderson, D.M., Glibert, P.M., Burkholder, J.M., 2002. Harmful Algal Blooms and Eutrophication Nutrient Sources, Composition, and Consequences. *Estuaries* 25, 704–726.
- Aquino-Cruz, A., Okolodkov, Y.B., 2016. Impact of increasing water temperature on growth, photosynthetic efficiency, nutrient consumption, and potential toxicity of *Amphidinium* cf. *carterae* and *Coolia monotis* (Dinoflagellata). *Rev. Biol. Mar. Oceanogr.* 51, 565–580. <https://doi.org/10.4067/S0718-19572016000300008>
- Azad, H.S., Borchardt, J.A., 1970. Variations in phosphorus uptake by algae. *Environ. Sci. Technol.* 4, 737–743. <https://doi.org/10.1021/es60044a008>
- Bachmann, R.W., Hoyer, M. V., Fernandez, C., Canfield, D.E., 2003. An Alternative to Proposed Phosphorus TMDLs for the Management of Lake Okeechobee. *Lake Reserv. Manag.* 19, 251–264. <https://doi.org/10.1080/07438140309354090>

- Bais, H.P., 2003. Allelopathy and Exotic Plant Invasion: From Molecules and Genes to Species Interactions. *Science* (80-.). 301, 1377–1380. <https://doi.org/10.1126/science.1083245>
- Baker, N.R., 2008. Chlorophyll Fluorescence: A Probe of Photosynthesis In Vivo. *Annu. Rev. Plant Biol.* 59, 89–113. <https://doi.org/10.1146/annurev.arplant.59.032607.092759>
- Berg, G.M., Driscoll, S., Hayashi, K., Ross, M., Kudela, R., 2017. Variation in growth rate, carbon assimilation, and photosynthetic efficiency in response to nitrogen source and concentration in phytoplankton isolated from upper San Francisco Bay. *J. Phycol.* 53, 664–679. <https://doi.org/10.1111/jpy.12535>
- Berges, J., 1997. Miniview: algal nitrate reductases. *Eur. J. Phycol.* 32, 3–8. <https://doi.org/10.1080/09541449710001719315>
- Bidle, K.D., Bender, S.J., 2008. Iron Starvation and Culture Age Activate Metacaspases and Programmed Cell Death in the Marine Diatom *Thalassiosira pseudonana*. *Eukaryot. Cell* 7, 223–236. <https://doi.org/10.1128/EC.00296-07>
- Boesch, D.F., Brinsfield, R.B., Magnien, R.E., 2001. Chesapeake Bay eutrophication: scientific understanding, ecosystem restoration, and challenges for agriculture. *J. Environ. Qual.* 30, 303–20.
- Bourland, W.A., Wendell, L., Hampikian, G., Vd'áčný, P., 2014. Morphology and phylogeny of *Bryophryoides ocellatus* n. g., n. sp. (Ciliophora, Colpodea) from in situ soil percolates of Idaho, U.S.A. *Eur. J. Protistol.* 50, 47–67. <https://doi.org/10.1016/J.EJOP.2013.09.001>
- Bower, C.E., Holm-Hansen, T., 1980. A Salicylate–Hypochlorite Method for Determining Ammonia in Seawater. *Can. J. Fish. Aquat. Sci.* 37, 794–798. <https://doi.org/10.1139/f80-106>
- Burford, M.A., Pearson, D.C., 1998. Effect of different nitrogen sources on phytoplankton composition in aquaculture ponds. *Aquat. Microb. Ecol.* 15, 277–284.
- Burkill, P.H., Mantoura, R.F.C., Llewellyn, C.A., Owens, N.J.P., 1987. Microzooplankton grazing and selectivity of phytoplankton in coastal waters. *Mar. Biol.* 93, 581–590. <https://doi.org/10.1007/BF00392796>

- Calbet, A., Landry, M.R., 2004. Phytoplankton growth, microzooplankton grazing, and carbon cycling in marine systems. *Limnol. Oceanogr.* 49, 51–57. <https://doi.org/10.4319/lo.2004.49.1.0051>
- Calbet, A., Saiz, E., 2017. How much is enough for nutrients in microzooplankton dilution grazing experiments? *J. Plankton Res.* 0, 1–9. <https://doi.org/10.1093/plankt/fbx070>
- Camargo, J.A., Alonso, Á., 2006. Ecological and toxicological effects of inorganic nitrogen pollution in aquatic ecosystems: A global assessment. *Environ. Int.* 32, 831–849. <https://doi.org/10.1016/j.envint.2006.05.002>
- Casamayor, E.O., Massana, R., Benlloch, S., Ovreas, L., Diez, B., Goddard, V.J., Gasol, J.M., Joint, I., Rodriguez-Valera, F., Pedros-Alio, C., 2002. Changes in archaeal, bacterial and eukaryal assemblages along a salinity gradient by comparison of genetic fingerprinting methods in a multipond solar saltern. *Environ. Microbiol.* 4, 338–348. <https://doi.org/10.1046/j.1462-2920.2002.00297.x>
- Chariton, A.A., Ho, K.T., Proestou, D., Bik, H., Simpson, S.L., Portis, L.M., Cantwell, M.G., Baguley, J.G., Burgess, R.M., Pelletier, M.M., Perron, M., Gunsch, C., Matthews, R.A., 2014. A molecular-based approach for examining responses of eukaryotes in microcosms to contaminant-spiked estuarine sediments. *Environ. Toxicol. Chem.* 33, 359–369. <https://doi.org/10.1002/etc.2450>
- Clarke, K.R., Gorley, R.N., 2015. PRIMER v7 : User Manual/Tutorial.
- Coats, D.W., Kim, S., Bachvaroff, T.R., Handy, S.M., Delwiche, C.F., 2010. *Tintinnophagus acutus* n. g., n. sp. (Phylum Dinoflagellata), an Ectoparasite of the Ciliate *Tintinnopsis cylindrica* Daday 1887, and Its Relationship to *Duboscquodinium collini* Grassé 1952. *J. Eukaryot. Microbiol.* 57, 468–482. <https://doi.org/10.1111/j.1550-7408.2010.00504.x>
- Collos, Y., Harrison, P.J., 2014. Acclimation and toxicity of high ammonium concentrations to unicellular algae. *Mar. Pollut. Bull.* 80, 8–23. <https://doi.org/10.1016/j.marpolbul.2014.01.006>
- Cosgrove, J., Borowitzka, M.A., 2010. Chlorophyll fluorescence terminology: an introduction, in: Suggett, D.J., Prasil, O.J., Borowitzka, M.A. (Eds.), *Chlorophyll a Fluorescence in Aquatic Sciences: Methods and Applications*. Springer, Dordrecht, The Netherlands, pp. 1–18.

- Countway, P.D., Caron, D.A., 2006. Abundance and Distribution of *Ostreococcus* sp. in the San Pedro Channel, California, as Revealed by Quantitative PCR. *Appl. Environ. Microbiol.* 72, 2496–2506. <https://doi.org/10.1128/AEM.72.4.2496-2506.2006>
- Coyne, K.J., Handy, S.M., Demir, E., Whereat, E.B., Hutchins, D.A., Portune, K.J., Doblin, M.A., Cary, S.C., 2005. Improved quantitative real-time PCR assays for enumeration of harmful algal species in field samples using an exogenous DNA reference standard. *Limnol. Oceanogr. Methods* 3, 381–391. <https://doi.org/10.4319/lom.2005.3.381>
- Coyne, K., Hutchins, D., Hare, C., Cary, S., 2001. Assessing temporal and spatial variability in *Pfiesteria piscicida* distributions using molecular probing techniques. *Aquat. Microb. Ecol.* 24, 275–285. <https://doi.org/10.3354/ame024275>
- Culman, S.W., Bukowski, R., Gauch, H.G., Cadillo-Quiroz, H., Buckley, D.H., 2009. T-REX: software for the processing and analysis of T-RFLP data. *BMC Bioinformatics* 10, 171. <https://doi.org/10.1186/1471-2105-10-171>
- Czerpak, R., Bajguz, A., Piotrowska, A., Dobrogowska, R., Matejczyk, M., Wiesławski, W., 2011. Biochemical activity of di- and polyamines in the green alga *Chlorella vulgaris* Beijerinck (Chlorophyceae). *Acta Soc. Bot. Pol.* 72, 19–24. <https://doi.org/10.5586/asbp.2003.003>
- Dai, X., Lu, D., Guan, W., Wang, H., He, P., Xia, P., Yang, H., 2014. Newly recorded *Karlodinium veneficum* dinoflagellate blooms in stratified water of the East China Sea. *Deep Sea Res. Part II Top. Stud. Oceanogr.* 101, 237–243. <https://doi.org/10.1016/j.dsr2.2013.01.015>
- Diaz, M.R., Jacobson, J.W., Goodwin, K.D., Dunbar, S.A., Fell, J.W., 2010. Molecular detection of harmful algal blooms (HABs) using locked nucleic acids and bead array technology. *Limnol. Oceanogr. Methods* 8, 269–284. <https://doi.org/10.4319/lom.2010.8.269>
- Doucette, G.J., McGovern, E.R., Babinchak, J.A., 1999. ALGICIDAL BACTERIA ACTIVE AGAINST *GYMNODINIUM BREVE* (DINOPHYCEAE). I. BACTERIAL ISOLATION AND CHARACTERIZATION OF KILLING ACTIVITY1,3. *J. Phycol.* 35, 1447–1454. <https://doi.org/10.1046/j.1529-8817.1999.3561447.x>
- DROOP, M.R., 1953. Phagotrophy in *Oxyrrhis marina* Dujardin. *Nature* 172, 250–251. <https://doi.org/10.1038/172250b0>

- Duran, R., Bonin, P., Jezequel, R., Dubosc, K., Gassie, C., Terrisse, F., Abella, J., Cagnon, C., Milton, C., Michotey, V., Gilbert, F., Cuny, P., Cravo-Laureau, C., 2015. Effect of physical sediments reworking on hydrocarbon degradation and bacterial community structure in marine coastal sediments. *Environ. Sci. Pollut. Res.* 22, 15248–15259. <https://doi.org/10.1007/s11356-015-4373-2>
- FREUDENTHAL, H.D., LEE, J.J., 1963. *Glenodinium halli* * n. sp. and *Gyrodinium instriatum* n. sp., Dinoflagellates from New York Waters**. *J. Protozool.* 10, 182–189. <https://doi.org/10.1111/j.1550-7408.1963.tb01659.x>
- Gleason, F.K., Baxa, C.A., 1986. Activity of the natural algicide, cyanobacterin, on eukaryotic microorganisms. *FEMS Microbiol. Lett.* 33, 85–88. <https://doi.org/10.1111/j.1574-6968.1986.tb01217.x>
- Gleason, F.K., Paulson, J.L., 1984. Site of action of the natural algicide, cyanobacterin, in the blue-green alga, *Synechococcus* sp. *Arch. Microbiol.* 138, 273–277. <https://doi.org/10.1007/BF00402134>
- Glibert, P.M., Anderson, D.M., Gentien, P., Graneli, E., Sellner, K.G., 2005. Harmful Algal Blooms Th e Global, of Phenomena Complex. *Oceanography* 18, 136–147.
- Glibert, P.M., Wilkerson, F.P., Dugdale, R.C., Raven, J.A., Dupont, C.L., Leavitt, P.R., Parker, A.E., Burkholder, J.M., Kana, T.M., 2016. Pluses and minuses of ammonium and nitrate uptake and assimilation by phytoplankton and implications for productivity and community composition, with emphasis on nitrogen-enriched conditions. *Limnol. Oceanogr.* 61, 165–197. <https://doi.org/10.1002/lno.10203>
- Gobler, C.J., Deonaraine, S., Leigh-Bell, J., Gastrich, M.D., Anderson, O.R., Wilhelm, S.W., 2004. Ecology of phytoplankton communities dominated by *Aureococcus anophagefferens*: the role of viruses, nutrients, and microzooplankton grazing. *Harmful Algae* 3, 471–483. <https://doi.org/10.1016/j.hal.2004.06.013>
- Gopal, B., Goel, U., 1993. Competition and Allelopathy in Aquatic Plant Communities. *Bot. Rev.* 59, 155–210.
- Graham, S., Strom, S., 2010. Growth and grazing of microzooplankton in response to the harmful alga *Heterosigma akashiwo* in prey mixtures. *Aquat. Microb. Ecol.* 59, 111–124. <https://doi.org/10.3354/ame01391>
- Gross, E.M., 2003. Allelopathy of Aquatic Autotrophs. *CRC. Crit. Rev. Plant Sci.* 22, 313–339. <https://doi.org/10.1080/713610859>

- Gruber, N., 2008. The marine nitrogen cycle: overview and challenges, in: Capone, D.G., Bronk, D.A., Mulholland, M.R., Carpenter, E.J. (Eds.), Nitrogen in the Marine Environment. Academic Press, Cambridge, MA, pp. 1–50.
- Guerrero, M.G., Vega, J.M., Losada, M., 1981. The Assimilatory Nitrate-Reducing System and its Regulation. *Annu. Rev. Plant Physiol.* 32, 169–204.
<https://doi.org/10.1146/annurev.pp.32.060181.001125>
- Guillard, R.R.L., 1975. Culture of Phytoplankton for Feeding Marine Invertebrates, in: Culture of Marine Invertebrate Animals. Springer US, Boston, MA, pp. 29–60.
https://doi.org/10.1007/978-1-4615-8714-9_3
- Gustafsson, S., Hultberg, M., Figueroa, R.I., Rengefors, K., 2009. On the control of HAB species using low biosurfactant concentrations. *Harmful Algae* 8, 857–863.
<https://doi.org/10.1016/J.HAL.2009.04.002>
- Gutiérrez-Rodríguez, A., Selph, K.E., Landry, M.R., 2016. Phytoplankton growth and microzooplankton grazing dynamics across vertical environmental gradients determined by transplant *in situ* dilution experiments. *J. Plankton Res.* 38, 271–289. <https://doi.org/10.1093/plankt/fbv074>
- Hallegraeff, G.M., 1993. A review of harmful algal blooms and their apparent global increase*. *Phycologia* 32, 79–99.
- Hallegraeff, G.M., Anderson, D.M. (Donald M., Cembella, A.D., Enevoldsen, H.O. (Henrik O., Unesco., 2003. Manual on harmful marine microalgae. UNESCO, Paris, France.
- Handy, S.M., Demir, E., Hutchins, D.A., Portune, K.J., Whereat, E.B., Hare, C.E., Rose, J.M., Warner, M., Farestad, M., Cary, S.C., Coyne, K.J., 2008. Using quantitative real-time PCR to study competition and community dynamics among Delaware Inland Bays harmful algae in field and laboratory studies. *Harmful Algae* 7, 599–613. <https://doi.org/10.1016/J.HAL.2007.12.018>
- Hansen, F., Witte, H., Passarge, J., 1996. Grazing in the heterotrophic dinoflagellate *Oxyrrhis marina*: size selectivity and preference for calcified *Emiliania huxleyi* cells. *Aquat. Microb. Ecol.* 10, 307–313. <https://doi.org/10.3354/ame010307>
- Hansen, G., 1995. Analysis of the thecal plate pattern in the dinoflagellate *Heterocapsa rotundata* (Lohmann) comb. nov. (= *Katodinium rotundatum* (Lohmann) Loeblich), *Phycologia*.

- Hare, C.E., Demir, E., Coyne, K.J., Craig Cary, S., Kirchman, D.L., Hutchins, D.A., 2005. A bacterium that inhibits the growth of *Pfiesteria piscicida* and other dinoflagellates. *Harmful Algae* 4, 221–234.
<https://doi.org/10.1016/j.hal.2004.03.001>
- Hecky, R.E., Kilham, P., 1988. Nutrient limitation of phytoplankton in freshwater and marine environments: A review of recent evidence on the effects of enrichment I. *Limnol. Ocean.* 33, 196–822.
- Heisler, J., Glibert, P.M., Burkholder, J.M., Anderson, D.M., Cochlan, W., Dennison, W.C., Dortch, Q., Gobler, C.J., Heil, C.A., Humphries, E., Lewitus, A., Magnien, R., Marshall, H.G., Sellner, K., Stockwell, D.A., Stoecker, D.K., Suddleson, M., 2008. Eutrophication and harmful algal blooms: A scientific consensus. *Harmful Algae* 8, 3–13. <https://doi.org/10.1016/j.hal.2008.08.006>
- Higo, S., Maung-Saw-Htoo-Thaw, Yamatogi, T., Ishida, N., Hirae, S., Koike, K., 2017. Application of a pulse-amplitude-modulation (PAM) fluorometer reveals its usefulness and robustness in the prediction of *Karenia mikimotoi* blooms: A case study in Sasebo Bay, Nagasaki, Japan. *Harmful Algae* 61, 63–70.
<https://doi.org/10.1016/j.hal.2016.11.013>
- Hii, Y.S., Soo, C.L., Chuah, T.S., Mohd-Azmi, A., Abol-Munafi, A.B., 2011. Interactive effect of ammonia and nitrate on the nitrogen uptake by *Nannochloropsis* sp. *J. Sustain. Sci. Manag.* 6, 60–68.
- Hoagland, P., Scatasta, S., 2006. The Economic Effects of Harmful Algal Blooms, in: *Ecology of Harmful Algae*. Springer Berlin Heidelberg, pp. 391–402.
https://doi.org/10.1007/978-3-540-32210-8_30
- Iglesias-Rodriguez, D., Croot, P., Cai, Z., Zhou, J., Richlen, M.L., Sehein, T.R., Kulis, D.M., Anderson, D.M., 2018. Microbial Community Structure and Associations During a Marine Dinoflagellate Bloom.
<https://doi.org/10.3389/fmicb.2018.01201>
- Inderjit, Dakshini, K.M.M., 1994. Algal allelopathy. *Bot. Rev.* 60, 182–196.
<https://doi.org/10.1007/BF02856576>
- Janofske, D., 2000. *Scrippsiella trochoidea* and *scrippsiella regalis*, nov. comb. (peridinales, dinophyceae): a comparison. *J. Phycol.* 36, 178–189.
<https://doi.org/10.1046/j.1529-8817.2000.98224.x>
- Jeong, S.-Y., Ishida, K., Ito, Y., Okada, S., Murakami, M., 2003. Bacillamide, a novel algicide from the marine bacterium, *Bacillus* sp. SY-1, against the harmful

- dinoflagellate, *Cochlodinium polykrikoides*. *Tetrahedron Lett.* 44, 8005–8007. <https://doi.org/10.1016/J.TETLET.2003.08.115>
- Jia, Y., Yang, Z., Su, W., Johnson, D., Kong, F., 2014. Controlling of cyanobacteria bloom during bottleneck stages of algal cycling in shallow Lake Taihu (China). *J. Freshw. Ecol.* 29, 129–140. <https://doi.org/10.1080/02705060.2013.844206>
- Johnk, K.D., Huisman, J., Sharples, J., Sommeijer, B., Visser, P.M., Stroom, J.M., 2008. Summer heatwaves promote blooms of harmful cyanobacteria. *Glob. Chang. Biol.* 14, 495–512. <https://doi.org/10.1111/j.1365-2486.2007.01510.x>
- Kim, D.Y., Countway, P.D., Yamashita, W., Caron, D.A., 2012. A combined sequence-based and fragment-based characterization of microbial eukaryote assemblages provides taxonomic context for the Terminal Restriction Fragment Length Polymorphism (T-RFLP) method. *J. Microbiol. Methods* 91, 527–536. <https://doi.org/10.1016/j.mimet.2012.09.026>
- Kim, Y.S., Lee, D.-S., Jeong, S.-Y., Lee, W.J., Lee, M.-S., 2009. Isolation and characterization of a marine algicidal bacterium against the harmful raphidophyceae *Chattonella marina*. *J. Microbiol.* 47, 9–18. <https://doi.org/10.1007/s12275-008-0141-z>
- Kolber, Z.S., Prášil, O., Falkowski, P.G., 1998. Measurements of variable chlorophyll fluorescence using fast repetition rate techniques: defining methodology and experimental protocols. *Biochim. Biophys. Acta - Bioenerg.* 1367, 88–106. [https://doi.org/10.1016/S0005-2728\(98\)00135-2](https://doi.org/10.1016/S0005-2728(98)00135-2)
- Kotzabasis, K., Strasser, B., Navakoudis, E., Senger, H., Dörnemann, D., 1999. The regulatory role of polyamines in structure and functioning of the photosynthetic apparatus during photoadaptation. *J. Photochem. Photobiol. B Biol.* 50, 45–52. [https://doi.org/10.1016/S1011-1344\(99\)00067-6](https://doi.org/10.1016/S1011-1344(99)00067-6)
- Lananan, F., Jusoh, A., Ali, N., Lam, S.S., Endut, A., 2013. Effect of Conway Medium and f/2 Medium on the growth of six genera of South China Sea marine microalgae. *Bioresour. Technol.* 141, 75–82. <https://doi.org/10.1016/j.biortech.2013.03.006>
- Landry, M.R., Hassett, R.P., 1982. Estimating the grazing impact of marine microzooplankton. *Mar. Biol.* 67, 283–288. <https://doi.org/10.1007/BF00397668>
- Leu, E., Krieger-Liszkay, A., Goussias, C., Gross, E.M., 2002. Polyphenolic Allelochemicals from the Aquatic Angiosperm *Myriophyllum spicatum* Inhibit

- Photosystem II. *PLANT Physiol.* 130, 2011–2018.
<https://doi.org/10.1104/pp.011593>
- Levine, J.M., Vila, M., Antonio, C.M.D., Dukes, J.S., Grigulis, K., Lavorel, S., 2003. Mechanisms underlying the impacts of exotic plant invasions. *Proc. R. Soc. B Biol. Sci.* 270, 775–781. <https://doi.org/10.1098/rspb.2003.2327>
- Li, A., Stoecker, D.K., Coats, D.W., Coats, D.W., 2000. MIXOTROPHY IN *GYRODINIUM GALATHEANUM* (DINOPHYCEAE): GRAZING RESPONSES TO LIGHT INTENSITY AND INORGANIC NUTRIENTS 1, *J. Phycol.*
- Li, Z., Lin, S., Liu, X., Tan, J., Pan, J., Yang, H., 2014. A freshwater bacterial strain, *Shewanella* sp. Lzh-2, isolated from Lake Taihu and its two algicidal active substances, hexahydropyrrolo[1,2-a]pyrazine- 1,4-dione and 2, 3-indolinedione. *Appl. Microbiol. Biotechnol.* 98, 4737–4748. <https://doi.org/10.1007/s00253-014-5602-1>
- Linacre, L., 2017. Microzooplankton grazing impact on the phytoplankton community at a coastal upwelling station off northern Baja California, Mexico. *Ciencias Mar.* 40, 93–108. <https://doi.org/10.7773/cm.v43i2.2753>
- Lindström, S., Rowe, O., Timonen, S., Sundström, L., Johansson, H., 2018. Trends in bacterial and fungal communities in ant nests observed with Terminal-Restriction Fragment Length Polymorphism (T-RFLP) and Next Generation Sequencing (NGS) techniques—validity and compatibility in ecological studies. *PeerJ* 6, e5289. <https://doi.org/10.7717/peerj.5289>
- Liu, W., Marsh, T., Cheng, H., Forney, L., 1997. Characterization of microbial diversity by determining terminal restriction fragment length polymorphisms of genes encoding 16S rRNA. *Appl. Environ. Microbiol.* 63, 4516–4522.
- Lord, N.S., Kaplan, C.W., Shank, P., Kitts, C.L., Elrod, S.L., 2002. Assessment of fungal diversity using terminal restriction fragment (TRF) pattern analysis: comparison of 18S and ITS ribosomal regions. *FEMS Microbiol. Ecol.* 42, 327–337. <https://doi.org/10.1111/j.1574-6941.2002.tb01022.x>
- Main, C.R., Salvitti, L.R., Whereat, E.B., Coyne, K.J., 2015. Community-Level and Species-Specific Associations between Phytoplankton and Particle-Associated *Vibrio* Species in Delaware’s Inland Bays. *Appl. Environ. Microbiol.* 81, 5703–5713. <https://doi.org/10.1128/AEM.00580-15>

- Malerba, M.E., Connolly, S.R., Heimann, K., 2015. An experimentally validated nitrate-ammonium-phytoplankton model including effects of starvation length and ammonium inhibition on nitrate uptake. *Ecol. Modell.* 317, 30–40. <https://doi.org/10.1016/j.ecolmodel.2015.08.024>
- Manahan, D., Crisp, D., 1982. The Role of Dissolved Organic Material in the Nutrition of Pelagic Larvae: Amino Acid Uptake by Bivalve Veligers. *Am. Zool.* 22, 635–646.
- Miller, C.A., Penry, D.L., Glibert, P.M., 1995. The impact of trophic interactions on rates of nitrogen regeneration and grazing in Chesapeake Bay. *Limnol. Oceanogr.* 40, 1005–1011. <https://doi.org/10.4319/lo.1995.40.5.1005>
- Millette, N.C., Pierson, J.J., Aceves, A., Stoecker, D.K., 2017. Mixotrophy in *Heterocapsa rotundata*: A mechanism for dominating the winter phytoplankton. *Limnol. Oceanogr.* 62, 836–845. <https://doi.org/10.1002/lno.10470>
- Mills, J.D., 1986. Photophosphorylation, in: Hipkins, M.F., Baker, N.R. (Eds.), *Photosynthesis: Energy Transduction: A Practical Approach*. IRL Press, Oxford, UK, pp. 143–186.
- Møller, E.F., 2007. Production of dissolved organic carbon by sloppy feeding in the copepods *Acartia tonsa*, *Centropages typicus*, and *Temora longicornis*. *Limnol. Oceanogr.* 52, 79–84. <https://doi.org/10.4319/lo.2007.52.1.0079>
- O’Neil, J.M., Davis, T.W., Burford, M.A., Gobler, C.J., 2012. The rise of harmful cyanobacteria blooms: The potential roles of eutrophication and climate change. *Harmful Algae* 14, 313–334. <https://doi.org/10.1016/J.HAL.2011.10.027>
- Orsi, W., Biddle, J.F., Edgcomb, V., 2013. Deep Sequencing of Subseafloor Eukaryotic rRNA Reveals Active Fungi across Marine Subsurface Provinces. *PLoS One* 8, 56335. <https://doi.org/10.1371/journal.pone.0056335>
- Osborn, A.M., Moore, E.R.B., Timmis, K.N., 2000. An evaluation of terminal-restriction fragment length polymorphism (T-RFLP) analysis for the study of microbial community structure and dynamics. *Environ. Microbiol.* 2, 39–50. <https://doi.org/10.1046/j.1462-2920.2000.00081.x>
- Pokrzywinski, K.L., Place, A.R., Warner, M.E., Coyne, K.J., 2012. Investigation of the algicidal exudate produced by *Shewanella* sp. IRI-160 and its effect on dinoflagellates. *Harmful Algae* 19, 23–29. <https://doi.org/10.1016/j.hal.2012.05.002>

- Pokrzywinski, K.L., Tilney, C.L., Modla, S., Caplan, J.L., Ross, J., Warner, M.E., Coyne, K.J., 2017. Effects of the bacterial algicide IRI-160AA on cellular morphology of harmful dinoflagellates. *Harmful Algae* 62, 127–135. <https://doi.org/10.1016/j.hal.2016.12.004>
- Pokrzywinski, K.L., Tilney, C.L., Warner, M.E., Coyne, K.J., 2017. Cell cycle arrest and biochemical changes accompanying cell death in harmful dinoflagellates following exposure to bacterial algicide IRI-160AA. *Sci. Rep.* 7, 1–13. <https://doi.org/10.1038/srep45102>
- Prakash, A., Medcof, J.C., Tennant, A.D., 1971. *Paralytic Shellfish Poisoning in Eastern Canada*. Ottawa, Canada.
- Rasher, D.B., Hay, M.E., 2010. Chemically rich seaweeds poison corals when not controlled by herbivores. *Proc. Natl. Acad. Sci. U. S. A.* 107, 9683–8. <https://doi.org/10.1073/pnas.0912095107>
- Reigosa Roger, M.J., Pedrol, N., González, L., 2006. *Allelopathy : a physiological process with ecological implications*. Springer, Dordrecht, The Netherlands.
- Richardson, K., Fogg, G.E., 1982. The role of dissolved organic material in the nutrition and survival of marine dinoflagellates, *Phycologia*.
- Saba, G.K., Steinberg, D.K., Bronk, D.A., 2009. Effects of diet on release of dissolved organic and inorganic nutrients by the copepod *Acartia tonsa*. *Source Mar. Ecol. Prog. Ser.* 386, 147–161. <https://doi.org/10.3354/meps08070>
- Salas, R., Tillmann, U., John, U., Kilcoyne, J., Burson, A., Cantwell, C., Hess, P., Jauffrais, T., Silke, J., 2011. The role of *Azadinium spinosum* (Dinophyceae) in the production of azaspiracid shellfish poisoning in mussels. *Harmful Algae* 10, 774–783. <https://doi.org/10.1016/j.hal.2011.06.010>
- Sambrook, J., Fritsch, E.F., Maniatis, T., 1989. *Molecular cloning: A laboratory manual*, 2nd ed. Cold Spring Harbor Laboratory Press, Cold Spring Harbor, NY.
- Schmitz, A., Nagel, R., 1995. Influence of 3,4-Dichloroaniline (3,4-DCA) on Benthic Invertebrates in Indoor Experimental Streams. *Ecotoxicol. Environ. Saf.* 30, 63–71. <https://doi.org/10.1006/eesa.1995.1007>
- Schultz, M., Kiorboe, T., 2009. Active prey selection in two pelagic copepods feeding on potentially toxic and non-toxic dinoflagellates. *J. Plankton Res.* 31, 553–561. <https://doi.org/10.1093/plankt/fbp010>

- Schütte, U.M.E., Abdo, Z., Bent, S.J., Shyu, C., Williams, C.J., Pierson, J.D., Forney, L.J., 2008. Advances in the use of terminal restriction fragment length polymorphism (T-RFLP) analysis of 16S rRNA genes to characterize microbial communities. *Appl. Microbiol. Biotechnol.* 80, 365–380. <https://doi.org/10.1007/s00253-008-1565-4>
- Sebaugh, J.L., 2011. Guidelines for accurate EC50/IC50 estimation. *Pharm. Stat.* 10, 128–134. <https://doi.org/10.1002/pst.426>
- Sellner, K.G., Doucette, G.J., Kirkpatrick, G.J., 2003. Harmful algal blooms: causes, impacts and detection. *J. Ind. Microbiol. Biotechnol.* 30, 383–406. <https://doi.org/10.1007/s10295-003-0074-9>
- Selph, K., Goetze, E., Jungbluth, M., Lenz, P., Kolker, G., 2018. Microbial food web connections and rates in a subtropical embayment. *Mar. Ecol. Prog. Ser.* 590, 19–34. <https://doi.org/10.3354/meps12432>
- Sengco, M.R., 2009. Prevention and control of *Karenia brevis* blooms. *Harmful Algae* 8, 623–628. <https://doi.org/10.1016/J.HAL.2008.11.005>
- Singh, D.P., Tyagi, M.B., Kumar, A., Thakur, J.K., Kumar, A., 2001. Antialgal activity of a hepatotoxin-producing cyanobacterium, *Microcystis aeruginosa*. *World J. Microbiol. Biotechnol.* 17, 15–22. <https://doi.org/10.1023/A:1016622414140>
- Smayda, T.J., 1997. Harmful algal blooms: Their ecophysiology and general relevance to phytoplankton blooms in the sea. *Limnol. Oceanogr.* 42, 1137–1153. https://doi.org/10.4319/lo.1997.42.5_part_2.1137
- Smayda, T.J., 1989. Primary production and the global epidemic of phytoplankton blooms in the sea: A linkage?, in: Coper, E.M., Bricelj, V.M., Carpenter, E.J. (Eds.), *Novel Phytoplankton Blooms*. American Geophysical Union (AGU), pp. 449–483. <https://doi.org/10.1029/CE035p0449>
- Smith, G.D., Thanh Doan, N., 1999. Cyanobacterial metabolites with bioactivity against photosynthesis in cyanobacteria, algae and higher plants. *J. Appl. Phycol.* 11, 337–344. <https://doi.org/10.1023/A:1008115818348>
- Smith, V.H., Schindler, D.W., 2009. Eutrophication science: where do we go from here? *Trends Ecol. Evol.* 24, 201–207. <https://doi.org/10.1016/j.tree.2008.11.009>
- Sogin, M.L., Gunderson, J.H., 1987. Structural diversity of eukaryotic small subunit ribosomal RNAs. Evolutionary implications. *Ann. N. Y. Acad. Sci.* 503, 125–39.

- Strom, S.L., Benner, R., Ziegler, S., Dagg, M.J., 1997. Planktonic grazers are a potentially important source of marine dissolved organic carbon. *Limnol. Oceanogr.* 42, 1364–1374. <https://doi.org/10.4319/lo.1997.42.6.1364>
- Tada, K., Suksomjit, M., Ichimi, K., Funaki, Y., Montani, S., Yamada, M., Harrison, P.J., 2009. Diatoms grow faster using ammonium in rapidly flushed eutrophic Dokai Bay, Japan. *J. Oceanogr.* 65, 885–891. <https://doi.org/10.1007/s10872-009-0073-1>
- Terrado, R., Monier, A., Edgar, R., Lovejoy, C., 2015. Diversity of nitrogen assimilation pathways among microbial photosynthetic eukaryotes. *J. Phycol.* 51, 490–506. <https://doi.org/10.1111/jpy.12292>
- Theiss, C., Bohley, P., Bisswanger, H., Voigt, J., 2004. Uptake of polyamines by the unicellular green alga *Chlamydomonas reinhardtii* and their effect on ornithine decarboxylase activity. *J. Plant Physiol.* 161, 3–14. <https://doi.org/10.1078/0176-1617-00987>
- Tillmann, U., Elbrächter, M., John, U., Krock, B., 2011. A new non-toxic species in the dinoflagellate genus *Azadinium*: *A. poporum* sp. nov. *Eur. J. Phycol.* 46, 74–87. <https://doi.org/10.1080/09670262.2011.556753>
- Tillmann, U., Elbrächter, M., John, U., Krock, B., Cembella, A., 2010. *Azadinium obesum* (Dinophyceae), a new nontoxic species in the genus that can produce azaspiracid toxins. *Phycologia* 49, 169–182.
- Tillmann, U., Elbrächter, M., Krock, B., John, U., Cembella, A., 2009. *Azadinium spinosum* gen. et sp. nov. (Dinophyceae) identified as a primary producer of azaspiracid toxins. *Eur. J. Phycol.* 44, 63–79. <https://doi.org/10.1080/09670260802578534>
- Tilney, C.L., Pokrzywinski, K.L., Coyne, K.J., Warner, M.E., 2014. Growth, death, and photobiology of dinoflagellates (Dinophyceae) under bacterial-algicide control. *J. Appl. Phycol.* 26, 2117–2127. <https://doi.org/10.1007/s10811-014-0248-z>
- Tilney, C.L., Pokrzywinski, K.L., Coyne, K.J., Warner, M.E., 2014. Effects of a bacterial algicide, IRI-160AA, on dinoflagellates and the microbial community in microcosm experiments. *Harmful Algae* 39, 210–222. <https://doi.org/10.1016/j.hal.2014.08.001>
- Twiner, M.J., Rehmann, N., Hess, P., Doucette, G.J., 2008. Azaspiracid shellfish poisoning: a review on the chemistry, ecology, and toxicology with an emphasis

- on human health impacts. *Mar. Drugs* 6, 39–72.
<https://doi.org/10.3390/md20080004>
- Twomey, L.J., Piehler, M.F., Paerl, H.W., 2005. Phytoplankton uptake of ammonium, nitrate and urea in the Neuse River Estuary, NC, USA. *Hydrobiologia* 533, 123–134. <https://doi.org/10.1007/s10750-004-2403-z>
- Uchida, T., Kamiyama, T., Matsuyama, Y., 1997. Predation by a photosynthetic dinoflagellate *Gyrodinium instriatum* on loricated ciliates. *J. Plankton Res.* 19, 603–608. <https://doi.org/10.1093/plankt/19.5.603>
- United States Environmental Protection Agency, 1996. Ecological effects test guidelines II. OPPTS 850.5400 Algal Toxicity, Tiers I II 1–9.
- Van Dolah, F.M., 2000. Marine algal toxins: origins, health effects, and their increased occurrence. *Environ. Health Perspect.* 108 Suppl 1, 133–41.
- Vardi, A., Eisenstadt, D., Murik, O., Berman-Frank, I., Zohary, T., Levine, A., Kaplan, A., 2007. Synchronization of cell death in a dinoflagellate population is mediated by an excreted thiol protease. *Environ. Microbiol.* 9, 360–369.
<https://doi.org/10.1111/j.1462-2920.2006.01146.x>
- Vavilala, S.L., Gawde, K.K., Sinha, M., D’Souza, J.S., 2015. Programmed cell death is induced by hydrogen peroxide but not by excessive ionic stress of sodium chloride in the unicellular green alga *Chlamydomonas reinhardtii*. *Eur. J. Phycol.* 50, 422–438. <https://doi.org/10.1080/09670262.2015.1070437>
- Vd’ačn, P., Orsi, W., Foissner, W., 2010. Molecular and morphological evidence for a sister group relationship of the classes Armophorea and Litostomatea (Ciliophora, Intramacronucleata, Lamellicorticata infraphyl. nov.), with an account on basal litostomateans. *Eur. J. Protistol.* 46, 298–309.
<https://doi.org/10.1016/j.ejop.2010.07.002>
- Wolf, D., Georgic, W., Klaiber, H.A., 2017. Reeling in the damages: Harmful algal blooms’ impact on Lake Erie’s recreational fishing industry. *J. Environ. Manage.* 199, 148–157. <https://doi.org/10.1016/j.jenvman.2017.05.031>
- Yang, J.W., Wu, W., Chung, C.-C., Chiang, K.-P., Gong, G.-C., Hsieh, C., 2018. Predator and prey biodiversity relationship and its consequences on marine ecosystem functioning—interplay between nanoflagellates and bacterioplankton. *ISME J.* 12, 1532–1542. <https://doi.org/10.1038/s41396-018-0111-3>

Yang, Y., Liu, Q., Chai, Z., Tang, Y., 2015. Inhibition of marine coastal bloom-forming phytoplankton by commercially cultivated *Gracilaria lemaneiformis* (Rhodophyta). *J. Appl. Phycol.* 27, 2341–2352. <https://doi.org/10.1007/s10811-014-0486-0>

Appendix

PHOTOCHEMICAL RESPONSE TO NH₄⁺ ALONE VS. IRI-160AA

Table A1 Maximum yield of photosystem II (F_v/F_m) with standard deviation (SD) through after application of IRI-160AA at EC50 for *K. veneficum*. All values are representative of the mean of three biological replicates.

Treatment	Time (h)	F_v/F_m	SD
IRI-160AA	0	0.399	0.020
	18	0.423	0.025
	42	0.439	0.047
	66	0.480	0.010
NH ₄ ⁺	0	0.399	0.020
	18	0.456	0.034
	42	0.473	0.015
	66	0.456	0.007
Control	0	0.399	0.020
	18	0.448	0.025
	42	0.453	0.004
	66	0.465	0.005

Table A2 Maximum yield of photosystem II (F_v/F_m) with standard deviation (SD) through after application of IRI-160AA at EC50 for *P. minimum*. All values are representative of the mean of three biological replicates.

Treatment	Time (h)	F_v/F_m	SD
IRI-160AA	0	0.351	0.020
	18	0.408	0.016
	42	0.370	0.007
	66	0.417	0.029
NH ₄ ⁺	0	0.351	0.020
	18	0.412	0.016
	42	0.341	0.048
	66	0.403	0.008
Control	0	0.351	0.020
	18	0.408	0.014
	42	0.349	0.018
	66	0.396	0.016

Table A3 Maximum yield of photosystem II (F_v/F_m) with standard deviation (SD) through after application of IRI-160AA at EC50 for *G. instriatum*. All values are representative of the mean of three biological replicates.

Treatment	Time (h)	F_v/F_m	SD
IRI-160AA	0	0.489	0.031
	18	0.599	0.018
	42	0.477	0.019
	66	0.479	0.013
NH ₄ ⁺	0	0.489	0.031
	18	0.526	0.052
	42	0.500	0.030
	66	0.509	0.011
Control	0	0.489	0.031
	18	0.558	0.009
	42	0.474	0.027
	66	0.472	0.006

Table A4 Maximum yield of photosystem II (F_v/F_m) with standard deviation (SD) through after application of IRI-160AA at EC50 for *A. tamarense*. All values are representative of the mean of three biological replicates.

Treatment	Time (h)	F_v/F_m	SD
IRI-160AA	0	0.487	0.006
	18	0.541	0.013
	42	0.480	0.011
	66	0.524	0.030
NH ₄ ⁺	0	0.487	0.006
	18	0.534	0.005
	42	0.470	0.027
	66	0.524	0.032
Control	0	0.487	0.006
	18	0.516	0.011
	42	0.485	0.019
	66	0.505	0.057